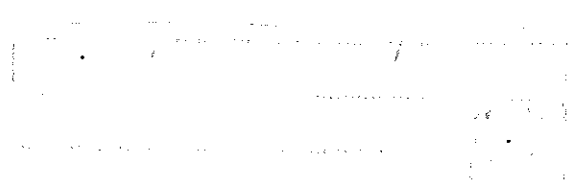


**Effects of the Missense Mutations and the Anticancer Drug Cisplatin on  
Ubiquitination of BRCA1 RING Finger Domain**

**Apichart Atipairin**



**A Thesis Submitted in Fulfillment of the Requirements for the Degree of  
Doctor of Philosophy in Pharmaceutical Sciences**

**Prince of Songkla University**

**2010**

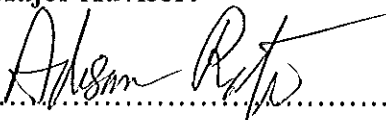
**Copyright of Prince of Songkla University**

เลขที่	RC211.GAD A64 2010.	C. 2.
Bib Key	955911	
	23.01.01.2555	

**Thesis Title**                Effects of the Missense Mutations and the Anticancer Drug  
   Cisplatin on Ubiquitination of BRCA1 RING Finger Domain  
**Author**                        Mr. Apichart Atipairin  
**Major Program**            Pharmaceutical Sciences

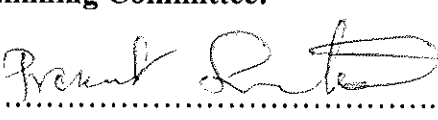
---

**Major Advisor:**

  
.....

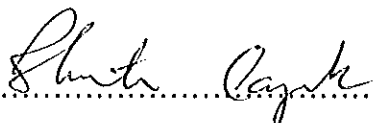
(Assoc. Prof. Dr. Adisorn Ratanaphan)

**Examining Committee:**

 ..... Chairperson

(Assoc. Prof. Dr. Prasert Suintanalert)

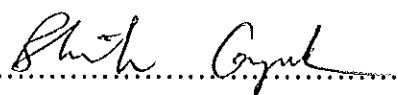
**Co-advisor:**

  
.....


(Assist. Prof. Dr. Bhutorn Banyuk)

  
.....

(Assoc. Prof. Dr. Adisorn Ratanaphan)

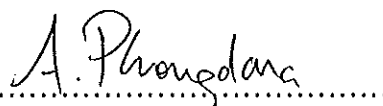
  
.....

(Assist. Prof. Dr. Bhutorn Banyuk)

  
.....

(Assoc. Prof. Dr. Chartchai Krittanai)

The Graduate School, Prince of Songkla University, has approved this thesis as fulfillment of the requirements for the Doctor of Philosophy Degree in Pharmaceutical Sciences

  
.....

(Prof. Dr. Amornrat Phongdara)

Dean of Graduate School

**Thesis Title**            Effects of the Missense Mutations and the Anticancer Drug  
                                  Cisplatin on Ubiquitination of BRCA1 RING Finger domain

**Author**                    Mr. Apichart Atipairin

**Major Program**        Pharmaceutical Sciences

**Academic Year**        2010

### Abstract

Tumor suppressor protein BRCA1 participates in genomic integrity maintenance through DNA repair, cell cycle checkpoint, protein ubiquitination, and transcriptional regulation. The N-terminus of BRCA1 contains a RING domain which forms two Zn<sup>2+</sup>-binding sites in an interleaved fashion. A number of deleterious BRCA1 missense mutations, which predispose individuals to a subset of hereditary breast and ovarian cancers, have been identified in the RING domain. An unprecedented D67E BRCA1 mutation, identified in Thai familial breast cancer patients, is located in the vicinity of the Zn<sup>2+</sup>-binding site II, and its pathogenic significance remains elusive. The present study revealed that the D67E BRCA1 RING protein assumed a preformed structure in the absence of Zn<sup>2+</sup>. The Zn<sup>2+</sup>-bound mutant protein was more folded, resulting in an enhanced proteolytic resistance and dimerization. It indicated that the mutation retained Zn<sup>2+</sup>-binding, and barely perturbed the native global structure of the BRCA1 RING domain. However, the D67E mutation was slightly less stable toward thermal denaturation. The complex between the D67E BRCA1 and BARD1 RING domains still maintained a substantial ubiquitin ligase activity compared with a defective complex containing the C61G BRCA1 mutation. It implied that the D67E mutation might be a neutral or mild cancer-risk modifier through the other defective mechanisms, underlying the BRCA1-mutation-related breast cancer. Preclinical and clinical studies have recently revealed that the inactivation of BRCA1 in cancer cells leads to chemosensitivity. Therefore,

approaching the BRCA1 RING domain as a potentially molecular target for a platinum-based drug might be of interest in cancer therapy. The *in vitro* platination of the BRCA1 RING domain by the anticancer drug cisplatin was observed. Cisplatin formed the intramolecular and intermolecular BRCA1 adducts by which His117 was the primary platinum-binding site. The cisplatin-modified BRCA1 also conferred conformational changes and induced thermostability. Additionally, the BRCA1-mediated E3 ubiquitin ligase activity was inhibited by a number of platinum complexes whose reactivity towards the BRCA1 protein was decreased in the following order: transplatin > cisplatin > oxaliplatin > carboplatin. The data could raise the possibility of selectively targeting the BRCA1 RING domain for cancer therapy with less toxicity or improved response to conventional regimens.



ชื่อวิทยานิพนธ์ ผลของการผ่าเหล่าแบบ missense และยาด้านมะเร็งซิสพลาตินต่อ ubiquitination  
ของ BRCA1 RING finger domain

ผู้เขียน นาย อภิชาติ อธิไกริน

สาขาวิชา เกษศาสตร์

ปีการศึกษา 2553

### บทคัดย่อ

โปรตีนกดการเกิดมะเร็ง BRCA1 ทำหน้าที่เกี่ยวข้องในการรักษาเสถียรภาพของจีโนมโดยอาศัยกระบวนการซ่อมแซมดีเอ็นเอที่เสียหาย การควบคุมวงจรชีวิตของเซลล์ กระบวนการ ubiquitination และการควบคุมการถอดรหัส บริเวณด้านปลายอะมิโนของ BRCA1 เป็นส่วนที่เรียกว่า RING domain ซึ่งมีการจัดเรียงตัวของกรดอะมิโนในบริเวณดังกล่าวเพื่อจับกับโลหะสังกะสี 2 ตัว การผ่าเหล่าแบบ missense ในบริเวณ RING domain จำนวนมากมีความเกี่ยวข้องกับการเกิดมะเร็งเต้านมและมะเร็งรังไข่แบบที่มีการถ่ายทอดทางกรรมพันธุ์ BRCA1 ที่มีการการผ่าเหล่าแบบ D67E (D67E BRCA1) ซึ่งพบเฉพาะในผู้ป่วยคนไทยที่เป็นมะเร็งเต้านมอยู่ในบริเวณใกล้เคียงกับกรดอะมิโนที่จับกับโลหะสังกะสี และความสำคัญของการผ่าเหล่าชนิดนี้กับการก่อโรคมะเร็งยังไม่เป็นที่ทราบแน่ชัด การศึกษาครั้งนี้แสดงให้เห็นว่าการผ่าเหล่าแบบ D67E ทำให้ BRCA1 ในส่วน RING domain ยังคงรูปอยู่ได้แม้อยู่ในสภาวะปราศจากโลหะสังกะสี โปรตีนผ่าเหล่าชนิดนี้ในสภาวะที่มีโลหะสังกะสีมีการม้วนตัวที่มากขึ้นซึ่งทำให้คงตัวต่อการถูกย่อยสลายและเป็น dimer เพิ่มมากขึ้นแสดงให้เห็นว่าการผ่าเหล่าชนิดนี้ไม่ได้รับกวนความสามารถในการจับกับโลหะสังกะสีและโครงสร้างโดยรวมของ BRCA1 ในส่วน RING domain อย่างไรก็ตาม D67E BRCA1 ทำให้ความคงตัวต่อความร้อนลดลงเล็กน้อยและการทำหน้าที่เป็นเอนไซม์ ubiquitin ligase ร่วมกับ BARD1 ยังคงเหมือนเดิมเมื่อเปรียบเทียบกับ C61G BRCA1 ที่สูญเสียการทำหน้าที่ดังกล่าวไป ดังนั้น D67E BRCA1 อาจเป็น neutral หรือ mild cancer-risk modifier โดยผ่านกลไกที่มีความบกพร่องอื่น ๆ ที่มีความสัมพันธ์กับ BRCA1 ที่ผ่าเหล่า การศึกษาทางพีรีคลินิกและทางคลินิกแสดงให้เห็นว่าการยับยั้งการทำงานของ BRCA1 ในเซลล์มะเร็งทำให้เซลล์มะเร็งไวต่อยาเคมีบำบัด ดังนั้นที่น่าสนใจที่ BRCA1 RING domain น่าจะเป็นเป้าหมายระดับโมเลกุลของยาในกลุ่มพลาตินัมในการรักษามะเร็ง

การศึกษาในหลอดทดลองระหว่างโปรตีน BRCA1 RING กับยาด้านมะเร็งซิสพลาตินพบว่าซิสพลาติน  
เกิดพันธะกับโปรตีน BRCA1 ทั้งภายในและระหว่างโมเลกุล BRCA1 โดยที่อะตอมพลานัมของ  
ซิสพลาตินเกิดพันธะกับกรดอะมิโนฮิสติดีนที่ตำแหน่ง 117 ของ BRCA1 RING domain ซิสพลาติน  
ยังทำให้ BRCA1 มีการเปลี่ยนแปลงโครงสร้างและมีความคงตัวต่อความร้อนเพิ่มขึ้น นอกจากนี้การทำ  
หน้าที่ของ BRCA1 ในการเป็นเอนไซม์ ubiquitin ligase ยังถูกยับยั้งโดยสารประกอบเชิงซ้อนใน  
กลุ่มพลานัมโดยที่ความไวในการยับยั้งการทำงานของ BRCA1 จากมากไปหาน้อยคือ ทรานพลานิน  
> ซิสพลาติน > อ็อกซะลิพลาติน > และคาร์โบพลานิน ตามลำดับ ข้อมูลที่ได้จากการศึกษาครั้งนี้อาจ  
เพิ่มความเข้าใจได้ที่ BRCA1 RING domain เป็นเป้าหมายจำเพาะสำหรับการรักษามะเร็งเพื่อให้มี  
ความเป็นพิษลดน้อยลงหรือเพิ่มผลการตอบสนองของยากลุ่มเดิม

## ACKNOWLEDGEMENTS

I would like to express my gratitude and sincere appreciation to my thesis advisor, Assoc. Prof. Dr. Adisorn Ratanaphan, for providing an important opportunity of Ph.D. degree study. I wish to thank him for valuable suggestions, comments, support, and constant encouragement throughout this work.

My sincere thanks are expressed to my thesis co-advisor and examining committee, Assist. Prof. Dr. Bhutorn Canyuk, Prof. Dr. Udo Heinemann, Assoc. Prof. Dr. Prasert Sutinanalert, and Assoc. Prof. Dr. Chartchai Krittanai for kindness, assistance, and valuable suggestions.

I am thankful to Prof. Dr. Udo Heinemann and his colleagues for kindly assistance during my research stay at Max-Delbrück Center for Molecular Medicine (MDC), Berlin, Germany.

I would like to express my appreciation to Faculty of Pharmaceutical Sciences, Prince of Songkla University, the Graduate Study Scholarship during 2003-2005, and the grants from the Synchrotron Light Research Institute (Public organization)(1-2548/LS01), the National Research Council of Thailand (PHA5111990041S and PHA530097S), and Prince of Songkla University (PHA530188S). I also would like to extend my sincere thanks to the Pharmaceutical Laboratory Service Center, Faculty of Pharmaceutical Sciences, Prince of Songkla University, for research facilities.

I also would like to thank all my dear friends, the members and staff of BRCA1 Laboratory in PSU and Macromolecular Structure and Interaction in MDC.

Finally, I would like to express my sincere gratitude to my father, mother, brothers, and relatives for their loves, understanding, and support.

Apichart Atipairin

## CONTENTS

	<b>Page</b>
Contents	(viii)
List of Tables	(xi)
List of Figures	(xii)
List of Abbreviations and Symbols	(xv)
Chapter	
1. Introduction	1
2. Literature review	
2.1 Breast cancer	4
2.1.1 Incidence and mortality rates of breast cancer	4
2.1.2 Classification of the breast cancer	4
2.2 Risk factors	6
2.3 Breast cancer susceptibility gene 1 ( <i>BRCA1</i> )	11
2.3.1 Mutation spectrum of <i>BRCA1</i>	13
2.4 Breast cancer susceptibility protein 1 (BRCA1)	16
2.4.1 The BRCA1 RING finger domain	16
2.4.2 The large central segment of BRCA1	19
2.4.3 The BRCA1 C-terminal domain	19
2.5 BRCA1 and its cellular function	20
2.5.1 BRCA1 and cell growth control	21
2.5.2 BRCA1 and transcriptional regulation	23
2.5.3 BRCA1 and DNA repair	25
2.5.4 BRCA1 and protein ubiquitination	27
2.6 Targeting the ubiquitin system	31
2.7 Cisplatin	34
2.7.1 Introduction	34
2.7.2 DNA adducts	37

## CONTENTS (Continued)

	Page
2.7.3 Effect of cisplatin on DNA replication and mutagenicity	38
2.7.4 Repair of cisplatin-damaged DNA	42
2.7.5 Effect of cisplatin on transcription inhibition	44
2.7.6 Effect of cisplatin on protein translation	47
2.7.7 Effect of cisplatin on cell death pathways	48
2.7.8 Protein adducts	51
2.8 Dysfunctional BRCA1 as a therapeutic strategy	54
2.8.1 Targeting BRCA1 for the anticancer platinum-based drugs for cancer therapy	57
3. Materials and Methods	
Materials	61
Methods	
3.1 Preparation of the complementary DNA fragments of the <i>BRCA1</i> gene (GenBank no. U14860)	66
3.2 DNA amplification of the <i>BRCA1</i> , <i>BARD1</i> , <i>ubiquitin</i> , and <i>UbcH5c</i> genes	69
3.3 Extraction and purification of the PCR products	71
3.4 Plasmid constructions	72
3.5 Site-directed mutagenesis of the BRCA1 RING domain	74
3.6 Verification of the recombinant plasmids by automated DNA sequencing	76
3.7 Expression and purification of the recombinant proteins	76
3.8 Gel-filtration chromatography	78
3.9 Glutaraldehyde cross-linking	78
3.10 Limited proteolysis and mass spectrometry	78
3.11 Circular dichroism	79

## CONTENTS (Continued)

	Page
3.12 X-ray absorption near-edge structure (XANES)	80
3.13 Three-dimensional structure modeling	80
3.14 Preparation of the platinum-BRCA1 complexes	81
3.15 <i>In vitro</i> ubiquitin ligase assay	81
4. Results	
4.1 Expression and purification of the recombinant proteins	82
4.2 Secondary structure and zinc(II)-binding of the D67E BRCA1 protein	84
4.3 Proteolytic resistance of the D67E BRCA1 mutation	90
4.4 Thermal stability of the D67E BRCA1 mutation	92
4.5 <i>In vitro</i> ubiquitin ligase activity of the D67E BRCA1 protein	95
4.6 Cisplatin binding to the BRCA1 RING domain	99
4.7 Thermal stability of the cisplatin-BRCA1 adducts	105
4.8 <i>In vitro</i> ubiquitin ligase activity of the cisplatin-BRCA1 adducts	109
5. Discussion	
5.1 The structural consequence of the D67E BRCA1 mutation	113
5.2 The functional consequence of the D67E BRCA1 mutation	115
5.3 The interaction between the anticancer drug cisplatin and the BRCA1 RING domain	118
5.4 The BRCA1 E3 ligase activity inactivated by the platinum-based drugs	120
6. Conclusion	123
References	125
Appendix	159
Vitae	165

## LIST OF TABLES

Table		Page
1	Age-standardized incidence and mortality rates for breast cancer in the major industrialized countries of the world in 2008	6
2	Summary of known breast cancer-predisposing genetic factors	12
3	Cumulative incidences (standard error) of breast and ovarian cancers by age for <i>BRCA1</i> carriers	13
4	Total number of mutations, polymorphisms, and variants from the Breast Cancer Information Core Database	14
5	Relative frequencies of <i>BRCA1</i> mutation in Thais	15
6	Summary of the consequences of protein adducts by cisplatin	52
7	Summary of the cisplatin-based therapy in breast cancer patients and the pathological complete response	59
8	Reaction components for the One-step RT-PCR	69
9	Thermal cycling conditions for the One-step RT-PCR	69
10	The oligonucleotide primers for the amplifications of the <i>BRCA1</i> , <i>BARD1</i> , <i>ubiquitin (ub)</i> , and <i>UbcH5c</i> genes	70
11	Reaction components for PCR amplification	71
12	Thermal cycling conditions for PCR	71
13	The oligonucleotide primers for site-directed mutagenesis	75
14	The sample reaction for site-directed mutagenesis	75
15	Thermal cycling condition for site-directed mutagenesis	75

## LIST OF FIGURES

Figure		Page
1	Ball and stick representation of the Zn <sup>2+</sup> -binding site II of the BRCA1 RING domain (1JM7.pdb)	2
2	The global cancer incidence and mortality rates	5
3	Schematic illustration of breast anatomy	6
4	Schematic diagram of BRCA1 and its binding partners	18
5A	Solution structure of the BRCA1-BARD1 RING complex	18
5B	Crystal structure of the BRCA1-BRCT domain (PDB: 1JNX)	18
6	Multiple cellular functions of BRCA1	21
7	An overview of BRCA1-transcriptionally regulated targets and their impact on cell cycle progression	22
8	The ubiquitination pathway	27
9	Potential roles for the BRCA1-BARD1 E3 ligase in the known BRCA1 functions	28
10	Molecular structures of the platinum complexes	35
11	Hydrolysis of cisplatin	36
12	The formations of different cisplatin-modified DNA adducts	37
13	Effects of a bifunctional intrastrand cisplatin adduct on DNA replication	40
14	Possible mechanisms of transcription inhibition by cisplatin-DNA adduct	46
15	Schematic overview of the proposed biochemical pathways of cell death induced by cisplatin	49
16	Loss of functional BRCA1 affects the choice of DNA double-strand break (DSB) repair pathway	55
17	Potential mechanisms of BRCA1 dysfunction	56
18	The potential role of BRCA1 in response to chemotherapy	58



## LIST OF FIGURES (Continued)

Figure		Page
19	Nucleotide sequence of the <i>BRCA1</i> gene fragment (nucleotide 1-912)	68
20	Schematic representations of the bacterial expression plasmids	73
21	Expression and purification of the BRCA1 RING domain analyzed by 15% SDS-PAGE with Coomassie blue staining	83
22	Amino acid sequencing of the peptides after tryptic digestion	83
23	Purification of the affinity-tagged proteins	84
24	The CD spectra of the BRCA1 RING proteins	85
25	Gel-filtration chromatography of the BRCA1 RING domain	86
26	15% SDS-PAGE of glutaraldehyde cross-linking	88
27	Titration curves of Zn <sup>2+</sup> -binding to the BRCA1 RING proteins	89
28	X-ray absorption near-edge structure (XANES) of the wild-type BRCA1(1-139) RING proteins	89
29	Limited proteolysis of the D67E BRCA1 protein	91
30	Limited proteolysis of the wild-type BRCA1 protein	91
31	Thermal transition of the D67E BRCA1 protein	93
32	Thermal transition of the wild-type BRCA1 protein	94
33	Thermal unfolding curve of the BRCA1 RING domains	95
34	The extended BRCA1 RING domain exhibited the higher ubiquitination	96
35	Time-dependence of the ubiquitination reaction	97
36	<i>In vitro</i> ubiquitination	97
37	<i>In vitro</i> ubiquitin ligase activity of the mutant BRCA1 RING proteins	98
38	15% SDS-PAGE of the cisplatin-BRCA1 intermolecular crosslinks	99
39	Mass spectrometric analyses of the cisplatin-BRCA1 adducts	100
40	The CD spectra of the cisplatin-BRCA1 adducts	102
41	Titration curve of cisplatin binding to the BRCA1(1-139) protein	103

## LIST OF FIGURES (Continued)

Figure		Page
42	Mass spectrometric analyses of the cisplatin-BRCA1(1-139) adduct digests	104
43	The product-ion spectrum of the MS/MS analysis for the 656.29 <sup>2+</sup> ion	105
44	Thermal transition of the cisplatin-BRCA1 adducts in the absence of Zn <sup>2+</sup>	106
45	Thermal transition of the cisplatin-BRCA1 adducts in the presence of Zn <sup>2+</sup>	107
46	Thermal denaturation curves of the cisplatin-BRCA1 adducts	109
47	<i>In vitro</i> ubiquitin ligase activity of the platinum-BRCA1 complexes	110
48	<i>In vitro</i> ubiquitin ligase activity of the platinum-BRCA1 or platinum-BARD1 complexes	111
49	Inhibition of the BRCA1 E3 ligase activity by the platinum complexes	112
50	Superposition of the model structures in the Zn <sup>2+</sup> -binding site II	114
51	Surface representation of the model structures	115
52	Information of pET28a(+)_BARD1 (Addgene plasmid 12646)	160
53	Information of pET28a(+)_UbcH5c (Addgene plasmid 12643)	161
54	Information of pET15_ubiquitin (Addgene plasmid 12647)	162
55	Nucleotide sequence of the <i>BARD1</i> gene fragment (nucleotide 76-981)	163
56	Nucleotide sequence of the full-length <i>UbcH5c</i> gene	164
57	Nucleotide sequence of the full-length ubiquitin gene	164

## LIST OF ABBREVIATIONS AND SYMBOLS

°C	Degree celcius
$A_{600\text{ nm}}$	Absorbance at 600 nm
ACN	Acetonitrile
AIB1	Amplified in breast cancer 1
APC	Anaphase-promoting complex
ASR	Age-standardized rate
ATM	Ataxia telangiectasia mutated
ATR	Ataxia telangiectasia and RAD3-related
BACH1	BRAC1-associated C-terminal helicase 1
BAP1	BRCA1-associated protein 1
BARD1	BRCA1-associated RING domain 1
BIC	Breast Cancer Information Core Database
BRCA1	Breast cancer suppressor protein 1
BRCA2	Breast cancer suppressor protein 2
BRCT	BRCA1 C-terminal domain
BSA	Bovine serum albumin
BubR1	Budding uninhibited by benzimidazole 1-related kinase
CD	Circular dichroism
CtBP	C-terminal binding protein
CTD	Carboxyl terminal domain
CtIP	CtBP-interacting protein
Ctr1	Copper transporter 1
Cys	Cysteine
D67E	Substitution of aspartic acid with glutamic acid at position 67
DDT	Dichlorodiphenyl trichloroethane
DNA-PKcs	DNA-dependent protein kinase catalytic subunit

DSBs	DNA double-stranded breaks
DSC	Differential scanning calorimetry
DTT	Dithiothreitol
DUBs	Deubiquitylating enzymes
E1	Ubiquitin-activating enzyme
E2	Ubiquitin-conjugating enzyme
E3	Ubiquitin ligase
EDTA	Ethylenediamine tetraacetic acid
ER $\alpha$	Estrogen receptor $\alpha$
ERCC1	Excision repair cross-complementing-1
ESI-MS	Electrospray ionization mass spectrometry
FA	Fanconi anemia
FDA	Food and Drug Administration
FT-IR	Fourier-transform infrared spectroscopy
GADD45	Growth-arrest and DNA-damage-inducible protein 45
GGR	Global genomic repair
GST	Glutathione- <i>S</i> -transferase
h	Hour
HDAC1	Histone deacetylase 1
Hdm2	Human counterpart of Mdm2
HERC2	HECT domain and RCC1-like domain-containing protein 2
His	Histidine
HR	Homologous recombination
HRT	Hormone replacement therapy
IAP	Inhibitor of apoptosis protein
IPTG	Isopropyl-1-thio- $\beta$ -D-galactopyranoside
IR	Ionizing radiation
JNK/SAPK	c-Jun NH <sub>2</sub> -terminal kinase/stress-activated protein kinase

LB	Luria Broth
LC-MS	Liquid chromatography mass spectrometry
M	Molar
MAD2	Mitotic arrest-deficient protein 2
MDC1	Mediator of DNA damage checkpoint 1
Mdm2	Murine double minute 2
MMR	Mismatch repair
MS/MS	Tandem mass spectrometer
NAT2	<i>N</i> -acetyltransferase 2
NER	Nucleotide excision repair
NHEJ	Non-homologous end-joining
NLS	Nuclear localization signal
NMR	Nuclear magnetic resonance spectroscopy
OC	Oral contraceptives
PAGE	Polyacrylamide gel electrophoresis
PALB2	Partner and localizer of BRCA2
PARP	Poly(ADP-ribose) polymerase
PCBs	Polychlorinated biphenyls
PCR	Polymerase chain reaction
PDB	Protein data bank
PMSF	Phenylmethylsulphonyl fluoride
PRE	Progesterone response elements
RAD51	The mammalian homolog of the <i>Escherichia coli</i> RecA protein
RAP80	Receptor-associated protein 80
RING	Really interesting gene
RNA	Ribonucleic acid
RNAPII	RNA polymerase II
RNF8	RING finger protein 8

RR	Relative risk
RT-PCR	Reverse transcriptase-polymerase chain reaction
s	Second
SDS	Sodium dodecyl sulfate
siRNA	Small interfering RNA
SRC1	Steroid receptor co-activator 1
TBP	TATA-binding protein
TCR	Transcription-coupled repair
TFIIE	Transcription factor E
TFIIH	Transcription factor H
T <sub>m</sub>	Melting temperature
Ub	Ubiquitin
UIM	Ubiquitin-interacting motif
wt	Wild-type
XANES	X-ray absorption near-edge structure

## CHAPTER 1

### INTRODUCTION

The breast cancer susceptibility protein BRCA1 is a tumor suppressor protein and has been implicated in a variety of cellular processes such as cell-cycle checkpoint control, transcriptional regulation, protein ubiquitination, and the cellular response to DNA damage (Huen *et al.*, 2010; O'Donovan and Livingston, 2010; Rosen *et al.*, 2003). Germline mutations of BRCA1 undoubtedly predispose individuals to cancer development with 50% for hereditary breast cancer, and at least 80% for hereditary breast and ovarian cancer (Ford *et al.*, 1995). Due to being a large protein, BRCA1 is characterized into 3 major domains, including the N-terminal RING domain, large central segment, and the BRCA1 C-terminal domain (BRCT). The BRCA1 RING domain is located at the N-terminus whose sequence contains the conservative pattern of cysteine and histidine (C<sub>3</sub>HC<sub>4</sub>) necessary for the specific coordination with two Zn<sup>2+</sup> ions. Atomic structure of the BRCA1 RING domain has recently been elucidated. Both ends of the domain are antiparallel  $\alpha$ -helices, flanking the central RING motif characterized by a short antiparallel three-stranded  $\beta$ -sheets, two large Zn<sup>2+</sup>-binding loops, and a central  $\alpha$ -helix. Two metal-binding sites are formed in an interleaved fashion, which the first and third pairs of cysteines (Cys24, Cys27, Cys44, and Cys47) form site I, and the second and fourth pairs of cysteines and a histidine (Cys39, His41, Cys61, and Cys64) form site II (Brzovic *et al.*, 2001). It is an important domain since it might mediate a central role in macromolecular interactions to exert the tumor suppression function. Intriguingly, the BARD1 (BRCA1-associated RING domain 1) protein was well identified to form a heterodimer with BRCA1 through the formation of an extensive four-helix-bundle dimerization interface that is the flanking region of each RING domain (Brzovic *et al.*, 2001). The BRCA1-BARD1 RING complex exhibited an E3 ubiquitin ligase

activity, and the mutations in the residues of the first  $Zn^{2+}$  loop, the central helix, and the second  $Zn^{2+}$  loop of BRCA1 abolished its E3 ligase activity, (Brzovic *et al.*, 2003; Dizin and Irminger-Finger, 2010; Eakin *et al.*, 2007; Hashizume *et al.*, 2001). It was suggested that there was a direct relationship between the BRCA1-mediated ubiquitination and cancer development (Morris *et al.*, 2006; Nishikawa *et al.*, 2004; Ruffner *et al.*, 2001).

An unprecedented D67E BRCA1 mutation has only been identified in Thai familial and isolated breast cancer patients (Patmasiriwat *et al.*, 2002). Aspartic acid at position 67 is located in the vicinity of the  $Zn^{2+}$ -binding site II. Its carboxylic side-chain is not directly involved in  $Zn^{2+}$ -binding, but projects into the bulk solvent. The extension of the negatively charged side-chain of the D67E mutant could potentially alter the native molecular surface by interacting with the proximal residues such as Lys38, Gln60, and Asn66 (Figure 1). Therefore, the alteration of the protein surface could affect protein stability and interfere protein-protein interactions that are crucial for exerting BRCA1 functions. It is of great interest to investigate in the structural and functional consequences of the D67E BRCA1 RING mutation. This would provide insights into the BRCA1 mutation-related breast carcinogenesis.

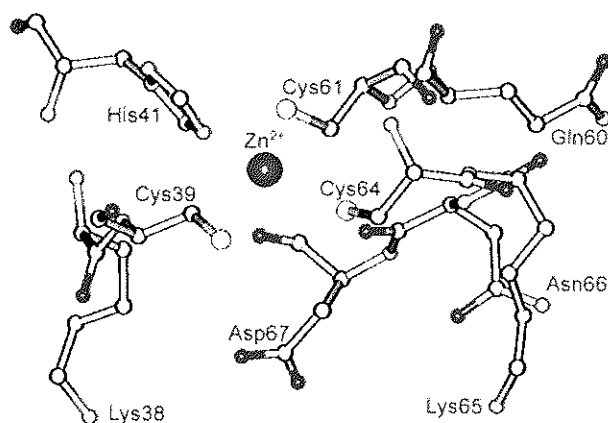


**Figure 1.** Ball and stick representation of the  $Zn^{2+}$ -binding site II of the BRCA1 RING domain (1JM7.pdb). The spheres represented the bound  $Zn^{2+}$  atom, and the highly conserved residues (Cys39, His41, Cys61, and Cys64) constituted the  $Zn^{2+}$ -binding site II were shown.



A new approach for cancer therapy involves alterations to the DNA repair pathways by which the cancer cells with dysfunctional DNA repair pathways accumulate high levels of DNA damage that eventually resulted in major genomic instability and cell death (Amir *et al.*, 2010; Price and Monteiro, 2010; Tassone *et al.*, 2009). Recently, extensive investigations have examined the relevance of the BRCA1-mediated E3 ubiquitin ligase activity to its tumor suppression function, and several preclinical and clinical studies have demonstrated the utilization of a dysfunctional BRCA1 as a clinically validated target for breast and ovarian cancer treatment (Byrski *et al.*, 2009; Byrski *et al.*, 2010; Font *et al.*, 2010; Silver *et al.*, 2010). It is of interest to approach the BRCA1 RING domain as a potentially molecular target for platinum-based drugs for cancer therapy. To raise the possibility that the BRCA1 RING domain could be a molecular target for platinum-based drugs, the functional consequences of the platinated BRCA1 on its effect on the E3 ubiquitin ligase activity have been investigated. The data would provide an insight into the feasibility of selectively targeting the BRCA1 RING domain for cancer therapy with less toxicity or improved response to conventional regimens.

## CHAPTER 2

### LITERATURE REVIEW

#### 2.1 Breast cancer

##### 2.1.1 Incidence and mortality rates of breast cancer

Breast cancer is one of the major health problems by which the estimated age-standardized incidence and mortality rates (ASR) for women are 39.0 and 12.5 in 2008, respectively (Figure 2) (Ferlay *et al.*, 2008). The disease has gradually increased worldwide, and it is the leading cause of death in approximately 22.9% of all females who die from cancer. The estimated incidence and mortality rates (ASR) for women in the major industrialized countries are shown in Table 1 (Ferlay *et al.*, 2008). There are marked differences in the incidence of breast cancer in different places in which the predominant prevalence of the disease is more common among western countries. The recent global breast cancer statistics indicates that mortality rate is currently declining in the United States and other countries where the disease historically has been a leading cancer-related mortality cause (Metin, 1999). This has been due to the early detection of disease, and the use of chemotherapeutics and endocrine therapy. In Thailand, breast cancer has become the most common cancer in women with the estimated incidence and death rates (ASR) of 30.7 and 10.8, respectively in 2008 (Ferlay *et al.*, 2008).

##### 2.1.2 Classification of the breast cancer

Breast cancer is a form of cancer that originates from breast tissue which is made up of three main parts; mammary glands, ducts, and connective tissues (Figure 3). Mammary glands produce milk. The ducts are passages that carry milk to the nipple. The connective tissues, which consist of fibrous and fatty tissues, connect

and hold everything together. There are different kinds of breast cancers, depending on which cells in the breast turn into cancer. Common types of breast cancers are

**Ductal carcinoma.** It is the most common type of breast cancer that begins in the cells that line the milk ducts in the breast.

- **Ductal carcinoma in situ (DCIS).** The abnormal cancer cells are only in the lining of the milk ducts, and have not spread to other tissues in the breast.

- **Invasive ductal carcinoma (IDC).** It is the most common type of breast cancer which accounts for 75% of breast carcinomas. The abnormal cancer cells break through the ducts, and spread (metastatize) into other parts of the breast tissue. Invasive cancer cells can also spread to other parts of the body.

**Lobular carcinoma.** The cancer cells begin in the lobes or lobules that are the glands that produce milk.

- **Lobular carcinoma in situ (LCIS).** The cancer cells are found only in the breast. It does not spread to other tissues.

- **Invasive lobular carcinoma (ILC).** It is the second most common type of breast cancer which accounts for 10-15% of breast carcinomas. The cancer cells spread from the lobules to the surrounding breast tissues, and can also spread to other parts of the body.

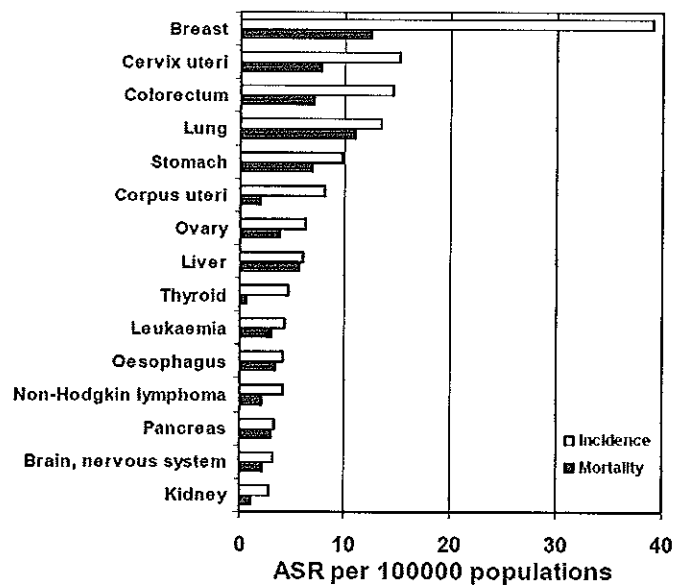


**Figure 2.** The global cancer incidence and mortality rates (Ferlay *et al.*, 2008).

**Table 1.** Age-standardized incidence and mortality rates for breast cancer in the major industrialized countries of the world in 2008 (Ferlay *et al.*, 2008).

Country	Age-standardized incidence rate (per 100000 population)	Age-standardized mortality rate (per 100000 population)
England	87.9	18.6
France	99.7	17.6
Germany	81.8	16.9
Italy	86.3	16.1
Canada	83.2	15.6
USA	76.0	14.7
Japan	42.7	9.1
Thailand	30.7	10.8

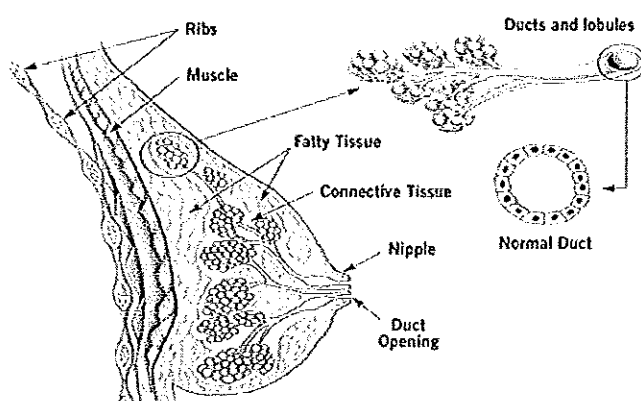


**Figure 3.** Schematic illustration of breast anatomy (Ramsay *et al.*, 2006).

## 2.2 Risk factors

The pathology of breast cancer is poorly characterized. However, there are several well-established risk factors associated with the cancer development.

### 2.2.1 Gender

Breast cancer is relatively uncommon in men whose the female-to-male breast cancer ratio is approximately 100:1. An estimated 207090 and 1970 new cases of breast cancers will be diagnosed among American women and men, respectively in 2010, and about 39840 women and 390 men will die from the disease

(Jemal *et al.*, 2010). The higher risk in women is attributed to the responsiveness of breast tissues to ovarian hormones which are active from puberty to menopause.

### **2.2.2 Age**

The risk of developing breast cancer increases with age. The disease is uncommon in women younger than 40 years of age which occur only 6.4% of all patients diagnosed with a first primary breast cancer. Women, who are 40 years of age or older at time of diagnosis, are accounted for the remaining portion (93.6%) of all breast cancers (Gnerlich *et al.*, 2009). The biological characteristics of tumors in younger women are significantly different from tumor characteristics in older women. Younger women have a more aggressive form of tumors with poorer prognosis, and therefore the mortality rate in this population is higher compared with older women.

### **2.2.3 Family history**

Family history is one of the most well-established breast-cancer risk factors. The overall relative risk of breast cancer in a woman with a positive family history in a first-degree relative (mother, daughter, or sister) is  $> 1.7$  (Anderson *et al.*, 2008). Premenopausal onset of the disease in a first-degree relative is associated with a threefold increase in breast cancer risk, whereas postmenopausal diagnosis increases the relative risk by only 1.5. When the first-degree relative has bilateral disease, there is a fivefold increase in risk. Recent advances in molecular biological techniques have correlated certain inherited genes with the susceptibility to breast cancer.

### **2.2.4 Race**

Female breast cancer incidence rates vary considerably across racial and ethnic groups. The average annual age-adjusted incidence rate is 140.8 cases per 100000 among white women, 121.7 among African Americans, 97.2 among Asian Americans/Pacific Islanders, 89.8 in Hispanics, and 58 in American Indians/Alaska Natives in 2000 (Jatoi *et al.*, 2005). The lifestyle factors between populations can be attributed to the different risks of breast cancers. Probable reasons for the higher incidence rates in whites than in other racial and ethnic groups are the differences in

underlying reproductive risk factors (older age at first birth), use of hormone replacement therapy (HRT), and access to and use of screening. White women tend to have delayed child bearing, and more commonly use HRT. Mammography use for diagnosing the patient at an early stage is also higher in white than in African American women.

### **2.2.5 Hormonal and reproductive factors**

Hormonal and reproductive factors have long been recognized to be the important risk factors of breast cancer development. Bilateral prophylactic oophorectomy has a significant impact on breast cancer risk. The risk reduction will be greater than 50% if the oophorectomy is performed in women before age 40 compared to those after age 40 (Eisen *et al.*, 2005). This observation suggests a hormonal role in breast cancer etiology. Early onset of menarche (< 12 years old) has been associated with a modest increase in breast cancer risk (twofold or less). Women who undergo menopause before age 30 have a twofold reduction in breast cancer risk when compared with those who undergo menopause after age 55 (Hulka and Stark, 1995). It implies that the length of exposure time to cycling ovarian hormones is attributed to the risk of breast cancer. A first full-term pregnancy before age 30 appears to have a protective effect against breast cancer, whereas a late first full-term pregnancy or nulliparity may be associated with a higher risk. This is directly related to breast-feeding by which lactation delays the return of ovulation after pregnancy. Breast-feeding is associated with an increased prolactin which results in less estrogen exposure to the breast. Most epidemiologic evidence suggests that the reduction in risk associated with lactation is more pronounced for premenopausal than postmenopausal breast cancer, exhibiting the relative risk (RR) of 0.88 and 1.00, respectively (Martin *et al.*, 2005). Risk reduction has also been observed primarily with a longer duration of breast-feeding. Exogenous hormone uses whether hormonal contraceptives or hormone replacement therapy (HRT) have conferred the increased risk of breast cancer. The results indicated a slightly increased risk among current

users of oral contraceptives (OC) with the relative risk of 1.19, and the risk was declined in women who had discontinued use 5-10 years ago (Cibula *et al.*, 2010; Kahlenborn *et al.*, 2006). The small increase in breast cancer risk was likely associated with the new introduced low-dose regimens of OC. An elevation in breast cancer risk among menopausal women who received the hormone replacement therapy has also been observed. The use of estrogen plus progestin therapy was associated with a significantly increased risk (RR = 1.82), and the risk was higher (RR = 2.44) in women with prolonged use  $\geq 10$  years. In addition, women using only estrogen therapy showed a slightly increased risk (RR = 1.15) with no further evidence of increase seen for longer durations of use (Brinton *et al.*, 2008). Although the hormonal replacement therapy generally confers the increased risk in breast cancer, some clinicians have reconsidered whether the prohibition of external hormone use is always appropriate in postmenopausal women. Several studies reported a reduced mortality from breast cancer in women using hormone therapy before the disease diagnosis ( $\geq 5$  years) (Henderson *et al.*, 1991; Newcomb *et al.*, 2008; Toh *et al.*, 2010). The better quality of life due to menopausal symptoms, and the reduced risk of coronary artery disease and osteoporosis were also observed in those cases.

### **2.2.6 High-fat diet**

Diets that are high in fat have been associated with the increased risk for breast cancer. A meta-analysis of case-control and cohort studies showed a modest association between women who had diets high in animal fat from red meat and the breast cancer incidence (RR = 1.17). The risk of the disease was a 12% increase per 50 g increment of meat each day (Boyd *et al.*, 2003). Several hypotheses explained how consumption of high-fat diet could induce carcinogenesis such as growth-promoting hormones used in animal production, carcinogenic heterocyclic amines formed in cooking, and its specific fatty acid content (Mahoney *et al.*, 2008). In addition, women who take physical exercise such as walking for  $\geq 10$  hours per week

showed the greatest risk reduction in breast cancer (RR = 0.57) compared with those reporting no physical activity (Howard *et al.*, 2009).

### 2.2.7 Lifestyle factors

A direct association between alcohol consumption and the occurrence of breast cancer has been consistently observed in several epidemiologic studies. The increased breast cancer risk was varied between 13 and 35 percent, depending on the amount of alcohol intake. The relative risk was 1.35 among women who consumed alcohol > 35 g per day, and the modestly increased risk (RR = 1.05) was observed for an increment of 1 drink per day (Lew *et al.*, 2009). Several potential mechanisms for the alcohol and breast cancer association have been postulated. The role of alcohol as a mammary carcinogen was suggested by an evidence that it could affect cellular response and differentiation of breast tissue by stimulating estrogen signaling, and by down-regulating the tumor suppressor BRCA1 level (Fan *et al.*, 2000). By-products of alcohol metabolism such as acetaldehyde and reactive oxygen species, and the influences of alcohol on poor folate intake and its metabolism also led to DNA damage-induced carcinogenesis (Dumitrescu and Shields, 2005).

The relationship between smoking and the risk of breast cancer is still controversial. Some studies reported the lack of an association among smoking intensity, duration or age started smoking, and the increased breast cancer risk, while others highlighted a significantly increased risk in current smokers compared with never smokers (RR = 1.7) (Nagata *et al.*, 2006; Roddam *et al.*, 2007). Chemical carcinogens in cigarette smoke, which can cause mammary tumors in animals, have been detected in the breast fluid or tissue of smokers. Thus, it is biologically plausible that exposure to cigarette smoke is related to breast cancer. Certain genotype modifications such as *N*-acetyltransferase 2 (*NAT2*) have been suggested to increase the risk of breast cancer among individual women who smoke (Baumgartner *et al.*, 2009).



### **2.2.8 Environmental factors**

A number of environmental agents have been investigated in epidemiological studies with respect to their potential influences on breast cancer risk. Organochlorine pesticides such as dichlorodiphenyl trichloroethane (DDT), and polychlorinated biphenyls (PCBs) are lipid soluble that can accumulate in the food chain, and may be found in human adipose tissue, blood, and breast milk. Long-term exposure to these chemicals showed a positive correlation with breast cancer risk. Ionizing radiation is the most well established environmental risk factor for breast cancer. Increased rates of breast cancer have been found in laboratory animals and in human populations that have received relatively high doses of ionizing radiation. In addition, there are some evidences for supporting the hypothesis that delayed primary Epstein-Barr virus infection may contribute to the increased breast cancer risk (Coyle, 2004).

### **2.2.9 Genetic risk factors**

Approximately 5-10% of all breast cancer cases are related to a subset of hereditary (familial) breast cancers, while the other 90-95% of breast cancers are considered to be sporadic (non-familial). In recent years, better understanding of genetic predisposition to breast cancer has advanced significantly. The genetic factors associated with the increased breast cancer risk can be classified as (1) high-penetrance mutations that are rare in the population but associated with very high risk ( $RR \geq 5$ ) (2) moderate-penetrance variants associated with moderate increases in risk, and (3) low-penetrance mutations which are common and associated with small increases in risk ( $RR < 1.5$ ) (Mavaddat *et al.*, 2010). Some of the genetic factors that confer the increased risk in breast cancer are shown in Table 2.

## **2.3 Breast cancer susceptibility gene 1 (*BRCA1*)**

The most common cause of hereditary breast cancer is an inherited mutation in the breast cancer susceptibility genes 1 (*BRCA1*). Germline mutations in

*BRCA1* represent a predisposing genetic factor of 15-45% of hereditary breast cancers, and at least 80% of both breast and ovarian cancers (Miki *et al.*, 1994). *BRCA1* mutations also confer an increased risk for other hormone responsive cancers, such as uterine, cervical, and prostate cancers (Thompson *et al.*, 2002). The *BRCA1* gene, therefore, is identified as a tumor suppressor gene proposed by a two-hit hypothesis that the inactivation of two functional alleles of suppressor gene in normal cells leads to cancer development (Knudson, 1971). The cumulative incidence of breast cancer by age for *BRCA1* carries is summarized in Table 3.

**Table 2.** Summary of known breast cancer-predisposing genetic factors (Mavaddat *et al.*, 2010; Turnbull and Rahmann, 2008).

Genes	Locus	Syndrome associated with gene	Relative risk of breast cancer	Carrier frequency
<b>High-penetrance</b>				
<i>BRCA1</i>	17q21	Hereditary breast and ovarian cancer	5-45	0.1%
<i>BRCA2</i>	13q12.3	Fanconi anemia	9-21	0.1%
<i>TP53</i>	17p13.1	Li-Fraumeni syndrome	2-10	rare
<i>PTEN</i>	10q23.3	Cowden syndrome	2-10	rare
<b>Intermediate-penetrance</b>				
<i>ATM</i>	11q22.3	Ataxia-telangiectasia	2-3	0.4%
<i>CHEK2</i>	22q12.1		2-3	0.4%
<i>BRIP1</i>	17q22-q24	Fanconi anemia	2-3	0.1%
<i>PALB2</i>	16p12.1	Fanconi anemia	2-4	rare
<b>Low-penetrance</b>				
<i>FGFR2</i>	10q26		1.26	24-50%
<i>TOX3</i>	16q12		1.20	24-50%
<i>CASP8</i>	2q33		1.13	87%
<i>MAP3K1</i>	5q11		1.13	28-30%
<i>LSP1</i>	11p15		1.07	28-30%

**Table 3.** Cumulative incidences (standard error) of breast and ovarian cancers by age for *BRCA1* carries (Evans *et al.*, 2008).

Cancer risk to age	Breast cancer	Ovarian cancer
30	2%	0
40	16.5% (0.015)	3% (0.007)
50	48% (0.023)	21% (0.02)
60	55% (0.027)	40% (0.024)
70	68% (0.033)	60% (0.037)
80	79.5% (0.04)	65% (0.042)

### 2.3.1 Mutation spectrum of *BRCA1*

The *BRCA1* gene is identified based on its linkage to early onset familial breast and/or ovarian cancer syndromes (Hall *et al.*, 1990). The Breast Cancer Information Core (BIC) Database collects *BRCA1* mutation data in the human population. It indicates that there are more than 1600 distinct variants identified throughout the whole coding and non-coding regions of the *BRCA1* gene (Table 4) (BIC, 2010). Approximately 40% of all mutations are found in the exon 11 which is the largest exon in the *BRCA1* gene. The majority of known mutations in *BRCA1* results in the premature termination of protein caused by frameshift, nonsense, and splice site mutations (Szabo *et al.*, 2004). Frameshift mutation is the most common abnormality that accounts for 48.3% of all *BRCA1* variants, whereas missense and nonsense mutations are found in 29.6% and 10.9%, respectively (BIC, 2010). A previous study analyzed the *BRCA1* mutations in Thai patients from the central region of the country including Bangkok (Patmasiriwat *et al.*, 2002). It included a total of 23 patients with breast and/or ovarian cancers. Seventeen patients were from 12 families, having at least two affected cases of breast or ovarian cancers diagnosed at any age among first degree relatives. The other six out of 23 patients were isolated cases without family history of breast or ovarian cancer. PCR-based heteroduplex analysis

and DNA sequencing were used for screening *BRCA1* variants. Five distinct variants and their relative frequencies are shown in Table 5.

**Table 4.** Total number of mutations, polymorphisms, and variants from the Breast Cancer Information Core Database (BIC, 2010).

Exon type	Total number of entries	Distinct mutations, polymorphisms, and variants	Alterations reported only once
1	1	1	1
2	2125	50	33
3	167	43	26
5	420	44	21
6	183	28	16
7	159	34	18
8	145	30	18
9	137	18	8
10	42	16	11
11A	1098	209	111
11B	1082	212	117
11C	1385	217	112
11D	1445	201	103
12	108	40	23
13	409	46	27
14	106	26	17
15	214	41	20
16	534	78	45
17	150	48	25
18	218	48	20
19	115	30	18
20	1273	47	26
21	87	27	17
22	158	28	12
23	63	26	14
24	188	50	27
<b>total</b>	<b>12012</b>	<b>1638</b>	<b>886</b>

**Table 5.** Relative frequencies of *BRCA1* mutation in Thais.

Mutations	Relative frequencies
T320G	3/23 = 0.13
744ins20	1/23 = 0.04
3300delA	3/23 = 0.13
C3271G	2/23 = 0.08
IVS20+78 G>A	1/23 = 0.04

- T320G was a conservative missense mutation in exon 5 in which thymine at nucleotide 320 was changed to guanine. This mutation was identified in three unrelated Thai breast cancer patients, and no other mutations were found in the coding and non-coding regions of their *BRCA1* and *BRCA2* genes. Two of the patients had a family history of breast and ovarian cancers with onset age of 27 and 54 years, whereas the remaining patient was diagnosed with an isolated breast cancer with early onset of 25 years and one multiple myeloma case was found in her kindred. This mutation is probably a founder mutation in Thais which resulted in the substitution of aspartic acid with glutamic acid at position 67 (D67E). It is in the vicinity of Zn<sup>2+</sup>-binding site II, and is located in the second Zn<sup>2+</sup>-binding loop (residue 58-68) that forms a recognition interface with a ubiquitin-conjugating enzyme (Brzovic *et al.*, 2003). It is interesting to investigate the contribution of this mutation in the hereditary breast and ovarian cancers.

- 744ins20 was a frameshift mutation in exon 10 as a result of 20 base insertions (AGGGATGAAATCAGGAGCCA). It provided a stop codon at nucleotide 839, leading to a premature translational termination at codon 240. This mutation was identified in a single patient (42 years) with breast and ovarian cancers.

- 3300delA was a frameshift mutation in exon 11 whose adenine base at nucleotide 3300 was deleted. It introduced a stop codon at nucleotide 3300, and

resulted in a truncated BRCA1 protein of 1060 amino acids. This mutation was found in three patients from two apparently unrelated families. One patient revealed only 3300delA, while the other patients (daughter and mother) appeared to carry an additional *BRCA1* variant (C3271G).

- C3271G was a conservative missense mutation in exon 11 in which cytosine was replaced by guanine at nucleotide 3271. It caused the substitution of threonine with serine at residue 1051. This variant was a rare mutation identified in two patients from the same family (daughter and mother) that also carried 3300delA mutation.

- IVS20+78 G>A was a rare intronic variant in which guanine was replaced by adenine at upstream position 78 in intron 20. This mutation was only found in a single patient with age of onset of 60 years, and did not appear to segregate with disease.

## **2.4 Breast cancer susceptibility protein 1 (BRCA1)**

The BRCA1 protein is composed of 24 exons which only 22 ones encode for 1863 amino acid residues with a molecular weight of 220 kDa. It is characterized into 3 major domains, including (1) the N-terminal Zn<sup>2+</sup> finger RING domain (BRCA1 RING domain), (2) the large central segment with nuclear localization signal (NLS), and (3) the BRCA1 C-terminal domain (BRCT) (Figure 4). The BRCA1 protein plays an essential role in genomic stability maintenance associated with a number of cellular processes, including DNA repair, cell cycle checkpoint, transcriptional regulation, and protein ubiquitination (Huen *et al.*, 2010; O'Donovan and Livingston, 2010).

### **2.4.1 The BRCA1 RING finger domain**

The N-terminus of BRCA1 protein contains a RING finger domain which has the conservative sequences of cysteine and histidine residues (C<sub>3</sub>HC<sub>4</sub>)

necessary for the specific coordination with two  $Zn^{2+}$  ions. The solution structure of the BRCA1 RING domain revealed the existence of the antiparallel  $\alpha$ -helices at both ends, flanking the central RING motif (residues 24-64) characterized by a short antiparallel three-stranded  $\beta$ -sheets, two large  $Zn^{2+}$ -binding loops, and a central  $\alpha$ -helix (Figure 5) (Brzovic *et al.*, 2001). Two  $Zn^{2+}$ -binding sites are formed in an interleaved fashion in which the first and third pairs of cysteines (Cys24, Cys27, Cys44, and Cys47) form site I, and the second and fourth pairs of cysteines and a histidine (Cys39, His41, Cys61, and Cys64) form site II. It is an important domain since it might mediate a central role in macromolecular interactions to exert the tumor suppression function. The solution structure and yeast-two-hybrid studies revealed that BRCA1 RING domain preferentially formed a heterodimeric complex with another RING domain BARD1 (BRCA1-associated RING domain 1) through an extensive four-helix-bundle interface (Figure 5) (Brzovic *et al.*, 2001; Wu *et al.*, 1996). The binding interface is composed of residues 8-22 and 81-96 of BRCA1, and residues 36-48 and 101-116 of BARD1 which provide an extensive buried surface area of about 2200  $\text{\AA}^2$ . The BRCA1-BARD1 complex requires each other for their mutual stabilities, and they are co-localized in nuclear dots (sites in the nucleus concerned with transcription) during S phase of the cell cycle and in nuclear foci (site associated with repair of DNA caused by the damage agents or  $\gamma$ -irradiation) (Hashizume *et al.*, 2001). Of further interest is that the BRCA1-BARD1 complex has enzymatic activity of an E3 ubiquitin ligase that specifically transfers ubiquitin (a small peptide) to protein substrates that regulate some aspects of cell biology (Hashizume *et al.*, 2001; Xia *et al.*, 2003). Cancer-predisposing mutations in the  $Zn^{2+}$ -binding sites were demonstrated not only to alter  $Zn^{2+}$  affinity and native BRCA1 RING structure but also to abrogate the interaction with BARD1 and the E3 ligase activity (Morris *et al.*, 2006). The results supported an importance of  $Zn^{2+}$  as a structural component, playing critical roles in the stabilization and function of the BRCA1 RING domain.

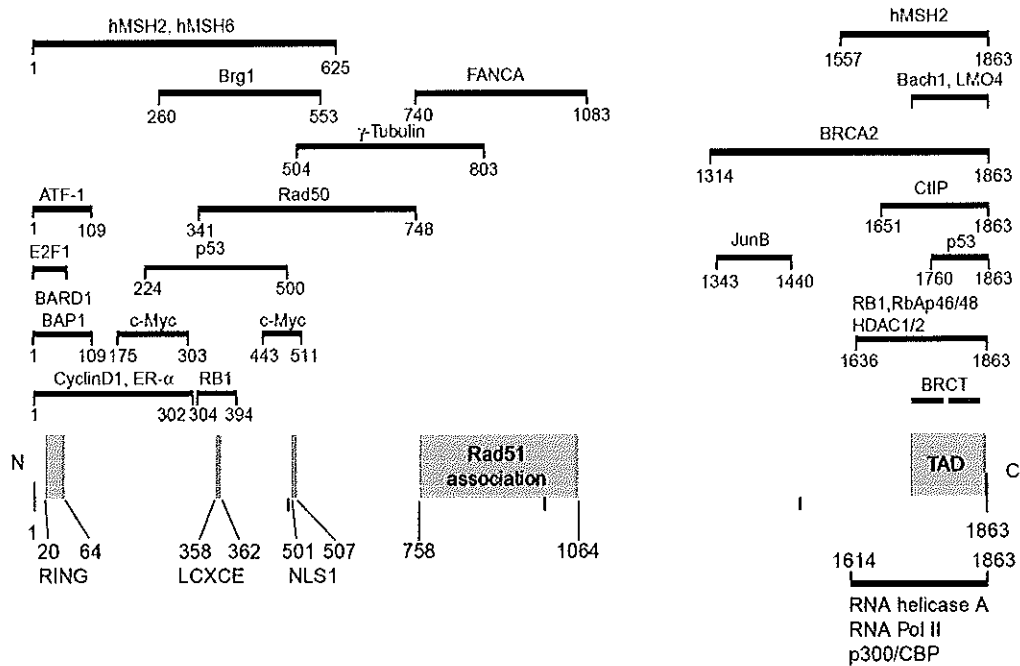


**Figure 4.** Schematic diagram of BRCA1 and its binding partners (Rosen *et al.*, 2003).

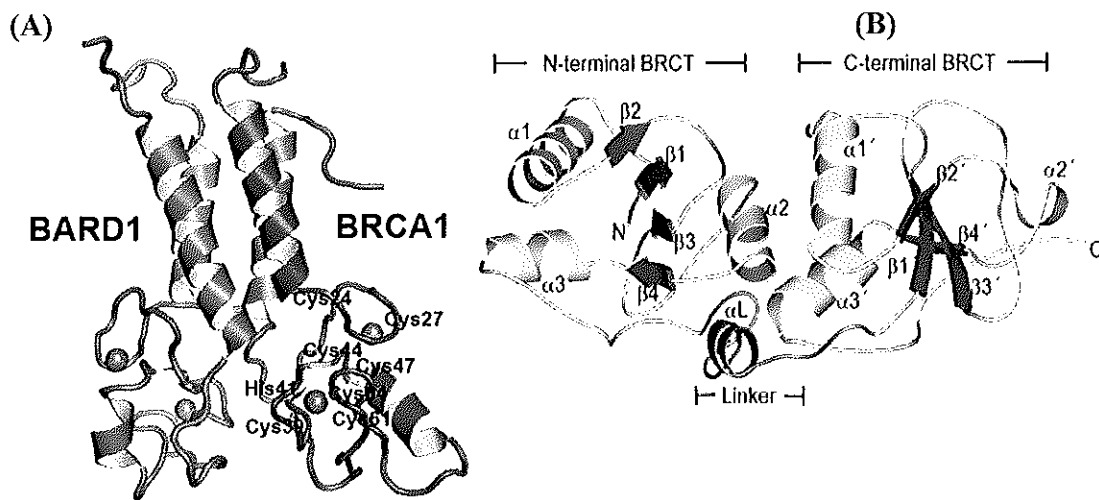


**Figure 5.** (A) Solution structure of the BRCA1-BARD1 RING complex. The spheres represent two Zn<sup>2+</sup> ions. Zn<sup>2+</sup>-ligating residues in site I and II of the BRCA1 RING domain are also indicated. The structure is generated with PyMOL software (<http://pymol.sourceforge.net>) based on the protein databank (PDB: 1JM7). (B) Crystal structure of the BRCA1-BRCT domain (PDB: 1JNX). The N-terminal and C-terminal BRCT repeats are joined through a linker in a head-to-tail fashion.



#### **2.4.2 The large central segment of BRCA1**

The central region of BRCA1 encompasses approximately 1500 residues that lack any substantial conserved sequence motifs. Biophysical characterization revealed that this domain was intrinsically disordered or natively unfolded at physiological conditions. This might potentially afford the BRCA1 central region as a long flexible scaffold, mediating interactions with DNA, and a number of other proteins involved in DNA damage response and repair (Mark *et al.*, 2005). The reported binding partners to the central region were c-Myc, RB, p53, FANCA, RAD50, RAD51, JunB, and BRCA2 (Rosen *et al.*, 2003). Recently, the BRCA1 central region has been shown to efficiently interact with p53, and stimulate p53-mediated DNA binding and transcriptional activities (Buck, 2008). The result also suggested that the BRCA1 central segment facilitated the induction of cell cycle arrest and apoptosis in response to DNA damage. However, it remains to be determined whether the interaction with p53 is critical for BRCA1 function since overexpression of BRCA1 is protective rather than a cause of apoptosis. Furthermore, the association between the central region of BRCA1 and PALB2 (partner and localizer of BRCA2, also known as FANCN) was observed primarily through apolar bonding between their respective coiled-coil domains (Sy *et al.*, 2009). PALB2 binds directly to BRCA1, and serves as the molecular scaffold in the formation of the BRCA1-PALB2-BRCA2 complex. BRCA1 mutations (L1407P and M1411T) identified in cancer patients were shown to disrupt the specific interaction between BRCA1 and PALB2, resulting in the defective homologous recombination (HR) repair and the compromised cell survival on DNA damage (Sy *et al.*, 2009). This suggested that impaired HR repair was one of the fundamental causes for genomic instability and tumorigenesis observed in patients, carrying *BRCA1*, *BRCA2*, or *PALB2* mutations.

#### **2.4.3 The BRCA1 C-terminal domain**

The C-terminal region (residues 1646-1863) of BRCA1 contains a tandem BRCT domain (BRCA1 carboxyl-terminal). Each BRCT domain (90-100

amino acids) is characterized by a central, parallel four-stranded  $\beta$ -sheet with a pair of  $\alpha$ -helices ( $\alpha 1$  and  $\alpha 3$ ) packed against one face, and a single  $\alpha$ -helix ( $\alpha 2$ ) packed against the opposite face of the sheet (Figure 5) (Williams *et al.*, 2001). The two BRCA1-BRCT repeats interact in a head-to-tail fashion in which bury about 1600  $\text{\AA}^2$  of hydrophobic, solvent accessible surface area in the interface with a 23-amino acid linker, connecting the two BRCT domains (Williams *et al.*, 2001). This domain serves as multipurpose protein-protein interaction modules that bind to other BRCT repeats or other protein domains with apparently unrelated structures (Watts and Brissett, 2010). Based on its physical interactions with other proteins, BRCA1 has been implicated in a wide array of cellular functions, including cell cycle regulation, DNA damage response, transcriptional regulation, replication and recombination, and higher chromatin hierarchical control (Starita and Parvin, 2003). Recently, the BRCA1-BRCT domain has been identified as a phosphopeptide recognition module, and is demonstrated to bind to the phosphorylated protein partners (BACH1 and CtIP, containing the consensus sequence pSer-X-X-Phe) involved mainly in the control of the G2/M phase checkpoint and DNA damage response (Varma *et al.*, 2005; Williams *et al.*, 2004). Several cancer-predisposing mutations in the BRCA1-BRCT domain resulted in the destabilization of the structural integrity at the BRCT active sites, and abolished their affinities to synthetic BACH1 and CtIP phosphopeptides (Rowling *et al.*, 2010). These findings provide the better understanding of the pathogenic BRCA1 mutations on functional mechanisms and tumorigenesis.

## **2.5 BRCA1 and its cellular function**

BRCA1 is a tumor susceptibility protein. It is essential for maintaining genomic stability, and is associated with a number of cellular processes, including cell cycle checkpoint control, transcriptional regulation, DNA repair, and protein

ubiquitination (Figure 6) (Huen *et al.*, 2010; O'Donovan and Livingston, 2010; Quinn *et al.*, 2009).

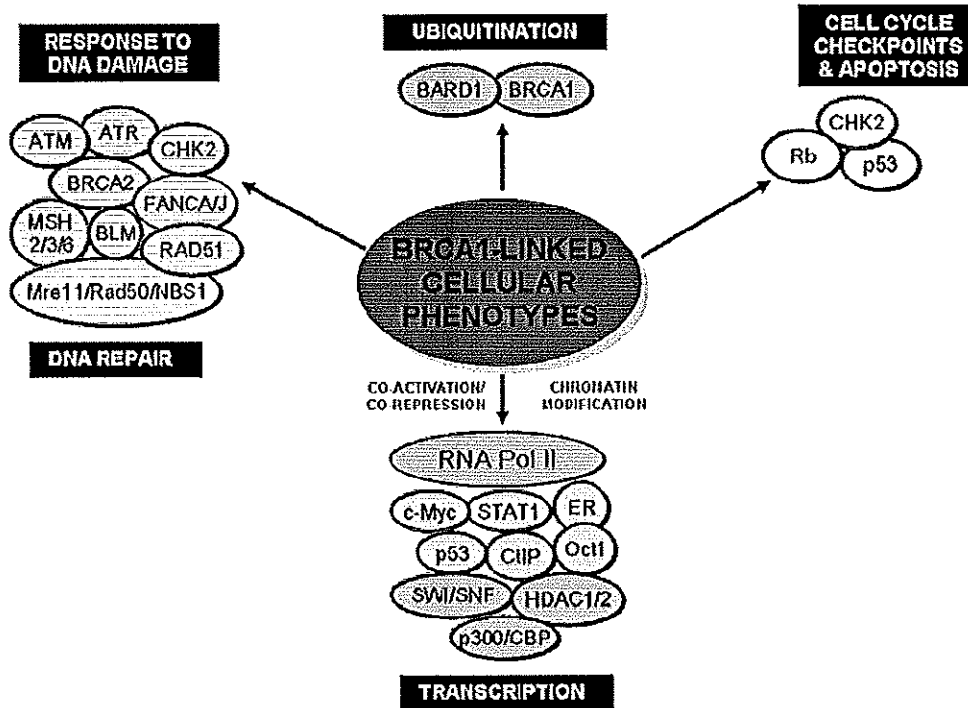


**Figure 6.** Multiple cellular functions of BRCA1 (Quinn *et al.*, 2009).

### 2.5.1 BRCA1 and cell growth control

Cell cycle checkpoints play an essential role in cell survival by preventing the propagation of DNA damage through cell cycle progression before DNA repair. Failure of cell cycle checkpoints can lead to the acquisition and accumulation of genetic alterations and chromosomal abnormalities. Several studies have recently revealed the implication of BRCA1 role in cell growth control (Figure 7) (Murray *et al.*, 2007). It was demonstrated that the BRCT domain of BRCA1 was associated with CtIP, which in turn interacted with the transcriptional corepressor CtBP (Li *et al.*, 1999). After DNA damage, BRCA1 was phosphorylated by ATM, and then the hyperphosphorylated BRCA1 no longer formed a complex with CtIP/CtBP and allowed BRCA1 to transactivate many cell cycle responsive genes.

BRCA1 was reported to stimulate the transcription of the *p21* gene, which resulted in cell cycle arrest at the G1/S phase boundary (Li *et al.*, 1999). It was also found to regulate *p21* transactivation and G1/S arrest in an indirect manner, involving ATM/ATR-directed phosphorylation of *p53* after ionizing radiation-induced DNA damage (Fabbro *et al.*, 2004). In addition, BRCA1 has been shown to have a direct transcriptional role in the regulation of the cyclin-dependent kinase inhibitor *p27*, resulting in S phase arrest (Williamson *et al.*, 2002).

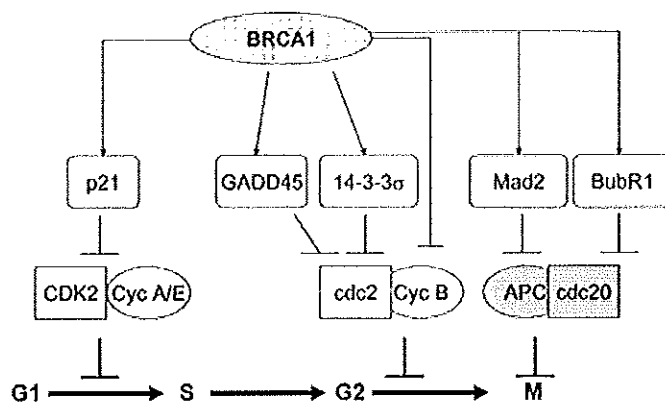


**Figure 7.** An overview of BRCA1-transcriptionally regulated targets and their impact on cell cycle progression. BRCA1 has been shown to transcriptionally up-regulate *p21* in a *p53*-independent manner to inhibit CDK2 and cyclin (Cyc) A/E, promoting transition from G1 to S phase. BRCA1 downstream signalling inhibits a number of proteins involved in transition from G2 to M phase and mitotic checkpoint activity (Murray *et al.*, 2007).

BRCA1 has also been demonstrated to be a transcriptional regulator of several genes associated with the regulation of the G2/M checkpoint. It has been reported to transcriptionally repress cyclin B that is responsible for activating *cdc2* (cell division cycle 2) kinase and mitotic entry (MacLachlan *et al.*, 2000). BRCA1 could transcriptionally regulate the chaperone protein 14-3-3σ which targeted and sequestered *cdc25C* in the cytoplasm, following DNA damage to prevent it from activating the cyclin B-*cdc2* kinase complex (Yarden *et al.*, 2002). Additionally,

BRCA1 stimulated the transcription of the *wee-1* kinase, leading to the inhibitory phosphorylation of *cdc2* and subsequent inhibition of cyclin B-*cdc2* kinase (Yarden *et al.*, 2002). However, the most compelling evidence for BRCA1 transcriptional regulation and G2/M cell cycle arrest came from its induction of GADD45 (growth-arrest and DNA-damage-inducible protein 45) that inhibited the activity of the cyclin B-*cdc2* complex by the sequestration of *cdc2* (Wang *et al.*, 1999). BRCA1 has also been shown to mediate the transactivation of MAD2 (mitotic arrest-deficient protein 2) (Wang *et al.*, 2004). MAD2 is a key component of the spindle assembly checkpoint, and inhibits the APC (anaphase-promoting complex). It is postulated that loss of transcriptionally active BRCA1 would down-regulate MAD2 expression, leading to loss of mitotic checkpoint activity and ultimately the higher levels of genomic instability found in BRCA1 mutant tumors (Wang *et al.*, 2004).

### **2.5.2 BRCA1 and transcriptional regulation**

BRCA1 has been implicated in the transcriptional regulation of several genes responsible for DNA damage. The ability of BRCA1 to act as either a co-activator or a co-repressor of transcription may involve in its ability to recruit the basal transcriptional machinery and other proteins that implicated in chromatin remodeling such as histone deacetylases or components of the SWI/SNF-related chromatin-remodeling complex (Mullan *et al.*, 2006). Transient transfection assays showed that the BRCA1-BRCT domain fused to a GAL4 DNA-binding domain could activate a reporter gene in both yeast and mammalian cells, suggesting that BRCA1 was a component of the core transcriptional machinery (Nadeau *et al.*, 2000; Ratanaphan *et al.*, 2009). Furthermore, germline mutations of this domain identified in patients with early onset breast and/or ovarian cancers were defective in the transcriptional activation, implicating that the ability of BRCA1 to regulate transcription was a key to its tumor suppressor activity (Nadeau *et al.*, 2000). The transcription function of BRCA1 was established by an association between the BRCA1-BRCT domain and RNA polymerase II in a large complex called RNA

polymerase II holoenzyme (Krum *et al.*, 2003). Previous studies using microarray technology showed that p53-responsive cell cycle progression inhibitors and stress-response factors such as p21, and GADD45, respectively are the target genes stimulated by BRCA1 overexpression (MacLachlan *et al.*, 2002). Further investigations revealed that BRCA1 participated in the stabilization of p53 in response to DNA damage, and served as a co-activator for p53 (Zhang *et al.*, 1998). The interaction of BRCA1 and p53 potentially resulted in the redirection of p53-mediated transactivation from proapoptotic targets to genes involved in DNA repair and cell cycle arrest (Zhang *et al.*, 1998). On the other hand, BRCA1 could repress the transcription of estrogen receptor  $\alpha$  (ER $\alpha$ ) and its downstream estrogen responsive genes (Fan *et al.*, 1999). The transcriptional repression activity of BRCA1 for ER $\alpha$  was occurred by the association of the N-terminus of BRCA1 (residues 1-300) with the C-terminal activation function (AF-2) of ER $\alpha$  (Fan *et al.*, 2001). Breast cancer-associated mutations of BRCA1 were found to abolish its ability to inhibit ER $\alpha$  activity (Fan *et al.*, 2001). The repression activity exerted by BRCA1 involved the ability of BRCA1 to down-regulate levels of the transcriptional coactivator p300, which has also been shown to interact with the AF-2 domain of ER $\alpha$  (Fan *et al.*, 2002). Ectopic expression of p300 could reverse BRCA1 inhibition of ER $\alpha$  transcription, suggesting that BRCA1 regulated the availability of p300 to compete for the AF-2 domain of ER $\alpha$  (Fan *et al.*, 2002). In addition, BRCA1 inhibited progesterone receptor (PR) activity, and blocked progesterone-stimulated gene expression and cell proliferation (Katiyar *et al.*, 2009). Further investigation revealed that BRCA1 overexpression could inhibit the recruitment of co-activators [steroid receptor co-activator 1 (SRC1), and amplified in breast cancer 1 (AIB1)], and enhanced the recruitment of a co-repressor [histone deacetylase 1 (HDAC1)] to the progesterone response elements (PRE) of c-Myc. Additionally, BRCA1 knockdown increased the abundance of AIB1, and decreased the abundance of HDAC1 at the c-Myc PRE. It suggested that BRCA1 inhibited progestin-stimulated PR activity by

preventing PR from its binding to the PRE, and then promoting the formation of the co-repressor complex rather than the coactivator complex (Katiyar *et al.*, 2009).

### 2.5.3 BRCA1 and DNA repair

Several lines of evidences indicated that BRCA1 was involved in DNA damage response and DNA repair by which, following DNA damage, BRCA1 was associated and co-localized with RAD51 at the damage-induced foci (Scully *et al.*, 1997). The DNA damage-induced foci, marked by the histone variant H2AX that was phosphorylated on Ser139 (known as  $\gamma$ H2AX), represent sites of DNA breaks (Rogakou *et al.*, 1998).  $\gamma$ H2AX is essential for the accumulation of numerous DNA damage repair factors, including BRCA1, at sites of DNA breaks, suggesting that  $\gamma$ H2AX is one of the initial recruiting factors for various checkpoint and DNA repair proteins to DNA breaks. The H2AX signaling cascade begins to emerge with the finding that MDC1 (mediator of DNA damage checkpoint 1) is the main downstream factor in the pathway, and is required for the damage-induced focal accumulation of a number of DNA damage repair factors at DNA breaks (Stucki *et al.*, 2005). MDC1 contains tandem BRCT domains that allow its direct interaction with phosphorylated  $\gamma$ H2AX. This event, in turn, results in BRCA1 accumulation and co-localization with other DNA repair proteins at sites of DNA damage through the interaction with RAP80 and phosphorylated Abraxas (Foulkes, 2010).

In eukaryotic cells, there are two primary mechanisms of DNA double-stranded breaks (DSBs) repair. Homologous recombination (HR) is the error-free process used in cells during the S and G2 phases of the cell cycle when sister chromatids are available as templates. Non-homologous end-joining (NHEJ) is a process of ligating DSB ends together without a homologous template. It is the predominant mechanism in cells during G0, G1, and early S phases of the cell progression, and is considered as an error-prone process (Yang and Xia, 2010). The significance of BRCA1 and HR was observed by the experiments that BRCA1-deficient mouse embryonic stem cells displayed a defective homologous repair of

chromosomal DSBs, and an increased frequency of non-homologous recombination (Snouwaert *et al.*, 1999). This impairment could be corrected by the reconstitution of wild-type BRCA1 (Snouwaert *et al.*, 1999). A role for BRCA1 in HR-mediated repair is involved in its stable complex formation with BRCA2, which has a well-defined role in HR through the direct interaction with RAD51 (Bhattacharyya *et al.*, 2000). RAD51 (the mammalian homolog of the *Escherichia coli* RecA protein) is a DNA recombinase that catalyzes strand exchange in an early step of HR (Baumann *et al.*, 1996). Recently, PALB2 (the partner and localizer of BRCA2) has been identified as the bridging factor required for the BRCA1-BRCA2 association (Rahman *et al.*, 2007). The BRCA1-PALB2 interaction was mediated by their respective coiled-coil domains, and was found to promote HR-mediated repair (Rahman *et al.*, 2007). Importantly, missense mutations identified in the PALB2-binding region on BRCA1 disrupted the specific interaction of BRCA1 with PALB2, and compromised DNA repair in a gene conversion assay (Sy *et al.*, 2009). Although these studies have revealed a molecular link between BRCA1 function and HR-mediated repair, the mechanism by which BRCA1 promotes HR through the PALB2-BRCA2-RAD51 axis remains unclear.

Alternatively to HR, there is a growing body of evidences, suggesting that a component of NHEJ is regulated by BRCA1. The exact role of BRCA1 in NHEJ, however, has not been well defined, and the studies have yielded, conflicting observations by which the different results may be the reflections of the different assays used to measure NHEJ and of the different sub-pathways of NHEJ (Zhang and Powell, 2005). In the NHEJ pathway, the DNA-dependent protein kinase catalytic subunit (DNA-PKcs) and a Ku heterodimer of Ku80 and Ku70 are recruited to the sites of DNA DSBs for preparing the DNA ends before the ligation by XRCC4 ligase IV. The most possible explanation for BRCA1 involved in NHEJ is its association with a NHEJ factor Ku80 (Chiba and Parvin, 2001; Wei *et al.*, 2008). Many studies provided the strong evidences that the NHEJ pathway was impaired, both *in vivo* and



*in vitro*, in BRCA1-deficient mouse embryonic fibroblasts and in the human breast cancer cell line HCC1937 which carries a homozygous mutation in the *BRCA1* gene (Bau *et al.*, 2004; Zhong *et al.*, 2002). It was also shown that the fidelity of NHEJ was severely decreased *in vitro* and *in vivo* in lymphoblastoid cell lines established from women, carrying a truncating BRCA1 mutation (Baldeyron *et al.*, 2002). In addition, a BRCA1 mutant (P142H) failed to associate with Ku80 and to restore resistance to irradiation in *BRCA1*-deficient cells (Wei *et al.*, 2008). These might provide a molecular basis of the involvement of BRCA1 in the NHEJ pathway of the DSB repair process.

#### 2.5.4 BRCA1 and protein ubiquitination

Protein ubiquitination is a form of post-translational modification. The process is responsible not only for traditionally targeting proteins for proteasome-dependent degradation but also for playing roles in diverse cellular pathways such as protein transport, and DNA repair (Figures 8 and 9) (Christensen and Klevit, 2009; Ohta and Fukuda, 2004). Ubiquitination is a multistep process initiated by an ATP-dependent activation through the formation of a thioester bond between the C-terminal glycine of ubiquitin and a cysteine residue of a ubiquitin-activating enzyme (E1). The ubiquitin is then transferred to the active cysteine site of a ubiquitin-conjugating enzyme (E2) by transesterification. Finally, ubiquitin is specifically attached to the  $\epsilon$ -amino group of a lysine on its protein substrates via an isopeptide bond mediated by a ubiquitin ligase (E3).

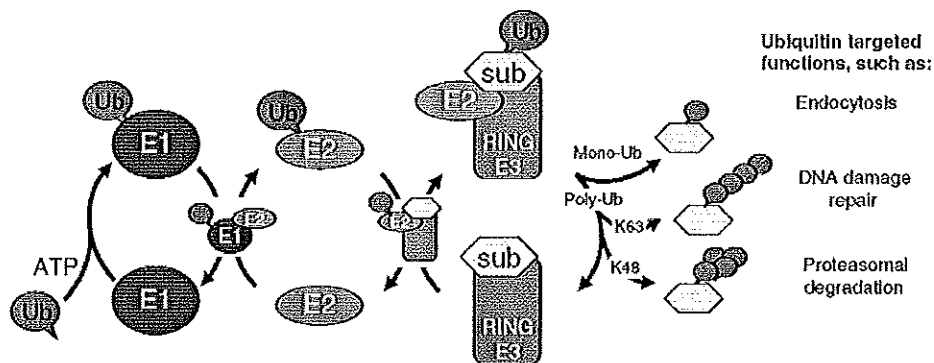
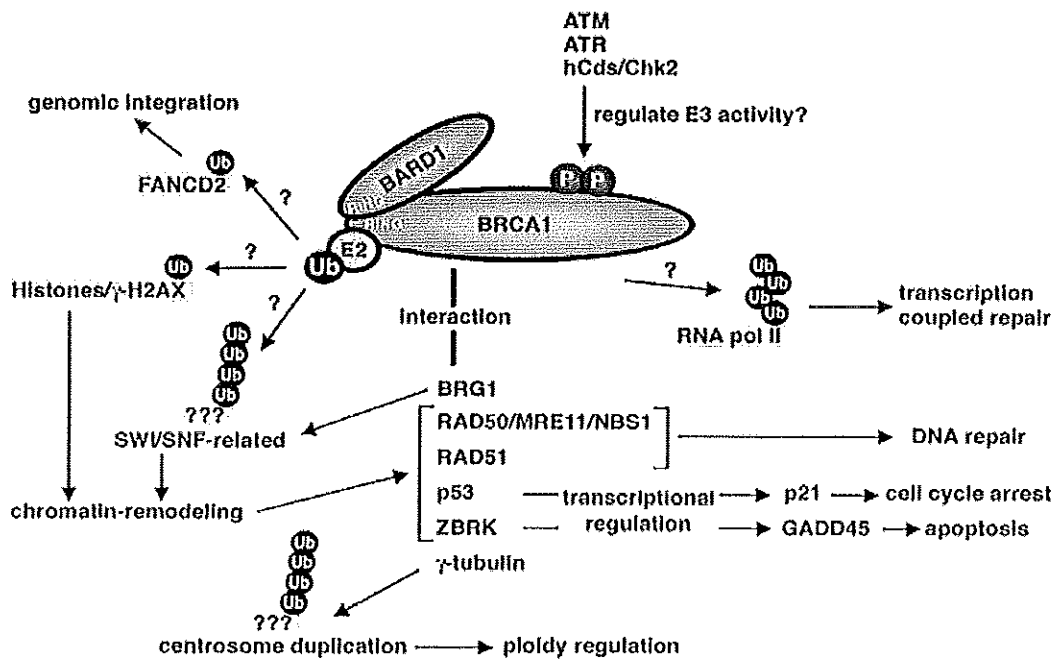


Figure 8. The ubiquitination pathway (Christensen and Klevit, 2009).



**Figure 9.** Potential roles for the BRCA1-BARD1 E3 ligase in the known BRCA1 functions. The BRCA1 protein interacts with a number of proteins, and functions in a variety of cellular processes, including DNA repair, cell cycle control, transcriptional regulation, apoptosis, and centrosome duplication. The BRCA1 E3 ligase activity may be involved in more than one of these known functions. P: phosphorylation. Ub: ubiquitin (Ohta and Fukuda, 2004).

The BRCA1 protein displays an E3 ubiquitin ligase activity through its RING domain, and this activity is enhanced when it heterodimerizes with the BARD1 RING domain (Xia *et al.*, 2003). Cancer-predisposing mutations in the BRCA1 RING domain inactivate the E3 ligase activity, and affect the other tumor suppressor activities of BRCA1 such as response to DNA damage, and ability to activate the G2-M checkpoint (Ruffner *et al.*, 2001). However, the substrate specificity of the BRCA1 E3 ligase activity and its biological relevance to tumor suppression function are still unknown. Putative substrates for the BRCA1-BARD1 RING complexes have recently emerged from *in vitro* and *in vivo* studies such as nucleosomal histones H2A and its variant H2AX, RNA polymerase II,  $\gamma$ -tubulin, nucleophosmin/B23, and estrogen

receptor  $\alpha$  (ER $\alpha$ ) (Eakin *et al.*, 2007; Horwitz *et al.*, 2007; Parvin, 2009; Sato *et al.*, 2004; Starita *et al.*, 2005; Thakar *et al.*, 2010). *In vitro* and *in vivo* studies indicated that the BRCA1-BARD1 complex was capable of autoubiquitination that paradoxically stabilized the protein complex, and that activated its *in vitro* E3 ligase activity (Chen *et al.*, 2002; Wu-Baer *et al.*, 2010). A special ubiquitin linkage through Lys6 (K6), instead of the conventional linkage through Lys48 (K48) that is commonly used when proteins are targeted for degradation, might be the key difference between protein destruction and stabilization of the polyubiquitinated BRCA1 (Nishikawa *et al.*, 2004). Thus, BRCA1-dependent ubiquitination is probably responsible for many cellular activities.

Several reports showed that the BRCA1 E3 ligase was capable of *in vitro* monoubiquitination of histones H2A and its variant H2AX (Thakar *et al.*, 2010). This implied a BRCA1 function in chromatin structure regulation in the context of transcriptional regulation and DNA repair. Hyperphosphorylated RNA polymerase II (RNAPII) at its carboxyl terminal domain (CTD), consisting of multiple repeats of the heptapeptides (YSPTSPS), is a generalized response to UV irradiation. It was also served as a substrate for the BRCA1-dependent ubiquitination that was proposed to facilitate BRCA1 function in DNA repair by inhibiting DNA transcription, and then recruiting other DNA repair proteins at a lesion (Starita *et al.*, 2005). Recently, It has found that the BRCA1-mediated ubiquitination of RNAPII prevented a stable association of some transcription factors (TFIIE and TFIIH) in the transcriptional preinitiation complex, and thus blocked the initiation of mRNA synthesis (Horwitz *et al.*, 2007). Ubiquitination of the preinitiation complex was not targeting proteins for degradation by proteasome but rather the ubiquitin moiety itself interfered with the assembly of basal transcription factors at the promoter (Horwitz *et al.*, 2007). Nucleoplasmin B23 and  $\gamma$ -tubulin were found to be the candidate substrates of the BRCA1 E3 ligase activity *in vivo* (Parvin, 2009; Sato *et al.*, 2004). Both proteins were present in centrosomes, and apparently were not targeted for degradation by BRCA1-

mediated modifications. The results suggested that ubiquitination of nucleoplasmin B23 and  $\gamma$ -tubulin played a vital role in regulating centrosome number and maintenance of genomic stability by unknown mechanisms. Recently, the BRCA1 protein has been shown to inhibit ER $\alpha$  transcriptional activity, and to induce repression of estrogen response genes and cell proliferation (Xu *et al.*, 2005). A potential explanation for the regulation of estrogen signaling by BRCA1 was the ER $\alpha$  ubiquitination and degradation mediated by the BRCA1 E3 ligase activity (Dizin and Irminger-Finger, 2010; Eakin *et al.*, 2007). Conversely, BRCA1-associated protein 1 (BAP1) is a deubiquitinating enzyme that can interact with the BRCA1 RING domain (Jensen *et al.*, 1998). It was shown that BAP1 inhibited the BRCA1 autoubiquitination, and the nucleophosmin/B23 ubiquitination mediated by the BRCA1 E3 ligase activity (Nishikawa *et al.*, 2009). Down-regulation of BAP1 in cells also resulted in the S phase retardation and ionizing irradiation hypersensitivity, a phenotype similar to BRCA1 deficiency, suggesting that the BRCA1-BARD1 complex and the BAP1 protein coordinately regulated ubiquitination during the DNA damage response and the cell cycle. Further elucidations are required for a better understanding of these biological significances.

Two RING finger E3 ubiquitin ligases (RNF8 and BRCA1) have recently been shown to sequentially recruit at the site of DNA damage (Foulkes, 2010). RNF8 catalyzes Lys63-linked polyubiquitin chains on H2AX (Wang and Elledge, 2007). Ubiquitinated H2AX then recruits the BRCA1-Abraxas-RAP80 complexes through the RAP80 ubiquitin-interacting motif (UIM) (Sobhian *et al.*, 2007). BRCA1 can form a RING heterodimer E3 ligase with BARD1, and is required for the recruitment of BRCA2 and RAD51 to damaged sites for homologous recombination (HR) repair (Ransburgh *et al.*, 2010). Many cancer-predisposing mutations in the BRCA1 RING domain, that inhibited the E3 ligase activity and its ability to accumulate at damaged sites, were defective in the homologous recombination that is critical for tumor suppression (Morris *et al.*, 2009; Ransburgh *et*

*al.*, 2010). Moreover, BRCA1 accumulation at the sites of DSBs occurred rapidly (within 20 s), and it required the RING structure (residue 1-200 of BRCA1) for the rapid recruitment with Ku80 at damaged sites in response to non-homologous end joining (Wei *et al.*, 2008). Missense mutations in the BRCA1 RING domain significantly reduced their accumulations at DSBs, and abolished the association with Ku80. Therefore, the loss of the BRCA1 E3 ligase activity rendered cancerous cells hypersensitive to DNA-damaging agents, indicating a significant role for ubiquitination in the DNA damage response and DNA repair activity (Ransburgh *et al.*, 2010; Ruffner *et al.*, 2001). Thus ubiquitination is involved in the key steps that properly conduct the DNA repair after DSBs. Targeting the ubiquitin-proteasome system is potentially exploited for both molecular diagnostics and novel strategies in cancer therapy (Ande *et al.*, 2009; Hoeller and Dikic, 2009).

## **2.6 Targeting the ubiquitin system**

Significant progress has been made in recent years in understanding not only the structure, function, and important regulatory roles of ubiquitin system but also the alterations of ubiquitin pathway in various human diseases including cancer. It is now possible to specifically target various components that involved in the ubiquitin pathway such as E3 ubiquitin ligases, deubiquitinases, and proteasome for potential anticancer therapies. Recently, proteasome inhibitors have been shown to inhibit nuclear foci formation of ubiquitin after exposures to ionizing radiation (IR) and chemotherapeutic agents (Mailand *et al.*, 2007; Takeshita *et al.*, 2009). It is possible that the inhibition of the 26S proteasome depletes the pool of the available nuclear ubiquitin because the undegraded polyubiquitinated proteins accumulate in the cytosol (Dantuma *et al.*, 2006). The depletion of the free nuclear ubiquitin results in the loss of nuclear foci formation of the conjugated ubiquitin accompanied by the loss of BRCA1- and 53BP1-induced nuclear foci formations (Mailand *et al.*, 2007).

This suggested the possibility that proteasome inhibitors might inhibit the DNA repair pathway and thereby have an additive or synergistic effect on cytotoxicity in response to IR and chemotherapeutic agents (Murakawa *et al.*, 2007; Takeshita *et al.*, 2009). Further investigations into the effectiveness of the combination between proteasome inhibitors and DNA damage-inducing agents are necessary for evaluating the treatment of breast cancer.

Developing the inhibitors for the ubiquitin-activating enzyme E1 is another plausible way of targeting ubiquitin in cancer. One such inhibitor developed recently is PYR41 which inhibits E1 enzyme and blocks the initiation of ubiquitination (Yang *et al.*, 2007). Previous studies have shown that it inhibits the degradation of p53, and exhibits the lower rate of transformed cell viability in a p53 dependent manner. However, more studies on this compound are needed to establish it as a potential anticancer drug (Yang *et al.*, 2007).

E3 ubiquitin ligases are a large family of proteins that are engaged in the regulation of the turnover and activity of many target proteins. Together with ubiquitin-activating enzyme E1 and ubiquitin-conjugating enzyme E2, E3 ubiquitin ligases specifically catalyze the ubiquitination of a variety of biologically significant protein substrates for either targeted degradation through the 26S proteasome or nonproteolytic regulation of their functions and subcellular localizations. E3 ubiquitin ligases, therefore, play an essential role in the regulation of many biological processes. Increasing amounts of evidences strongly suggest that the abnormal regulation of some E3 ligases is involved in cancer development. Furthermore, some E3 ubiquitin ligases are frequently overexpressed in human cancers that correlate well with the increased chemoresistance and poor clinic prognosis. E3 ubiquitin ligases, thus, offer a very attractive option for developing anticancer drugs. An interesting validated target would be Mdm2 (murine double minute 2), which is overexpressed in some human breast tumors (Bueso-Ramos *et al.*, 1996). It contains a p53-binding domain at the N-terminus and a RING domain at the C-terminus. The p53-binding

domain of Mdm2 or Hdm2 (human counterpart of Mdm2) binds to the tumor suppressor p53, whereas the RING domain acts as an E3 ubiquitin ligase to promote rapid degradation of p53 (Haupt *et al.*, 1997). Inhibition of MDM2, whether compounds that disrupt Hdm2-p53 binding (Nutlin and RITA) or those that inhibit Hdm2 E3 ligase (HLI98), resulted in the increased levels of p53, followed by transactivation of p53 downstream target genes and induction of growth arrest and apoptosis in breast tumors with wild-type p53 (Vassilev *et al.*, 2004; Yang *et al.*, 2005). Targeting the inhibitor of apoptosis protein (IAP) family is also of interest. IAP suppresses apoptosis by binding to and by inhibiting active caspase-3, -7, and -9 through its BIR (baculoviral IAP repeat) domains (Vaux and Silke, 2005). Furthermore, some IAP members have a RING finger domain at the C-terminus for the ubiquitination and degradation of caspases (Vaux and Silke, 2005). IAP, thus, has been a promising cancer target, using Smac peptide consisting of AVPI sequence or Smac mimic compounds that disrupt the IAP-caspase binding and that sensitize many human cancer cells to apoptosis induced by conventional cancer therapies both *in vitro* and *in vivo* (Oost *et al.*, 2004; Schimmer *et al.*, 2006). Additionally, IAPs have been shown to act as the ubiquitin ligases to promote the ubiquitination and degradation of caspase-3, -9, and Smac (Suzuki *et al.*, 2001). Targeting their ubiquitin ligases appear to be a feasible approach to increase the levels of caspases and Smac, thus inducing apoptosis in cancer cells or sensitizing cancer cells to conventional cancer therapies (Sun, 2006).

Removal of ubiquitin from the ubiquitinated proteins is an important regulatory step in the ubiquitin system. This process is mediated by the action of deubiquitylating enzymes (DUBs). Generally, DUBs, which are cysteine proteases, are divided into five sub families, including ubiquitin carboxy-terminal hydrolases (UCH), ubiquitin specific proteases (USP), ovarian tumor like proteases (OTU), JAMM/MPN metalloproteases, and Machado-Jacob-disease proteases (MJD) (Nijman *et al.*, 2005). Several deubiquitylating enzymes were shown to play the roles in

various events during the cell cycle progression, control of genomic instability, and the process of tumorigenesis (Ande *et al.*, 2009). Thus DUBs represent an alternative target in the ubiquitin system for cancer therapies. Small molecule inhibitors targeting ubiquitin C-terminal hydrolase (UCH-L1) have been identified using a high throughput screening, and are shown to induce the apoptotic cell death in lung tumor cell lines (Liu *et al.*, 2003). However, further studies need to be done for a better understanding of the DUBs in regard to their mechanisms of action and substrate recognition, and for evaluating the efficacy of these inhibitors in cancer therapy using *in vivo* model systems (Ande *et al.*, 2009).

## 2.7 Cisplatin

### 2.7.1 Introduction

Cisplatin [*cis*-diamminedichloroplatinum(II)] (Figure 10), a platinum-based anticancer drug, is widely used for the treatments against human testicular, ovarian, bladder, cervical, head and neck, oesophageal, and small cell lung cancers (Kelland, 2007; Muggia, 2009). The biological activity of cisplatin was discovered serendipitously in 1965 by Rosenberg and co-workers who studied the effects of electric fields on *E. coli* growth (Rosenberg *et al.*, 1965). The platinum complexes, which were the reaction products of platinum derived from the electrodes with ammonium chloride from the growth medium, were responsible for the inhibitory effects on bacterial cell division (Rosenberg *et al.*, 1969). Among the platinum complexes formed, cisplatin was identified as the most active compound with the antiproliferative property. Subsequently, cisplatin was developed into one of the most important anticancer drugs, and was approved by US Food and Drug Administration (FDA) in 1978. Cisplatin (Platinol<sup>®</sup> and Platinol-AQ<sup>®</sup>) is typically administered through intravenous route (IV) with a dosage ranging from 50-120 mg/m<sup>2</sup> once every 3-4 weeks (Brunton, 2006). After the injection of cisplatin, peak plasma drug occurs



immediately, and more than 90% of platinum are covalently bound to plasma proteins. Platinum concentrations are highest in liver, prostate, and kidney, somewhat lower in bladder, muscle, testicle, pancreas, and spleen, and lowest in bowel, adrenal, heart, lung, cerebrum, and cerebellum (Areberg *et al.*, 1999; Stewart *et al.*, 1982). Drug excretions are found in the urine (> 90%) and feces (10%) with the plasma elimination half-lives of 20-30 minutes in the initial phase, and of 30.5-107 h or possibly longer in the terminal phase (McEvoy *et al.*, 2009). Although cisplatin is an effective anticancer drug, it has several disadvantages including severe adverse effects such as nephrotoxicity, neurotoxicity, ototoxicity, and emetogenesis (Anderson *et al.*, 2002). Nephrotoxicity and emetogenesis can be alleviated by prehydration combined with the use of mannitol diuretics and serotonin receptor antagonists, respectively (Smith *et al.*, 1991). A number of protecting or rescue agents such as mesna, amifostine, thiosulfate, and diethyldithiocarbamate have been used for the reduction of cisplatin toxicity (Reedijk *et al.*, 1999).

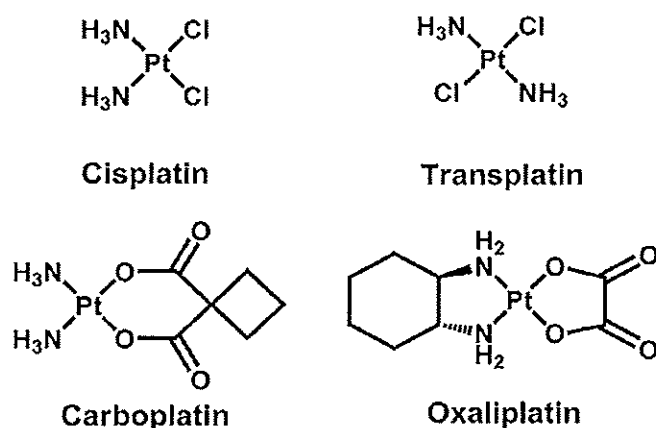


**Figure 10.** Molecular structures of the platinum complexes

The effectiveness of the anticancer drug cisplatin depends on the drug uptake, and its actual amount that reacts with the cellular targets. The physiological chloride concentration (100 mM) in blood and extracellular fluids is high enough to suppress cisplatin hydrolysis. Cisplatin can reach the surface of cells as a dichloro

form. Passive diffusion is believed to be the main mechanism that enables it to enter the cells. A study of drug uptake in the breast cancer MCF-7 cells was 0.197 ng platinum per mg protein with a high accumulation ratio of 5.04 between the intracellular and extracellular platinum concentrations after a 24 h continuous treatment with 0.1  $\mu\text{M}$  of cisplatin (Ghezzi *et al.*, 2004). The intracellular activation of cisplatin is required before it plays an important role in cytotoxicity, facilitating by the low cellular concentration of chloride ions about 2-3 mM. Chlorine groups of cisplatin are easily replaced by water molecules to allow the formation of aquated species in a stepwise manner (Figure 11). The hydration rate constant of monoqua form was faster than that of diaqua form ( $2.38 \times 10^{-5} \text{ s}^{-1}$  compared to  $1.4 \times 10^{-5} \text{ s}^{-1}$ ) (Cubo *et al.*, 2009). The aquated forms are more reactive to the cellular targets which contain the nucleophilic groups such as DNA and RNA at N7 position of guanine and adenine bases, and protein side-chains of cysteine, methionine, and histidine at sulfur and nitrogen atoms (Esteban-Fernández *et al.*, 2010).

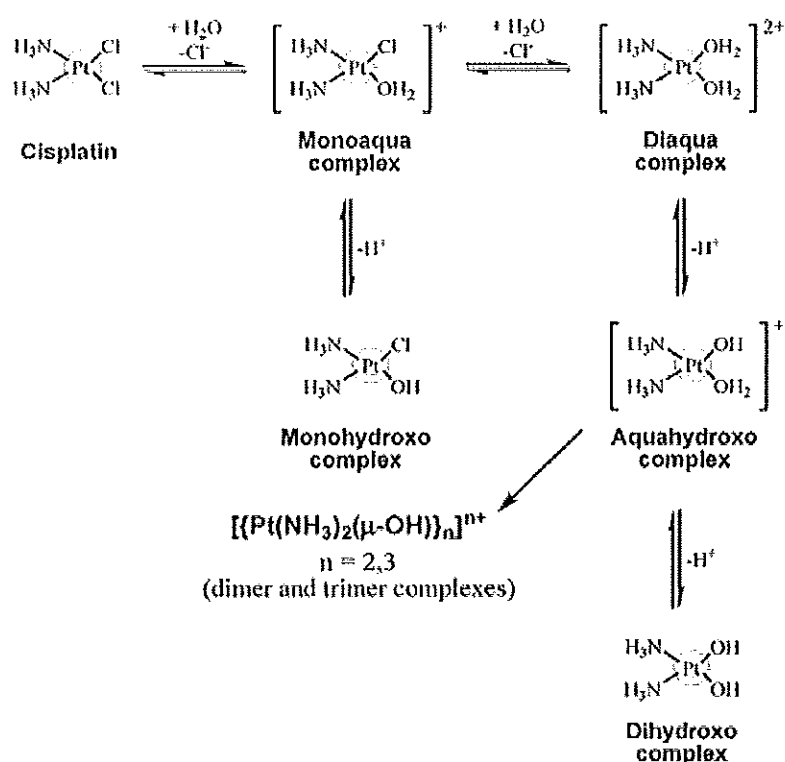
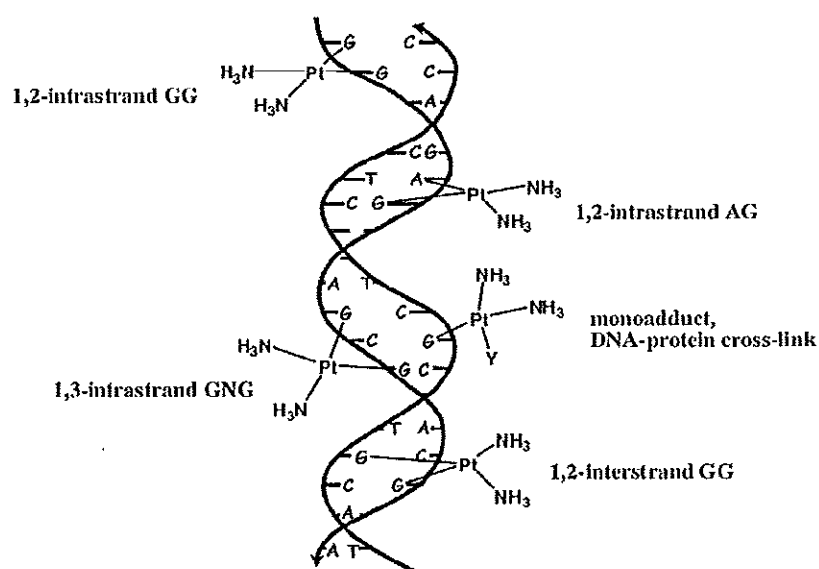


Figure 11. Hydrolysis of cisplatin (Esteban-Fernández *et al.*, 2010).

### 2.7.2 DNA adducts

The anticancer activity of cisplatin potentially results from the modification of DNA through covalent cross-linkings or platinum (Pt) -DNA adducts which account for 5-10% of all platinum adducts (Cepeda *et al.*, 2007). The DNA adducts interfere DNA replication and transcription, and ultimately lead to cancer cell death (Ahmad, 2010; Wang and Lippard, 2005). The N7 atoms of guanine and adenine bases are the putative platinum-binding sites, resulting in either monofunctional (via one leaving group) or bifunctional adducts (via two leaving groups) (Pizarro and Sadler, 2009). The predominant DNA adducts are the bifunctional forms, occurring on the same DNA strand so called intrastrand crosslinks. They involve the binding of platinum center to two adjacent bases; namely 1,2-intrastrand d(GpG) and d(ApG) crosslinks which account for 60-65% and 20-25% of all adducts, respectively. The 1,3-intrastrand d(GpNpG) crosslinks are approximately 2%, and the monofunctional adducts, occurring on guanine bases, are 2%. The interstrand crosslinks, which involve guanine bases on opposite DNA strands, are around 2% (Figure 12).



**Figure 12.** The formations of different cisplatin-modified DNA adducts (Pizarro and Sadler, 2009).

The consequences of cisplatin-modified DNA adducts are the bending and unwinding of DNA structures. Both 1,2-intrastrand d(GpG) and d(ApG) crosslinks unwind the synthetic DNA duplexes by 13° with a significant bend angle of 35° towards the major groove (Kartalou and Essigmann, 2001). The 1,3-intrastrand d(GpTpG) and the guanine interstrand adducts unwind the DNA helices by 23° and 79° with the bending of 35° and 45°, respectively. The predominant 1,2-intrastrand d(GpG) adduct presumably confers cisplatin cytotoxicity by which the DNA bending results in the widening and flattening of the minor groove. Some high mobility group (HMG) proteins specifically recognize this type of DNA adduct, and therefore may regulate the cellular processing of the platinated DNA (Ohndorf *et al.*, 1999). Two major mechanisms have been proposed for how HMG domain proteins can increase the sensitivity of cells to the anticancer drug cisplatin. The binding of HMG domain proteins to the DNA lesions protects the recognition of DNA repair proteins (referred to as the repair shielding model), and therefore the damaged DNAs still persist, and ultimately cause apoptosis (Huang *et al.*, 1994). Alternatively, the preferential bindings of HMG domain proteins and other nuclear proteins to DNA adducts rather than their natural binding sites can lead to the cellular stress and cell death (referred to as the hijack hypothesis) (Kartalou and Essigmann, 2001).

### **2.7.3 Effect of cisplatin on DNA replication and mutagenicity**

The inhibitory effect of cisplatin on DNA synthesis was subsequently observed after its discovery as the antiproliferative agent in *E. coli*, and this effect was believed to contribute to the cytotoxicity of cisplatin (Shimizu and Rosenberg, 1973). Cisplatin was shown to directly alter DNA synthesis below 5 µM in the inhibition of <sup>3</sup>H-thymidine incorporation into an acid-insoluble polymer in human amnion AV<sub>3</sub> cells (Harder and Rosenberg, 1970). *In vitro* platination of the *BRCA1* gene sequence by cisplatin revealed the complete inhibition of DNA amplification at 50 µM with about 2.5 platinum (Pt) atoms on DNA template (Ratanaphan *et al.*, 2005). The cisplatin-modified *BRCA1* protected a cleavage by some restriction endonucleases,

implying that cisplatin preferentially formed the 1,2-intrastrand d(GpG) crosslinks. In addition, cisplatin-induced inhibition of DNA replication occurred in African green monkey CV-1 cells transfected with SV40 chromosomal DNA (Ciccarelli *et al.*, 1985). A variety of cisplatin-DNA adducts that blocked DNA polymerases were more characterized. Most bifunctional adducts (intra- and interstrand crosslinks) effectively inhibited DNA polymerases, while monofunctional adducts seemed not to block the polymerases (Comess *et al.*, 1992). HIV-1 reverse transcriptase (RT) and T7 DNA polymerase strongly paused at a nucleotide, preceding the first guanine of 1,2-d(GpG) adduct, and at the positions opposite the two platinated guanines (Suo *et al.*, 1999). The binding affinity of HIV-1 RT on the cisplatin-modified DNA (10-20 nM) was similar to that of unmodified template (6-9 nM), whereas the cisplatin adduct moderately weakened the binding affinity of T7 DNA polymerase (12-115 nM) with a significantly slow rate of the next nucleotide incorporation. The nucleotide incorporation rate was slower when it was closer to the DNA adduct. It was suggested that cisplatin-modified DNA might cause misalignment of the twisted base pairs at the binding cleft of DNA polymerases, resulting in a significantly reduced rate of the protein conformational change before polymerization took place and then a replication arrest.

Several experiments have reported the ability of some DNA polymerases to synthesize DNA while ignoring various chemical lesions. This process is translesion synthesis or replication bypass, using specialized DNA polymerases which are less stringent than the major replicative DNA polymerases, and can accommodate damaged bases (Lehmann, 2005). Translesion synthesis through cisplatin-DNA adducts became interesting because of its correlation to drug sensitivity by which cisplatin-resistant cells exhibited more translesion synthesis than drug-sensitive cells (Hicks *et al.*, 2010). The process also conferred the mutagenic properties of cisplatin because of the nature of replication bypass which carried out error-prone DNA synthesis (Bassett *et al.*, 2004). The mutagenicity of cisplatin was

closely related to the evolution of resistance of cell lines against the drug. In particular, the cisplatin-resistant human ovarian carcinoma cell lines showed a 3-5 fold increase in the replicative bypass ability to proceed past a DNA adduct compared to their respective cisplatin-sensitive cells (Mamenta *et al.*, 1994).

Translesion synthesis of plasmid DNAs in *E. coli*, which contained cisplatin intrastrand d(GpG) and d(ApG) adducts, revealed the mutation frequencies of 1-2% occurred at the 5' base of the adducts (Bradley *et al.*, 1993; Burnouf *et al.*, 1990). Approximately 80% of the mutations were G→T and A→T transversions at the damaged sites, respectively (Figure 13). Alternatively, a part of human *H-ras* protooncogene, containing a cisplatin intrastrand d(GpG) adduct, was inserted into a single-stranded SV40-based shuttle vector able to replicate in simian COS7 cells. The observed mutation frequencies on codon 13 of *H-ras* gene were 21% by which the base substitutions occurred at one or both of the platinated guanines (Pillaire *et al.*, 1994). The single G→T transversion accounted for 65% of all mutations, and was located at the 3' base of the adduct. These findings might indicate differences in translesion synthesis by the prokaryotic and eukaryotic replication machineries.

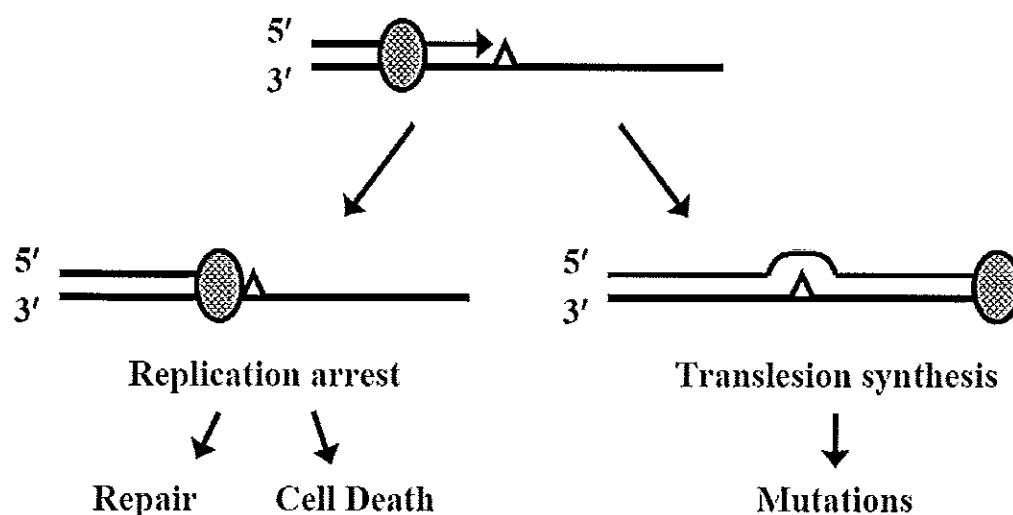


**Figure 13.** Effects of a bifunctional intrastrand cisplatin adduct on DNA replication.  $\Delta$  bifunctional cisplatin-d(GpG) adduct.  $\textcircled{\bullet}$  replicative complex (Bradley *et al.*, 1993).

A number of prokaryotic DNA polymerases to replicate linearized single-stranded M13 templates, carrying cisplatin intrastrand adducts at d(GpG), d(ApG), and d(GpCpG) were examined *in vitro* (Comess *et al.*, 1992). The intrastrand d(GpG) crosslink was found to be the most inhibitory lesion. Bacteriophage T7 polymerase and *E. coli* DNA polymerase I (Klenow fragment), which have low 3' to 5' exonuclease activity, exhibited a high frequency of translesion synthesis (25%) for the d(GpG) adduct. The extent of translesion syntheses for the d(ApG) and d(GpCpG) adducts were 19% and 25%, respectively. Bacteriophage T4 DNA polymerase and *E. coli* DNA polymerase III holoenzyme, which have a very active 3' to 5' exonuclease, were inhibited by all three types of cisplatin adducts, allowing only 2% translesion synthesis (Comess *et al.*, 1992). These results suggested that DNA polymerases with proofreading activity were halted at the damage site with an impaired elongation because they required an additional time frame for the proofreading exonuclease to remove the mutagenic bases substituted opposite the adducts (Belguise-Valladier *et al.*, 1994). Several experiments examined the abilities of eukaryotic DNA polymerases in translesion synthesis. Calf thymus DNA polymerases  $\alpha$ ,  $\beta$ ,  $\delta$ , and  $\epsilon$  were used to replicate a part of *H-ras* gene, bearing a single cisplatin-d(GpG) adduct (Hoffmann *et al.*, 1995). DNA polymerases  $\alpha$ ,  $\delta$  and  $\epsilon$  were blocked at the base preceding the lesion, while DNA polymerase  $\beta$  efficiently bypassed the cisplatin adduct. In addition, DNA polymerase  $\beta$  was able to elongate the arrested replication products of the other three DNA polymerases, showing its ability to compete with DNA polymerases  $\alpha$ ,  $\delta$ , and  $\epsilon$  at the stalled replication complex. Eukaryotic DNA polymerase  $\beta$  was the most inaccurate of the known DNA polymerases which exhibited the mutagenic replication frequency of 42% (Hoffmann *et al.*, 1996). Cells with the high level of DNA polymerase  $\beta$  acquired a spontaneous mutator phenotype. They displayed an increased genetic instability and a reduced sensitivity to alkylating chemotherapeutics such as cisplatin, melphalan, and mechlorethamine (Canitrot *et al.*, 1998). Error-prone translesion synthesis by DNA polymerase  $\beta$  overexpression was

one of the key determinants of tolerance phenotype and cancer predisposition during cancer treatment. Powerful replication bypass by DNA polymerase  $\eta$  was also observed in xeroderma pigmentosum cells by which functional pol  $\eta$  provided the cellular tolerance to cisplatin-induced damages (Albertella *et al.*, 2005).

#### 2.7.4 Repair of cisplatin-damaged DNA

Following cisplatin-induced DNA adducts, a number of cellular repair systems are responsible for recognizing and processing the removal of DNA damages. DNA repair pathways are related to drug sensitivity/tolerance and cell survival after chemotherapeutic treatments. The most important DNA repairs for cisplatin-DNA adducts are (1) nucleotide excision repair (2) mismatch repair, and (3) DNA recombination.

Nucleotide excision repair (NER) is a major process for removing platinum-damaged DNA. The process requires an ATP-dependent multiple protein complex that recognizes the bending induced on DNA by cisplatin. NER complex has a dual role that can unwind the DNA strands (helicase), and excise the damage strand (endonuclease) about 24-32 nucleotides in length, containing a platinum lesion. DNA resynthesis factors are recruited at the incised DNA, and employ the opposite strand as template to fill in the gap in concert with DNA ligases. There are two distinct sub-pathways of NER: transcription-coupled repair (TCR) and global genomic repair (GGR). TCR refers to the preferential repair of transcribed strands of RNA polymerase II-transcribed active gene, while GGR refers to repair throughout the genome (Shuck *et al.*, 2008). It suggested that the efficiently clinical response of human testicular cancer to cisplatin reflected its intrinsically low capacity for removal of cisplatin-DNA adducts, and low levels of the nucleotide-repair proteins XPA [xeroderma pigmentosum (XP) complementation group A], XPF (XP complementation group F), and ERCC1 (excision repair cross-complementing-1) (Welsh *et al.*, 2004). *Xeroderma pigmentosum* cell lines with defects in NER components were 5-10 fold more sensitive to cisplatin than normal cell (Furuta *et al.*,



2002). Greater levels of ERCC1 and XPAC mRNA, that implied an enhanced activity of DNA excision repair, were observed in ovarian cancer tissue of patients clinically resistant to cisplatin and other platinum-based drugs (Dabholkar *et al.*, 1994). Recently, the suppression of ERCC1 expression in the HeLa S3 cells by small interfering RNA (siRNA) led to a decrease in the repair activity of cisplatin-induced DNA damage along with a decrease in the cell viability against platinum-based drugs (Chang *et al.*, 2005).

Mismatch repair (MMR) is a repair process that acts during DNA replication to correct base misincorporation made by DNA polymerase. Several investigations showed that loss of MMR was closely correlated with cisplatin resistance. Human ovarian and colon carcinoma cell lines with known defects in mismatch repair (hMLH1 and hMSH6) resulted in the 1.5-4.8 fold increased cisplatin resistance, and the 2.5-6 fold increased replicative bypass of cisplatin adducts (Vaisman *et al.*, 1998). It was hypothesized that the repeated cycles of translesion synthesis past cisplatin-DNA adducts followed by removal of the newly synthesized DNA by an active mismatch repair system might trigger cell death. A recent study demonstrated the first finding of cisplatin-induced MMR-dependent apoptotic signaling (Topping *et al.*, 2009). Human endometrial carcinoma cell lines with wild-type copies of *MSH2* and *MSH6* showed cytochrome *c* relocalization to the cytoplasm beginning at 48 h after cells were treated with cisplatin. *MSH2*-proficient cells exhibited 2 and 17 fold increases, while *MSH6*-proficient cells presented 2.1 and 3.6 fold increases in the cytoplasmic cytochrome *c* at 48 and 72 h, respectively, compared with their deficient cells. In addition, cisplatin induced cleavage and activation of caspase-9 and caspase-3 in a *MSH2/MSH6*-dependent manner. These results implicated an intrinsic mitochondrial pro-death signaling as the mechanism of cisplatin-induced cell death in relation to MMR (Topping *et al.*, 2009).

Recombination pathway is also a repair system responsible for DNA damage induced by the anticancer drug cisplatin. Recombination-deficient *E. coli*

mutants were sensitive to cisplatin, exhibiting a decreased survival of four orders of magnitude in comparison with the parental strain at a cisplatin concentration of 75-80  $\mu\text{M}$  (Zdraveski *et al.*, 2000). Many recombination-deficient strains showed an equal sensitivity to the drug as the NER-deficient strains did. Double mutations in recombination and NER proteins were approximately 4-fold more sensitive to cisplatin than the corresponding single mutants, suggesting that recombination and NER pathways played the independent roles of each other in protecting cells from cisplatin-induced damage. Impaired recombination DNA repair in yeast and prostate cancer cell lines also showed an increased sensitivity to cisplatin (Wang *et al.*, 2005). Mutations of the homologous recombination repair (HR) pathway in mammalian cells resulted in an increased cisplatin sensitivity, while a knockout of the non-homologous endjoining repair (NHEJ) had no effect in cisplatin response (Raaphorst *et al.*, 2005). It indicated that DNA damage was affected differently by the various DNA repair pathways.

### **2.7.5 Effect of cisplatin on transcription inhibition**

Several investigations revealed the transcriptional inhibition on the DNA templates, containing the site-specific Pt-DNA adducts. The mammalian RNA polymerase II and *E. coli* RNA polymerase could not catalyze the transcriptional reactions when the DNA template strands carried the 1,2-intrastrand d(GpG) and d(ApG) adducts, whereas those polymerases could transcribed the complementary templates which there were no DNA lesions on the template strands (Corda *et al.*, 1991). Transcriptions of globally platinated DNA templates by SP6 and T7 RNA polymerases were also blocked primarily at 1,2-d(GpG) and d(ApG) Pt adducts, and to a lesser extent at the interstrand crosslink (Tornaletti, 2005). Bifunctional Pt-DNA adducts were much more effective at impeding transcription progression than monofunctional DNA adducts (Tornaletti, 2005). Moreover, cisplatin could cause a dose-dependent inhibition of mRNA synthesis. Treatment of human fibroblast cells with 50  $\mu\text{M}$  cisplatin for 24 h resulted in a 55% decrease in mRNA level and a

reduced expression of p21<sup>WAF1</sup> protein, suggesting that cisplatin inhibited the transcription of the p21<sup>WAF1</sup> gene (Ljungman *et al.*, 1999). A previous study have recently demonstrated that the platination of cisplatin on the *BRCA1* gene favorably formed the 1,2-intrastrand d(GpG) and d(ApG) adducts, and slightly caused the interstrand d(GpC) crosslink. These adduct formations dramatically inhibited a transcriptional transactivation of BRCA1 on the luciferase reporter gene transfected into MCF7 cells in a dose-dependent manner (Ratanaphan *et al.*, 2009). It suggested that transcription inhibition by cisplatin was a critical determinant in the pathway of cell-cycle arrest in G2 phase because cells could not synthesize the mRNA necessary to pass into mitosis, eventually leading to apoptosis. Possible mechanisms to explain this inhibitory process can be divided into three categories; (1) hijack of transcription factors (2) physical block of RNA polymerase, and (3) inhibition of chromatin remodeling (Figure 14) (Todd and Lippard, 2009).

A number of proteins have been identified to specifically recognize the distorted Pt-DNA adducts, including transcription factors. Upstream binding factor (UBF), a member of HMG-domain proteins, is a ribosomal RNA transcription factor. hUBF can bind the 1,2-intrastrand adducts with a high  $K_d$  of 60 pM (Jordan and Carmo-Fonseca, 1998). Treatment of DNA with cisplatin inhibited ribosomal RNA synthesis by competing hUBF from its natural binding site in an *in vitro* transcription assay (Zhai *et al.*, 1998). The TATA-binding protein (TBP) is a critical transcription factor for all three mammalian RNA polymerases (pol I, II, and III). TBP binding to the DNA duplex, containing the 1,2-intrastrand d(GpG) crosslink of cisplatin, was similar to that of TATA-promoter binding in terms of structural and affinity aspects with  $K_d$  of 0.3 nM (Jung *et al.*, 2001). It was shown that TBP interacted directly with cisplatin-damaged DNA, and the introduction of exogenous cisplatin-modified DNA into HeLa whole cell extract could sequester TBP and inhibited transcription 3- to 4-fold more than undamaged DNA (Vichi *et al.*, 1997). Collectively, failure of RNA synthesis resulted from the hijack of transcription factors by Pt-DNA adducts,

preventing the assembly of transcriptional elongation complexes at their normal promoter sequence and inhibiting the transcriptional process.

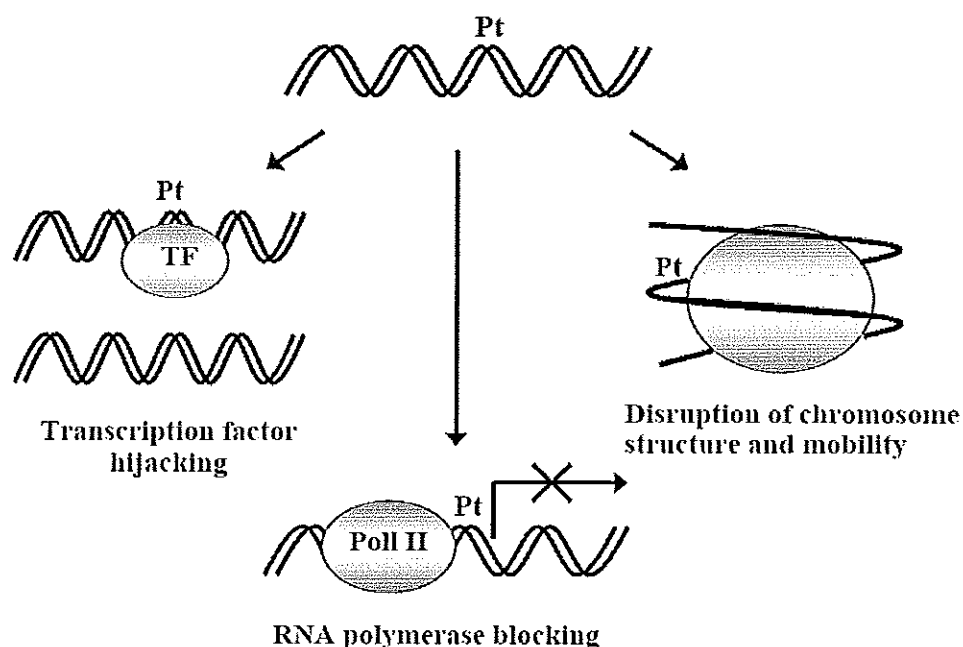


**Figure 14.** Possible mechanisms of transcription inhibition by cisplatin-DNA adduct (Todd and Lippard, 2009).

Recently, the processing of site-specific Pt-DNA crosslinks in mammalian cells was investigated (Ang *et al.*, 2010). Site-specifically platinated oligonucleotides, containing 1,2-d(GpG) and 1,3-d(GpTpG) adducts, were inserted into an expression vector between its promoter and luciferase reporter gene. Transcription inhibitions by blocking passage of the RNA polymerase complex through the 1,2-d(GpG) and 1,3-d(GpTpG) adducts were 50% and 37.7% of unplatinated controls for vectors, respectively. An X-ray crystal structure of RNA polymerase II stalled at the 1,2-intrastrand d(GpG) crosslink explained a physical block of transcription by cisplatin-DNA adduct (Damsma *et al.*, 2007). In this structure, the cisplatin dinucleotide lesion was favorably located downstream of Pol II in the position +2/+3 because it could not rotate properly to allow its entry into the enzyme active site. Attempts to place the cisplatin lesion in the active site (positions

+1/+2 and -1/+1) of the elongation complex apparently caused the backtracking of the polymerase so that the DNA lesion was occupied at position +2/+3. The physical translocation barrier resulted in the inhibition of transcription by Pol II stalling at damage site. RNA extension assays demonstrated that the elongation complex was impeded after AMP misincorporation opposite the first guanine of the cisplatin adduct. This terminal incorporation was a slow process, and it arose from nontemplated synthesis, according to an A-rule known for DNA polymerase (Strauss, 1991). Transcription could occur again as an artificial bypass if the DNA lesion was beyond the translocation barrier at position -2/-1, upstream of the Pol II active site.

Disruption of chromatin remodeling was another mechanism by which cisplatin adduct could interfere the transcription. Nucleosomal DNA, containing the 1,2-d(GpG) or 1,3-d(GpTpG) intrastrand crosslinks, enforced a characteristic rotational positioning of the DNA around the histone octamer such that the Pt adduct faced inward towards the histone core (Ober and Lippard, 2008). Increased solvent accessibility of the platinated DNA strand was observed, and it might be caused by a structural perturbation in proximity of the DNA lesion. In addition, the nucleosomes treated with cisplatin exhibited a significant decrease in the heat-induced mobility (Wu *et al.*, 2008). These effects suggested that cisplatin assault could inhibit transcription by altering the native nucleosomal organization, and limiting the nucleosomal sliding that protected an access of the RNA polymerase to the DNA template.

#### **2.7.6 Effect of cisplatin on protein translation**

Based on the results from *in vitro* translation studies, it was shown that the kinetics of cisplatin-induced inhibition of protein synthesis were biphasic, having an initial rate before a sudden decrease similar to those of inhibition caused by traditional inhibitors of translational initiation (Rosenberg and Sato, 1993). Analysis of cisplatin-inhibited reactions in sucrose density gradients presented a decrease in polyribosome formation. These results suggested that the maximum and half

inhibitions of translation activity were 110 and 23  $\mu\text{M}$  of cisplatin, respectively (Sato *et al.*, 1996). The inhibited protein synthesis by cisplatin occurred at the initiation step by which cisplatin prevented the joining of the 60S ribosomal subunit to the 48S preinitiation subunit (Rosenberg and Sato, 1993). The arrest of protein translation caused by cisplatin was also found in the elongation stage. Complete translation inhibition occurred within 10 min when the reactions contained 250  $\mu\text{M}$  of cisplatin (Heminger *et al.*, 1997). Agarose gel electrophoresis and northern blot analysis indicated that mRNA and rRNA in rabbit reticulocyte lysates were crosslinked to form high molecular weight adducts upon RNA extraction from polyribosomes of cisplatin-treated reactions. The arrest of elongation by cisplatin appeared to be due to the accumulation of cisplatin-RNA adducts at critical sites. The intramolecular mRNA crosslinks within hairpin loops or other secondary structures at the 5'-untranslated region or the open-reading frame may be the important events that inhibited the translocation ability of the ribosomes (Hostetter *et al.*, 2009). Diethyldithiocarbamate (DDTC), which reduces the cytotoxicity of cisplatin *in vivo*, was capable of partially reversing the inhibited protein synthesis by cisplatin. Cisplatin inhibited protein synthesis by 71% in the absence of DDTC, whereas the drug inhibited protein synthesis by only 37% in the presence of 1 mM DDTC added at the beginning of the incubation (Heminger *et al.*, 1997).

### **2.7.7 Effect of cisplatin on cell death pathways**

It is generally accepted that cisplatin confers cytotoxic processes that finally resulted in the triggering of cell death through apoptosis (programmed cell death) or necrosis (Figure 15) (Cepeda *et al.*, 2007). Necrosis is characterized by a cytosolic swelling and disruption of plasma membrane before organelle breakdown and cell lysis. The release of intracellular content after plasma membrane rupture is the cause of inflammation. In contrast to necrosis, apoptosis exhibits the different morphology and mechanistic aspects. It undergoes cell blebbing, cell shrinkage, chromatin condensation, and DNA fragmentation. The resultant apoptotic bodies are

eliminated by phagocytosis. The mode of cell death induced by cisplatin is dependent on drug concentration (Fuertes *et al.*, 2003).

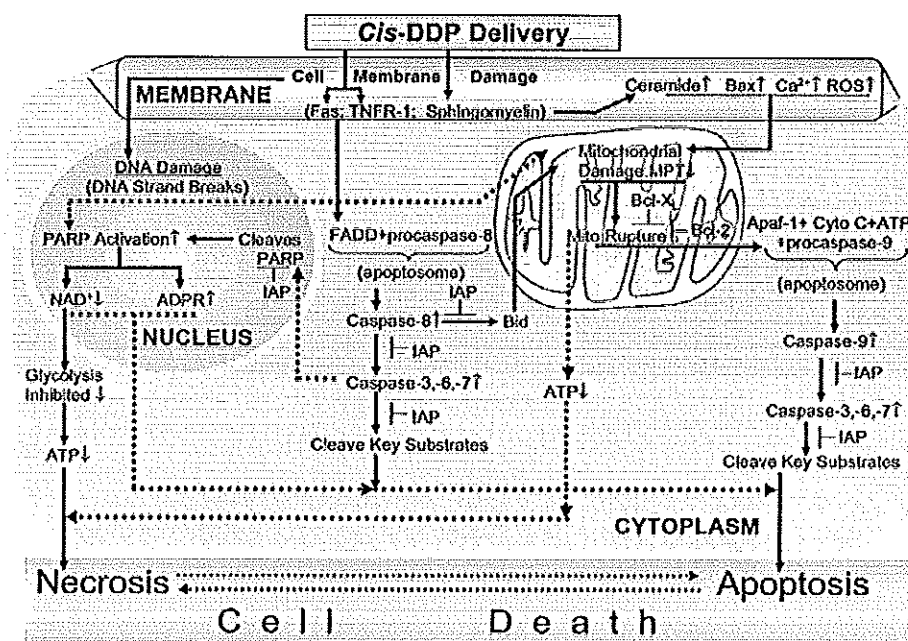


**Figure 15.** Schematic overview of the proposed biochemical pathways of cell death induced by cisplatin. Interconnections between apoptosis and necrosis are shown as discontinuous arrows. DNA strand breaks activate poly(ADP-ribose) polymerase (PARP), which cleaves NAD<sup>+</sup> and provokes the formation of poly(ADP-ribose) moieties (ADPR). It results in a decrease in NAD<sup>+</sup> with a concomitant fall of glycolysis and ATP depletion so that cell death by necrosis takes place. In contrast, if ATP levels are enough to sustain survival, caspase-3, -6, and -7 cleaves PARP, necrosis is blocked, and apoptosis occurs. If PARP cleavage is prevented, the continued activity of PARP leads to enhancement of both necrosis and apoptosis. Apaf-1, apoptotic protease-activating factor-1; Bid, a type of proapoptotic protein; FAAD, Fas-associated death domain; Fas, cell surface membrane receptor; TNFR-1, tumor necrosis factor receptor; IAP, inhibitor of apoptosis; ROS, reactive oxygen species; MPT, mitochondrial permeability transition; Cyto *c*, cytochrome *c*; Bax, Bcl-2-associated X protein; Bcl-2, B-cell lymphoma 2 (Cepeda *et al.*, 2007).

Primary cultures of mouse proximal tubular cells led to necrotic cell death over a few hours after treatment with a high concentration of cisplatin (800  $\mu\text{M}$ ), whereas cells underwent apoptosis, following exposure to a much lower concentration (8  $\mu\text{M}$ ) of the drug over several days (Lieberthal *et al.*, 1996). Excessive DNA damage caused by the anticancer agents induces the activation of poly(ADP-ribose) polymerase-1 (PARP-1). PARP-1 cleaves a glycolytic coenzyme  $\text{NAD}^+$  (nicotinamideadenine dinucleotide), and transfers ADP-ribose moieties to nuclear proteins. Depletion of  $\text{NAD}^+$  inhibits glycolytic production of ATP (ATP depletion), which results in necrotic cell death (Herceg *et al.*, 2001). In general, apoptosis is the main response of cancer cells to the most chemotherapeutic drugs. It is an ATP-dependent process in combination of the specific degradation of a series of proteins by cysteine aspartate-specific proteinases (caspase). Intracellular ATP level is important to dictate whether cisplatin or other anticancer drugs induce cell death by necrosis or apoptosis (Eguchi *et al.*, 1997; Leist *et al.*, 1997), and the interconnections of both processes are shown in Figure 15.

Cisplatin-induced DNA damage causes a fall in the mitochondrial permeability transition (MPT) (Custódio *et al.*, 2009). The altered MPT affords factors that facilitate the rupture of mitochondria such as reactive oxygen species, Bax, and  $\text{Ca}^{2+}$ , resulting in the releases of cytochrome *c* and procaspase-9 (Kroemer *et al.*, 1997). Those two proteins bind to cytosolic Apaf-1 and ATP in an apoptosome complex, leading to the activation of caspase-9. Activated caspase-9 causes the activation of caspase-3, -6, and -7 with the subsequent cleavage of key substrates (Reed, 2002). The final outcome is the formation of apoptotic bodies. A previous study demonstrated that cisplatin significantly inhibited the growth of cervical cancer HeLa cells in a dose- and time-dependent manner (Liu *et al.*, 2008). Flow cytometry and Hoechst 33258 staining showed that cisplatin inhibited HeLa cells through apoptosis. Western-blot analyses revealed the high expression levels of p53, p21, and Bax proteins, whereas Bcl-2 protein expression was not affected. It was confirmed



that apoptosis induced by cisplatin was occurred through the restoration of p53 function and Bax up-regulation. In addition, cleavage and activation of apoptosis-related regulators such as caspase-3, -8, and -9, and p53, were found in human bladder cancer cells treated with cisplatin (Konstantakou *et al.*, 2009). Semi-quantitative RT-PCR also revealed that the cells underwent cisplatin-induced apoptosis by the up-regulation of pro-apoptotic genes (*Bik*, *Bim*, *Fas*, *FasL*, *TRAIL*, and *caspase-10*), and the down-regulation of anti-apoptotic genes (*Bcl-2* and *FAP-1*) in p53-dependent and p53-independent responses. Alternative pathways of cisplatin-induced apoptosis may be initiated by an injury of phospholipids of the cell membrane, which triggers the sphingomyelin-ceramide signaling system of cell death (Noda *et al.*, 2001). Cisplatin also induces apoptosis through death receptors by which the drug increases the expression of Fas receptor and Fas ligand (Mansouri *et al.*, 2003). The formation of an apoptosome complex between Fas-associated death domain (FADD) and procaspase-8 activates caspase-8. Then active caspase-8 activates the caspase-3, -6, and -7 that finally cleaves key substrates, and the cell is digested through apoptosis. Caspase-8 may also activate the proapoptotic protein Bid that triggers the apoptotic cell death through the mitochondrial pathway.

#### 2.7.8 Protein adducts

The interaction of cisplatin with proteins is of particular significance, and it is believed to play an important role in drug distribution and inactivation responsible for determining its efficacy and toxicity (Casini *et al.*, 2008; Sun *et al.*, 2009; Timerbaev *et al.*, 2006). Intriguingly, the protein adducts affect some crucial aspects of protein structures and functions (Table 6). For instance, the platination of human serum albumin caused the partial unfolding of protein structure at high drug concentration, and induced intermolecular crosslinks possibly at Cys34 and/or Met298 via bifunctional adducts or via NH<sub>3</sub> release (Ivanov *et al.*, 1998; Neault and Tajmir-Riahi, 1998). Myoglobin, a small protein, which contains a heme group necessary for the oxygen transport in skeletal muscles and myocardial cells,

intramolecularly formed mono- and bi-functional adducts with cisplatin. Its putative platinum-binding sites were His116 and His119 (Zhao and King, 2010). A number of intramolecular crosslinks were also occurred in ubiquitin adducts (Casini *et al.*, 2009). The loss of activity in protein aggregation prevention of the C-terminal heat shock protein 90 was reported as the consequence of cisplatin binding but it did not exhibit any conformational change (Ishidaa *et al.*, 2008).

**Table 6.** Summary of the consequences of protein adducts by cisplatin.

Protein	Method	Protein conc. (M)	Drug conc. (M)	Incubation condition	Consequence
albumin (Neault and Tajmir-Riahi, 1998)	UV-vis FT-IR	$3 \times 10^{-4}$	$1 \times 10^{-7}$ - $1 \times 10^{-4}$	phosphate buffer pH 6.8-7.4, 25 mM NaCl, 37°C 2 h	- binding constant $8.52 \times 10^2 \text{ M}^{-1}$ - secondary structural changes
cytochrome <i>c</i> (Zhao and King, 2009)	ESI-MS	$1 \times 10^{-4}$	$4 \times 10^{-4}$ - $1.6 \times 10^{-3}$	5 mM $\text{NH}_4\text{OAc}$ pH 6.8, 37°C 24 h	- monoadduct at Met 65
hCtr1 (Crider <i>et al.</i> , 2010)	LC-MS	$8 \times 10^{-4}$	$8 \times 10^{-4}$	23.8 mM carbonate, 100 mM NaCl, 1.13 mM phosphate pH 7.4, 37°C 24 h	- intramolecular crosslinks through replacing of all platinum ligands by three Mets and an amide nitrogen of peptide backbone
lysozyme (Casini <i>et al.</i> , 2007)	ESI-MS X-ray crystallography	$1 \times 10^{-4}$	$3 \times 10^{-4}$	25 mM ammonium carbonate pH 7.4, 37°C 72 h	- monofunctional adduct at His 15
Hsp90 (Ishidaa <i>et al.</i> , 2008)	CD UV-vis	$5 \times 10^{-3}$ - $1.1 \times 10^{-6}$	$11 \times 10^{-6}$ - $2 \times 10^{-3}$	50 mM HEPES pH 7.4, 25°C	- dimer formation - inhibited aggregation prevention of HSP90C - altered secondary structure of HSP90N - increased protease resistance of HSP90N

Protein	Method	Protein conc. (M)	Drug conc. (M)	Incubation condition	Consequence
$\gamma$ -globulin (Chen <i>et al.</i> , 1994)	gel filtration- photometry	$1.9 \times 10^{-5}$	$1 \times 10^{-1}$ - 1.4	50 mM phosphate buffer, 100 mM NaCl pH 7.4, 37°C 14 d	- 12.4 mol platinum per a protein (30-fold excess of cisplatin) - protein precipitation
Na,K-ATPase (Neault <i>et al.</i> , 2001)	UV-vis FT-IR	$1 \times 10^{-4}$ - $1 \times 10^{-3}$	$1 \times 10^{-7}$ - $1 \times 10^{-3}$	25 mM Tris pH 7.5, 100 mM NaCl, 2 mM MgCl <sub>2</sub> , 2 mM ATP, 1 mM ouabain, 37°C 2 h	- binding constant $1.93 \times 10^4 \text{ M}^{-1}$ - secondary structural changes
transferrin (Cox <i>et al.</i> , 1999)	<sup>13</sup> C, <sup>15</sup> N NMR	$3 \times 10^{-4}$	$3 \times 10^{-4}$	100 mM KCl, 90% H <sub>2</sub> O/10% D <sub>2</sub> O pH 6.7, 37°C 24 h	- monofunctional adduct at Met256 or Met499 - unaffected conformational change
ubiquitin (Casini <i>et al.</i> , 2009)	ESI-MS	$1 \times 10^{-3}$ - $2 \times 10^{-3}$	$1 \times 10^{-3}$ - $2 \times 10^{-3}$	10 mM phosphate buffer pH 6.4, 37°C 24 h	- four distinct adducts: [Pt(Ub)(NH <sub>3</sub> ) <sub>2</sub> Cl], [Pt(Ub)(NH <sub>3</sub> ) <sub>2</sub> H <sub>2</sub> O], [Pt(Ub)(NH <sub>3</sub> ) <sub>2</sub> ], and [Pt(Ub)(NH <sub>3</sub> )]
urease (Du <i>et al.</i> , 1999)	CD DSC	$25 \times 10^{-8}$ - $9.2 \times 10^{-7}$	$8 \times 10^{-4}$ - $4 \times 10^{-3}$	HEPES pH 7.0, 4°C 24 h	- secondary structural change - reduced denaturation temperature - urease inactive

Intriguingly, cisplatin can cause the structural perturbation of a synthetic peptide containing a Zn<sup>2+</sup> finger domain. The platinum coordination to Zn<sup>2+</sup>-binding sites resulted in Zn<sup>2+</sup> ejection and subsequently loss of protein tertiary structure, implying the inhibition of critically biological functions regulated by Zn<sup>2+</sup> finger protein. Such a mechanism has been discussed in the apoptosis process mediated by the interaction of cisplatin and platinum-based compounds with Zn<sup>2+</sup>

finger transcriptional factors (Bose *et al.*, 2005). Likewise, the nucleocapsid Zn<sup>2+</sup> finger NCp7 protein, a protein required for the recognition and packaging of viral RNA, was attracted by some platinum compounds, thereby inhibiting its nucleic acid binding and preventing the viral infectivity (de Paula *et al.*, 2009; Musah, 2004). The Zn<sup>2+</sup> finger protein, therefore, is a potential target for platinum compounds in medicinal application.

## 2.8 Dysfunctional BRCA1 as a therapeutic strategy

The goal of all therapies aimed at eradicating cancer is to selectively destroy cancer cells while sparing normal tissue. Most chemotherapeutic or radiotherapeutic agents function by damaging DNA or interfering with DNA replication. The cellular responses to DNA damage, especially related to repair or tolerance of the damage as well as the activation of apoptosis, are thus critical factors in determining the effectiveness of most cancer therapies (Figure 16) (Ashworth, 2008). Recently, rapid advances in molecular biology have significantly contributed to identify and to understand the roles of key proteins in DNA damage response pathways. It is reasonable to assume that the effectiveness of the conventional cancer therapy can potentially be enhanced by modulating the cellular response to DNA damage perhaps through manipulating genes or proteins related to DNA repair, cell cycle checkpoint control, damage tolerance or apoptosis (Amir *et al.*, 2010; Helleday *et al.*, 2008; Lieberman, 2008; Powell and Bindra, 2009; Zhu *et al.*, 2009). It also improves the therapeutic ratio for cancer treatment by selectively sensitizing cancer cells relative to normal tissues. The DNA repair activity of the cell is an important determinant of cell sensitivity to the anticancer agents. In fact, it has been reported that resistance to DNA-damaging agents can be associated with the increased cellular repair activities, while defects in DNA repair pathways result in hypersensitivity to these agents (Kelley and Fishel, 2008; Quinn *et al.*, 2003; Quinn *et al.*, 2009). The

importance of DNA repair in cancer treatment is based on the following considerations: (1) most chemotherapeutic agents, including ionizing radiations, cause DNA damage, and their effects are influenced by the efficiency of DNA repair pathways (2) somatic or inherited mutations in DNA repair genes have been described in cancers, determining a selective loss of function that can be exploited to obtain the anticancer selectivity. In fact, cancerous cells will rely much more than normal cells on the remaining functional DNA repair mechanisms, and targeting of these pathways could have an advantage impact (3) an increased level of DNA repair proteins has been correlated with resistance to the anticancer agents, and (4) the unravelling of the DNA repair pathways and the definition of their molecular partners have provided available potentially druggable targets suitable for the identification of new anticancer therapies or for the enhanced antitumor activity of DNA-damaging agents (Damia and D'Incalci, 2007; Price and Monteiro, 2010).

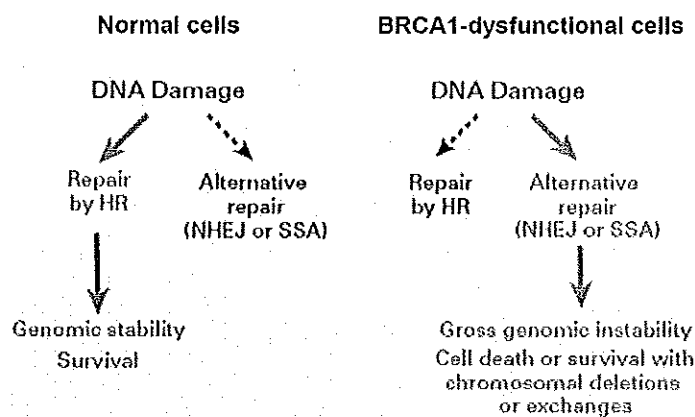


**Figure 16.** Loss of functional BRCA1 affects the choice of DNA double-strand break (DSB) repair pathway. DNA DSBs are repaired in normal cells, in part, by the homologous recombination (HR)-based mechanisms. The functional BRCA1 protein is required for efficient repair by HR and genomic stability. In the absence of BRCA1, alternative repair pathways such as nonhomologous end-joining (NHEJ) and single-strand annealing (SSA) are used, leading to cell death or survival with genomic damage (Ashworth, 2008).

Recently, a novel approach for cancer therapy involves alterations to the DNA repair processes by which the cancerous cells with dysfunctional DNA repair pathways accumulate high levels of DNA damage that eventually result in major genomic instability and cell death (Amir *et al.*, 2010; Helleday *et al.*, 2008; Lieberman, 2008; Powell and Bindra, 2009; Zhu *et al.*, 2009). In particular, several lines of evidences demonstrated that cancerous cells with BRCA1 inactivation had a defect in DNA repair of double strand breaks (DSBs) (Figure 17) (Farmer *et al.*, 2005; Kennedy *et al.*, 2004; Litman *et al.*, 2008). The DNA-damaging agents, that generate DSBs and require the BRCA1-mediated DNA repair, would be beneficial for treatment of such cancer cells. As described earlier, the extensive investigations have examined the relevance of the BRCA1-mediated ubiquitination to DNA repair function. Mutations in the BRCA1 RING domain resulted in loss of the E3 ubiquitin ligase activity, and conferred hypersensitivity of the cancerous cells to DNA-damaged chemotherapy and  $\gamma$ -irradiation (Ransburgh *et al.*, 2010; Ruffer *et al.*, 2001; Wei *et al.*, 2008).

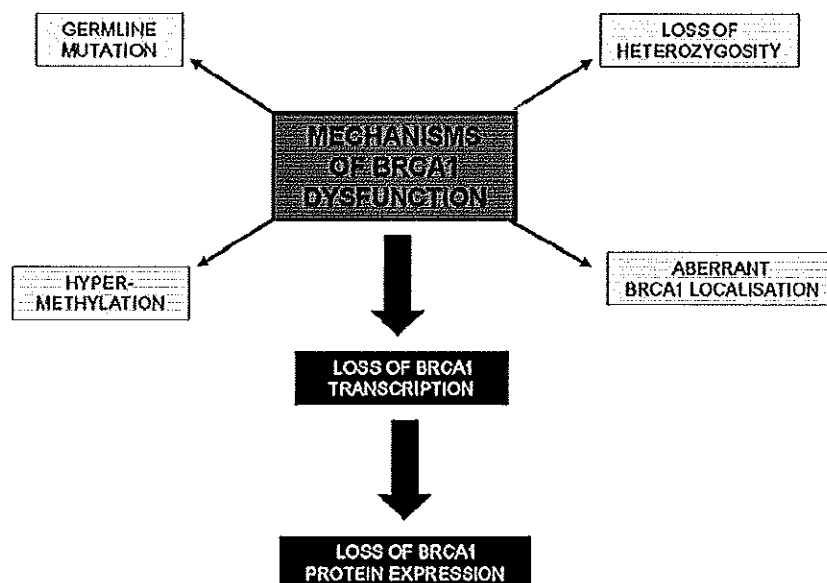


**Figure 17.** Potential mechanisms of BRCA1 dysfunction. It results in loss of BRCA1 associated transcriptional control and reduced BRCA1 protein expression (Quinn *et al.*, 2009).

### **2.8.1 Targeting BRCA1 for the anticancer platinum-based drugs for cancer therapy**

Preclinical and clinical studies have recently gained much attention on taking advantage of the inherent weakness of the BRCA1 dysfunction in cancer cells that increases their sensitivity to DNA-damaging agents such as platinum agents (Figure 18) (Ashworth, 2008; Quinn *et al.*, 2009; Tassone *et al.*, 2009). It was initially reported that overexpression of BRCA1 in the human breast cancer MCF7 cell line resulted in an increased resistance to cisplatin (Husain *et al.*, 1998). Furthermore, antisense or siRNA-based inhibition of endogenous BRCA1 expression promoted the increased sensitivity to cisplatin that was associated with the decreased DNA repair by NER and the increased apoptosis (Lafarge *et al.*, 2001; Quinn *et al.*, 2003). This suggests that the reduced BRCA1 expression observed in sporadic cancers may also be exploited for DNA damage-based chemotherapy (James *et al.*, 2007; Quinn *et al.*, 2009). Similarly, BRCA1-deficient mouse embryonic stem cells displayed defective DNA repair and a 100-fold increased sensitivity to the alkylating agent mitomycin C and cisplatin than those containing wild-type BRCA1 (Bhattacharyya *et al.*, 2000; Moynahan *et al.*, 2001). This sensitivity was reversed upon the correction of BRCA1 mutation in mouse embryonic fibroblast cells with a disrupted BRCA1 (Fedier *et al.*, 2003). The human breast cancer HCC1937 cell line derived from a patient with a BRCA1 mutation were significantly more sensitive to cisplatin (Tassone *et al.*, 2003). Recent studies have emphasized the potential of using BRCA1 dysfunction to predict response to therapy. It was demonstrated that inhibition of poly(ADP-ribose) polymerase (PARP) enzymatic activity could selectively target BRCA-mutant cells, sensitizing them to persistent DNA double-strand breaks and ultimately apoptosis (Farmer *et al.*, 2005; Fong *et al.*, 2009). PARP1 is a key enzyme in the repair of DNA single stranded breaks (SSBs) and its inhibition results in unrepaired SSBs, giving rise to DSBs when encountered by a replication fork during DNA replication. The inability of BRCA1-deficient cells to repair the indirectly induced DSBs results in a

specific sensitivity to PARP inhibition (Tutt *et al.*, 2010). Reconstitution of BRCA1 in the cells via transfection undoubtedly gained the BRCA1 functions, and resulted in a reduced level of cancer cell death, following treatment with cisplatin or other DNA damaging agents (Quinn *et al.*, 2003). Moreover, the recent evidences have revealed the implication of BRCA1 in cisplatin-resistant breast and ovarian cancer cell lines. These cells acquired the resistance to DNA-damaging agents mediated by the secondary mutation in *BRCA1*. This mutation restored the BRCA1 protein expression and function in DNA repair, causing the cancer cells to become more tolerant to cisplatin (Swisher *et al.*, 2008; Tassone *et al.*, 2003; Wang and Figg, 2008).

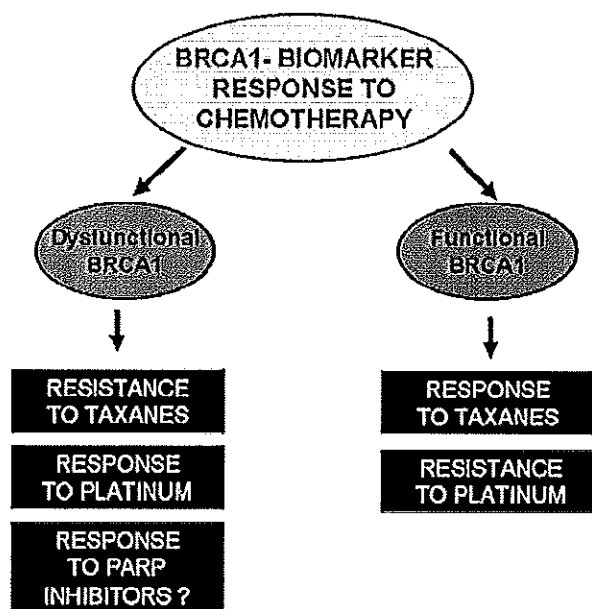


**Figure 18.** The potential role of BRCA1 in response to chemotherapy. Loss of BRCA1 function results in the enhanced sensitivity to platinum agents and potentially PARP inhibitor therapy and the reduced response to taxane based chemotherapy (Quinn *et al.*, 2009).

Recently, a number of clinical studies have examined the utilization of BRCA1 dysfunction in response to DNA-damaging drug cisplatin. Pathologic complete response (pCR) and excellent compliance were observed in nine (90%) out



of 10 breast cancer patients with *BRCA1* mutations after cisplatin chemotherapy every 3 weeks for four cycles (Byrski *et al.*, 2009). Irrespective of the *BRCA1* status, eighteen (64%) of 28 triple-negative breast cancer patients also had a good clinical response to neoadjuvant therapy with cisplatin (Silver *et al.*, 2010). Factors associated with a good cisplatin response included young age, low *BRCA1* mRNA expression, *BRCA1* promoter methylation, p53 mutations, and a gene expression signature of the activity of E2F3. Additionally, the significant benefits of the pathological response and overall survival rate from cisplatin-based chemotherapy were extended to the *BRCA1*-associated bladder, ovarian, and non-small cell lung (NSCL) cancers patients (Font *et al.*, 2010; Quinn *et al.*, 2007; Taron *et al.*, 2004). Table 7 is additionally represented the pathological complete response in breast cancer patients after the cisplatin-based therapy. It suggests that patients with *BRCA1* dysfunction gain more benefit from treatments which exert their effects by causing DNA damage (Figure 16). Therefore, targeting the *BRCA1* RING domain through the disruption of the  $Zn^{2+}$  coordination sites and the E3 ubiquitin ligase activity by cisplatin might be effective for the eradication of the *BRCA1*-associated cancers and its aggressively basal-like and triple negative subtypes, and the recurrently platinum-resistant cancers with lesser adverse effects than the empirical and historical treatment.

**Table 7.** Summary of the cisplatin-based therapy in breast cancer patients and the pathological complete response (pCR).

Investigations	N	Treatment regimen	pCR rate (%)	Comment
Byrski <i>et al.</i> , 2009	10	cisplatin 75 mg/m <sup>2</sup> every 3 weeks for four cycles	90	All breast cancer patients were <i>BRCA1</i> carriers (5382insC and C61G)
Byrski <i>et al.</i> , 2010	12	cisplatin 75 mg/m <sup>2</sup> every 3 weeks for four cycles	83	All breast cancer patients were <i>BRCA1</i> carriers (5382insC, C61G, and 4153delA)

Investigations	N	Treatment regimen	pCR rate (%)	Comment
Rocca <i>et al.</i> , 2008	147	Neoadjuvant cisplatin 60 mg/m <sup>2</sup> every 3 weeks for six cycles	23	cisplatin-based chemotherapy correlated with a high rate of pCR in patients with p63-positive breast cancer
Silver <i>et al.</i> , 2010	28	cisplatin 75 mg/m <sup>2</sup> every 3 weeks for four cycles	22	Eighteen (64%) triple-negative breast cancer patients had a clinical complete or partial response
Sirohi <i>et al.</i> , 2008	94	Neoadjuvant cisplatin 60 mg/m <sup>2</sup> and epirubicin 60 mg/m <sup>2</sup> every 3 weeks for six cycles	88	Platinum-based chemotherapy achieves the increased response rates for triple-negative breast tumors
Yerushalmi <i>et al.</i> , 2009	88	Neoadjuvant cisplatin 60 mg/m <sup>2</sup> and paclitaxel 90 mg/m <sup>2</sup> every 2 weeks for eight cycles	21.5	A cisplatin-based neoadjuvant regimen was well tolerated and achieved a pCR in locally advanced breast cancer

## CHAPTER 3

### MATERIALS AND METHODS

#### Materials

##### Bacterial plasmids

- pET15\_ubiquitin (plasmid 12647) (Addgene, USA)
- pET28a(+) derivatives (gift from Prof. Udo Heinemann)
- pET28a(+)\_BARD1 (plasmid 12646) (Addgene, USA)
- pET28a(+)\_UbcH5c (plasmid 12643) (Addgene, USA)
- pGEX-4T1 (gift from Prof. Udo Heinemann)

##### Cells

- *E. coli* BL21(DE3) (gift from Prof. Udo Heinemann)
- *E. coli* DH5 $\alpha$  (New England Biolab, USA)
- White blood cell (A normal healthy person)

##### Chemicals

- $\beta$ -Mercaptoethanol (Sigma-Aldrich, USA)
- Absolute ethanol (Merck, Germany)
- Acetone (Roth, Germany)
- Acetonitrile (Roth, Germany)
- Agarose powder (Promega, USA)
- Ammonium acetate (Ajax chemical, Australia)
- Ammonium persulfate (Sigma-Aldrich, USA)
- Ampicillin (Sigma-Aldrich, USA)
- Bacto<sup>TM</sup> agar (Becton, Dickson and company, USA)
- Bacto<sup>TM</sup> tryptone (Becton, Dickson and company, USA)
- Bacto<sup>TM</sup> yeast extract (Becton, Dickson and company, USA)

- Boric acid (Merck ,Germany)
- Bovine serum albumin (Sigma-Aldrich, USA)
- Bromphenol blue (Sigma-Aldrich, USA)
- Cacodylate sodium salt (Fluka, Switzerland)
- Calcium chloride (Merck ,Germany)
- Carboplatin (Sigma-Aldrich, USA)
- Cisplatin (Sigma-Aldrich, USA)
- Colbalt (II) chloride (Carlo Erba Reagenti, Italy)
- Coomassie brilliant blue G-250 (USB Corporation, USA)
- Coomassie brilliant blue R-250 (USB Corporation, USA)
- D(+)-glucose (Sigma-Aldrich, USA)
- dATP, dCTP, dGTP and dTTP (Promega, USA)
- Dialysis bag (Sigma-Aldrich, USA)
- Di-potassium hydrogen phosphate anhydrous  
(Merck ,Germany)
- Di-sodium hydrogen phosphate (Fluka, Switzerland)
- Dithiothreitol (Fluka, Switzerland)
- Elastase (Sigma-Aldrich, USA)
- Ethidium bromide (Gibco, USA)
- Ethylenediamine tetraacetic acid disodium salt (EDTA) (BDH  
laboratory supplier, England)
- Formaldehyde (Merck ,Germany)
- Glacial acetic acid (Merck ,Germany)
- Glutaraldehyde (Fluka, Switzerland)
- Glycerol (BDH laboratory supplies, England)
- Glycine Ultrapure (USB corporation, USA)
- Guanidine hydrochloride (Fluka, Switzerland)
- Hydrochloric acid (Merck, Germany)

- Imidazole (Fluka, Switzerland)
- Iodoacetamide (Sigma-Aldrich, USA)
- Isopropanol (J.T. baker, USA)
- Isopropyl-1-thio- $\beta$ -D-galactopyranoside (Applichem, Germany)
- Kanamycin (Roth, Germany)
- Lysozyme (Fluka, Switzerland)
- Magnesium chloride (Merck ,Germany)
- Methanol (Labscan Asia, Thailand)
- *N, N, N', N'*-tetramethylenediamine (TEMED) (Sigma-Aldrich, USA)
- *N,N'*-methylene-bis-acrylamide (Sigma-Aldrich, USA)
- Nonidet P-40 (Fluka, Switzerland)
- Oxaliplatin (Sigma-Aldrich, USA)
- Phenylmethylsulphonyl fluoride (Fluka, Switzerland)
- Potassium acetate (BDH laboratory supplier, England)
- Potassium dihydrogen phosphate (Merck ,Germany)
- Reduced glutathione (Sigma-Aldrich, USA)
- Silver nitrate (Merck ,Germany)
- Sodium acetate (APS Finechem, Australia)
- Sodium carbonate anhydrous (Ajax Finechem, Australia)
- Sodium chloride (Merck ,Germany)
- Sodium dodecyl sulfate (Promage, USA)
- Sodium hydrogen carbonate (Merck ,Germany)
- Sodium hydroxide (Carlo Erba Reagenti, Italy)
- Sodium thiosulfate (Fisher Chemicals, England)
- Transplatin (Sigma-Aldrich, USA)
- Trifluoroacetic acid (Fluka, Switzerland)

- Tris base (Promega, USA)
- Triton X-100 (Sigma-Aldrich, USA)
- Trypsin (Promega, USA)
- UltraPure™ Acrylamide (Invitrogen, USA)
- Urea (Roth, Germany)
- Xylene cyanol (Sigma-Aldrich, USA)
- Zinc(II) chloride (Fluka, Switzerland)
- Zinc sulfate (Fluka, Switzerland)

### **Enzymes**

- ProofStart DNA polymease (QIAGEN, Germany)
- Restriction enzyme *Bam*HI (New England Biolab, USA)
- Restriction enzyme *Nde*I (New England Biolab, USA)
- Restriction enzyme *Not*I (New England Biolab, USA)
- Restriction enzyme *Pst*I (New England Biolab, USA)
- Restriction enzyme *Xho*I (New England Biolab, USA)
- T4 DNA ligase (New England Biolab, USA)

### **Instruments**

- Agarose gel electrophoresis apparatus (EC 370, E-C Apparatus, USA)
- Autoclave (HD-3D, Hirayama Company, Japan)
- Bio-Rad GS-700 Imaging Densitometer (Bio-Rad, USA)
- Deep Freezer (-86°C) (Forma Scientific, USA)
- Desktop centrifuge (VSMC-13 minicentrifuge, Shelton Scientific, USA)
- DNA sequencer (ABI Prism 377, Perkin-Elmer, USA)
- Freezer (-20°C) (Hotpack, Forma Scientific, USA)
- French press (Spectronic Instruments, USA)
- Gel documentation equipment (Bio-Rad, USA)

- Hot air oven (Mammert GmbH Co., Germany)
- HPLC machine (Ultimate 3000, Dionex, Germany)
- Laboratory balance (Mettler Toledo, USA)
- Laminar air flow: biosafety cabinet class II (Ultrasafe 48, Faster, Italy)
- Mass spectrometer (QTRAP 4000, Applied Biosystem/MDS Sciex, USA)
- Mono Q HR 5/5 column (Amersham Biosciences, USA)
- PCR machine (GeneAmp 9600, Perkin-Elmer, USA)
- pH meter (Mettler Toledo 320, USA)
- Polyacrylamide gel electrophoresis apparatus (AE-6450 Dual mini slab kit, ATTO, Japan)
- Power supply (EC 135, E-C Apparatus Company, USA, and AE-8150 myPower 500. ATTO, Japan)
- Protein C4 column (Vydex, Grace, USA)
- Refrigerated centrifuge (Aventi J-26XP, Beckman Coulter, USA)
- Shaking bath (SBO 50 BIO, Heto lab equipment, USA)
- Sonicator (Vibracell, Sonic and Material, Inc., USA)
- Spectropolarimeter (J720, Jasco, Japan)
- Superose 12 HR10/30 column (Amersham Biosciences, USA)
- UV-spectrophotometer (Genesis 5, Spectronic, USA)
- Vortex (VSM-3 mixer, Shelton Scientific, USA)

### **Kits**

- Big Dye Terminator Cycle Sequencing Ready Reaction Kit (Applied Biosystem, USA)
- GSTrap column (Amersham Biosciences, USA)
- Low molecular standard kit (Amersham Biosciences, USA)

- Ni<sup>2+</sup>-NTA bead (QIAGEN, Germany)
- Oligonucleotide primers (Invitrogen, USA)
- QIAamp<sup>®</sup> RNA Blood Kit (QIAGEN, Germany)
- QIAGEN OneStep RT-PCR Kit (QIAGEN, Germany)
- QIAquick<sup>®</sup> Gel Extraction Kit (QIAGEN, Germany)
- QuikChange<sup>®</sup> site-directed mutagenesis kit (Stratagene, USA)

#### **Plasticware**

- Acrodisc<sup>®</sup> syring filter (Pall Life Sciences, USA)
- Amicon ultra concentrator (Milipore, USA)
- Econo-Pac<sup>®</sup> column (Bio-Rad)
- Macrosep centrifugal devices (Pall Life Sciences, USA)
- Microcentrifuge tube 1.5 ml (Axygen Scientific Inc, USA)
- PCR tube (Axygen Scientific Inc, USA)
- Pipet tip T-1000-B (200-1000 µl) (Axygen Scientific Inc, USA)
- Pipet tip T-200-Y (20-200 µl) (Axygen Scientific Inc, USA)
- Pipet tip T-300-STK-S (0.2-10 µl) (Axygen Scientific Inc, USA)

#### **Methods**

##### **3.1 Preparation of the complementary DNA fragments of the *BRCAl* gene (GenBank no. U14860)**

###### **Total RNA isolation**

Total RNA from human leukocytes was isolated using QIAamp<sup>®</sup> RNA Blood Kit (QIAGEN) by mixing 1 volume (1.5 ml) of the whole human blood with 5 volumes (7.5ml) of the hypotonic solution for erythrocyte lysis. The mixture was vortexed briefly 2 times during incubation on ice for 10-15 min, and subsequently centrifuged at 400xg for 10 min at 4°C. After the supernatant was



discarded, the cell pellet mainly containing leukocytes was resuspended with the hypotonic solution (3 ml per 1.5 ml of the whole blood), and centrifuged at 400xg for 10 min at 4°C for complete removal of erythrocytes. The pelleted leukocytes was resuspended with the leukocyte lysis buffer (600 µl), and loaded onto the QIAshredder spin column for efficient disruption of the cells and homogenization of the lysate, resulting in the optimal yield and purity. The QIAshredder spin column was centrifuged for 2 min at maximum speed to homogenize. The homogenized lysate was mixed with 70% ethanol (600 µl), and transferred to the QIAamp spin column, which allows RNAs longer than 200 bases to bind to the membrane. Small RNAs such as 5.8S RNA, 5S RNA, and tRNA (approximately 160, 120, and 70-90 nucleotides in length, respectively) do not bind in quantity under the conditions used. The QIAamp spin column was centrifuged at  $\geq 8000xg$  for 15 s, and transferred into a new 2-ml collection tube. The QIAamp spin column was applied with the washing buffer 1, and centrifuged at  $\geq 8000xg$  for 15 s to wash the RNA sample. The QIAamp spin column was placed in a new 2-ml collection tube, added with the washing buffer 2 (500 µl), and centrifuged at  $\geq 8000xg$  for 15 s. After the flow-through was discarded, the washing buffer 2 (500 µl) was added on the QIAamp spin column, and the column was centrifuged at full speed for 3 min. RNase-free water (50 µl) was directly added onto the membrane of the QIAamp spin column, sitting in a new 1.5-ml microcentrifuge tube, and finally centrifuged at  $\geq 8000xg$  for 1 min to elute total RNA.

#### **Reverse transcriptase-polymerase chain reaction (RT-PCR)**

The isolated total RNA was used as the template for complementary DNA (cDNA) synthesis, using QIAGEN OneStep RT-PCR Kit<sup>®</sup>. The combination of the Omniscript and Sensiscript reverse transcriptases was included in the enzyme mix, which provides the highly efficient and specific reverse transcription for the first strand cDNA synthesis from RNA templates with as little amount as 1 pg. The second strand cDNA synthesis was obtained by the function of HotStarTaq DNA

polymerase. The reactions were heated at 95°C for 15 min to activate the DNA polymerase, and simultaneously to inactivate the reverse transcriptase. The reaction mixture was prepared by mixing template RNA (< 2 µg/reaction), gene-specific primers for the cDNA synthesis of the *BRC1* gene fragment (nucleotides 1-912, Figure 19) (forward: 5'- ATGGATTTATCTGCTCTTCGC -3', reverse: 5'- GAA TTCAGCCTTTTCTAC -3'), dNTP mix, QIAGEN OneStep RT-PCR buffer, and QIAGEN OneStep RT-PCR enzyme (Table 8). Reactions were performed on a thermal cycler, according to the thermal cycling conditions (Table 9).

```

1   ATGGATTTAT CTGCTCTTCG CGTTGAAGAA GTACAAAATG TCATTAATGC TATGCAGAAA
61  ATCTTAGAGT GTCCCATCTG TCTGGAGTTG ATCAAGGAAC CTGTCTCCAC AAAGTGTGAC
121 CACATATTTT GCAAATTTTG CATGCTGAAA CTCTCAACC AGAAGAAAGG GCCTTCACAG
181 TGTCTTTTAT GTAAGAATGA TATAACCAA AGGAGCCTAC AAGAAAGTAC GAGATTTAGT
241 CAACTTGTTG AAGAGCTATT GAAAATCATT TGTGCTTTTC AGCTTGACAC AGGTTTGGAG
301 TATGCAAACA GCTATAATTT TGCAAAAAG GAAAATAACT CTCCTGAACA TCTAAAAGAT
361 GAAGTTTCTA TCATCCAAAG TATGGGCTAC AGAAACCGTG CCAAAGACT TCTACAGAGT
421 GAACCCGAAA ATCCTTCCTT GCAGGAAACC AGTCTCAGTG TCCAACCTC TAACCTTGA
481 ACTGTGAGAA CTCTGAGGAC AAAGCAGCGG ATACAACCTC AAAAGACGTC TGTCTACATT
541 GAATTGGGAT CTGATTCTTC TGAAGATACC GTTAATAAGG CAACTTATTG CAGTGTGGGA
601 GATCAAGAAT TGTTACAAAT CACCCCTCAA GGAACCAGGG ATGAAATCAG TTTGGATTCT
661 GCAAAAAGG CTGCTTGTA ATTTTCTGAG ACGGATGTAA CAAATACTGA ACATCATCAA
721 CCCAGTAATA ATGATTGAA CACCACTGAG AAGCGTGCAG CTGAGAGGCA TCCAGAAAAG
781 TATCAGGGTA GTTCTGTTTC AAACCTGCAT GTGGAGCCAT GTGGCACAAA TACTCATGCC
841 AGCTCATTAC AGCATGAGAA CAGCAGTTTA TTAICTACTA AAGACAGAAT GAATGTAGAA
901 AAGGCTGAAT TC

```

**Figure 19.** Nucleotide sequence of the *BRC1* gene fragment (nucleotide 1-912).

**Table 8.** Reaction components for the One-step RT-PCR.

Components	Volume ( $\mu$ l)	Final concentration
RNase-free water	27	-
5x QIAGEN One-step RT-PCR buffer	10	1x
dNTP mix (10 mM of each dNTP)	2	400 $\mu$ M of each
10 $\mu$ M forward primer	3	0.6 $\mu$ M
10 $\mu$ M reverse primer	3	0.6 $\mu$ M
QIAGEN One-step RT-PCR enzyme mix	2	-
Template RNA	3	1 pg -2 $\mu$ g / reaction
<b>Total volume</b>	<b>50</b>	<b>-</b>

**Table 9.** Thermal cycling conditions for the One-step RT-PCR.

<b>Reverse transcription</b>	50°C, 30 min
<b>Initial PCR activation</b>	95°C, 15 min
<b>3-step cycling</b>	
denaturation	94°C, 30 s
annealing	55°C, 45 s
extension	72°C, 1 min
<b>Number of cycles</b>	30 cycles
<b>Final extension</b>	72°C, 10 min

### 3.2 DNA amplification of the *BRCA1*, *BARD1*, *ubiquitin*, and *UbcH5c* genes

The *BRCA1* gene fragments, containing the nucleotides 1-417, and 1-912, were amplified by the polymerase chain reaction (PCR) using the *BRCA1* cDNA as the templates. The *BARD1* gene fragment (nucleotides 76-981), and the full-length *ubiquitin (Ub)* and *UbcH5c* genes were amplified by PCR using the Addgene plasmids 12646, 12647, and 12643 as the templates, respectively. The reaction

mixtures were prepared by mixing template DNA, primer solutions (Table 10), dNTP mix, 10X ProofStart PCR buffer, and water followed by the addition of the ProofStart DNA polymease (QIAGEN) to the individual PCR tubes. The reactions (Table 11) were performed on a thermal cycler, according to the thermal cycling conditions (Table 12). The PCR products were electrophoresed on 1% agarose gel, and then extracted by QIAquick<sup>®</sup> gel extraction kit (QIAGEN).

**Table 10.** The oligonucleotide primers for the amplifications of the *BRCA1*, *BARD1*, *ubiquitin (ub)*, and *UbcH5c* genes.

Construct name	Protein residue	Primer	Direction (5' → 3')
BRCA1 (1-139-wt)	1-139	forward	GACACGCGGATCCATGGATTTATCTGCTCTTCG
		reverse	GACACCGCTCGAGTCACTGTAGAAGTCTTTTGGCAC
BRCA1 (1-304-wt)	1-304	forward	GACACGCGGATCCATGGATTTATCTGCTCTTCG
		reverse	GACACCGCTCGAGTCAGAATTCAGCCTTTTCTACATTC
BARD1 (26-327)	26-327	forward	GACACGCGGATCCATGGAACCGGATGGTCGCGG
		reverse	GACACCGCTCGAGTCATCTATTGTGATGGCCACGTTTTC
Ubiquitin (Ub)	1-76	forward	GACACGCGGATCCATGCAGATCTTCGTC AAGAC
		reverse	GACACCGGCGCCGCTCAACCACCTCTTAGTCTTAAG
UbcH5c	1-147	forward	GACACGCGGATCCATGGCGCTGAAACGGATTAATAAG
		reverse	GACACCGCTCGAGTCACATGGCATACTTCTGAG

**Table 11.** Reaction components for PCR amplification.

Components	Volume ( $\mu$ l)	Final concentration
Double distilled water	variable	-
10X ProofStart PCR buffer	10	1x
dNTP mix (10 mM of each dNTP)	3	300 $\mu$ M of each
10 $\mu$ M forward primer	10	1 $\mu$ M
10 $\mu$ M reverse primer	10	1 $\mu$ M
ProofStart DNA polymerase	2	5 units
Template DNA	variable	100 ng - 1 $\mu$ g / reacion
<b>Total volume</b>	100	-

**Table 12.** Thermal cycling conditions for PCR.

<b>Initial denauration</b>	95°C, 5 min
<b>3-step cycling</b>	
denaturation	95°C, 30 s
annealing	55-63°C, 45 s
extension	72°C, 1 min
<b>Number of cycles</b>	35 cycles
<b>Final extension</b>	72°C, 10 min

### 3.3 Extraction and purification of the PCR products

The PCR products from 3.2 were electrophoresed on 1% agarose gel. DNA fragments were detected by staining with ethidium bromide, and visualizing by illumination with 300 nm UV light. Targeted DNA fragments were sliced from the agarose gel with a clean and sharp scalpel, and extracted by QIAquick<sup>®</sup> gel extraction kit (QIAGEN). Three volumes of the solubilizing buffer were added to a volume of gel (100 mg ~ 100  $\mu$ l) to dissolve the agarose gel slice, and to provide the appropriate conditions (high salt and pH  $\leq$  7.5) for binding of DNA to the silica gel membrane while the contaminants pass through the column. The mixture was incubated at 50°C

for 10 min, then loaded onto a QIAquick spin column, and centrifuged at 10000xg for 1 min. The flow-through was discarded, and the washing buffer (750  $\mu$ l) was added to the QIAquick spin column that was subsequently centrifuged at 10000xg for 1 min. The flow-through was discarded, and the QIAquick spin column was additionally centrifuged at 10000xg for 1 min to completely eliminate the washing buffer. Water (50  $\mu$ l) was directly added onto the membrane of the QIAquick spin column, sitting in a new 1.5-ml microcentrifuge tube, and finally centrifuged at full speed for 1 min to elute purified DNA.

### 3.4 Plasmid constructions

The short N-terminal fragment of the BRCA1 protein amino acid residues 1-139 was produced as the intact protein by inserting the respective gene fragment (the *BRCA1* gene nucleotides 1-417) into the *Bam*HI/*Xho*I sites of a bacterial plasmid pET28a(+) derivative (Figure 20). The BRCA1 protein amino acid residues 1-304 (the *BRCA1* gene nucleotides 1-912), and those of the BARD1 protein amino acid residues 26-327 (the *BARD1* gene nucleotides 76-981) were produced as a GST fusion by cloning the respective genes into the *Bam*HI/*Xho*I sites of the pGEX-4T1 (Amersham Biosciences). The full-length *ubiquitin* (*Ub*) and *UbcH5c* genes were inserted into the *Bam*HI/*Not*I and the *Bam*HI/*Xho*I sites, respectively, of the pET28a(+) derivatives for the expressions of the His<sub>6</sub>-tagged proteins. The digestion reactions (50  $\mu$ l) contained 5  $\mu$ l of 10x enzyme buffer, 0.5  $\mu$ l of 100x BSA, DNA fragments or 10  $\mu$ g of plasmids (pGEX4T1 and pET28a(+) derivatives), 1  $\mu$ l of each endonuclease (20 units), and water. The reactions were then incubated at 37°C for 6 h, and subsequently electrophoresed on 1% agarose gel. The digested DNA fragments were purified using QIAquick<sup>®</sup> gel extraction kit. The digested DNA fragments were ligated into the respective endonuclease sites of the plasmids by T4 DNA ligase. The ligated constructs were transformed to *E. coli* DH5 $\alpha$  by mixing the ligation reactions with 100  $\mu$ l of competent cells, and then the cells were incubated on ice for 30 min. The cells were shocked at 42°C for 90 s, and immediately placed on ice for 5 min. LB

broth (800  $\mu$ l) was added to the cells, and further incubated at 37°C for 1 h. The cells were centrifuged at 5000xg for 1 min. The medium was discarded, and the cell pellet was resuspended in 100  $\mu$ l of the fresh LB broth. The cells were grown on LB agar, containing 100  $\mu$ g/ml ampicillin (for pGEX-4T1) or 50  $\mu$ g/ml kanamycin [for pET28a(+)] derivatives] for clone selection. All Recombinant plasmids were isolated, and characterized by restriction analysis and DNA sequencing.

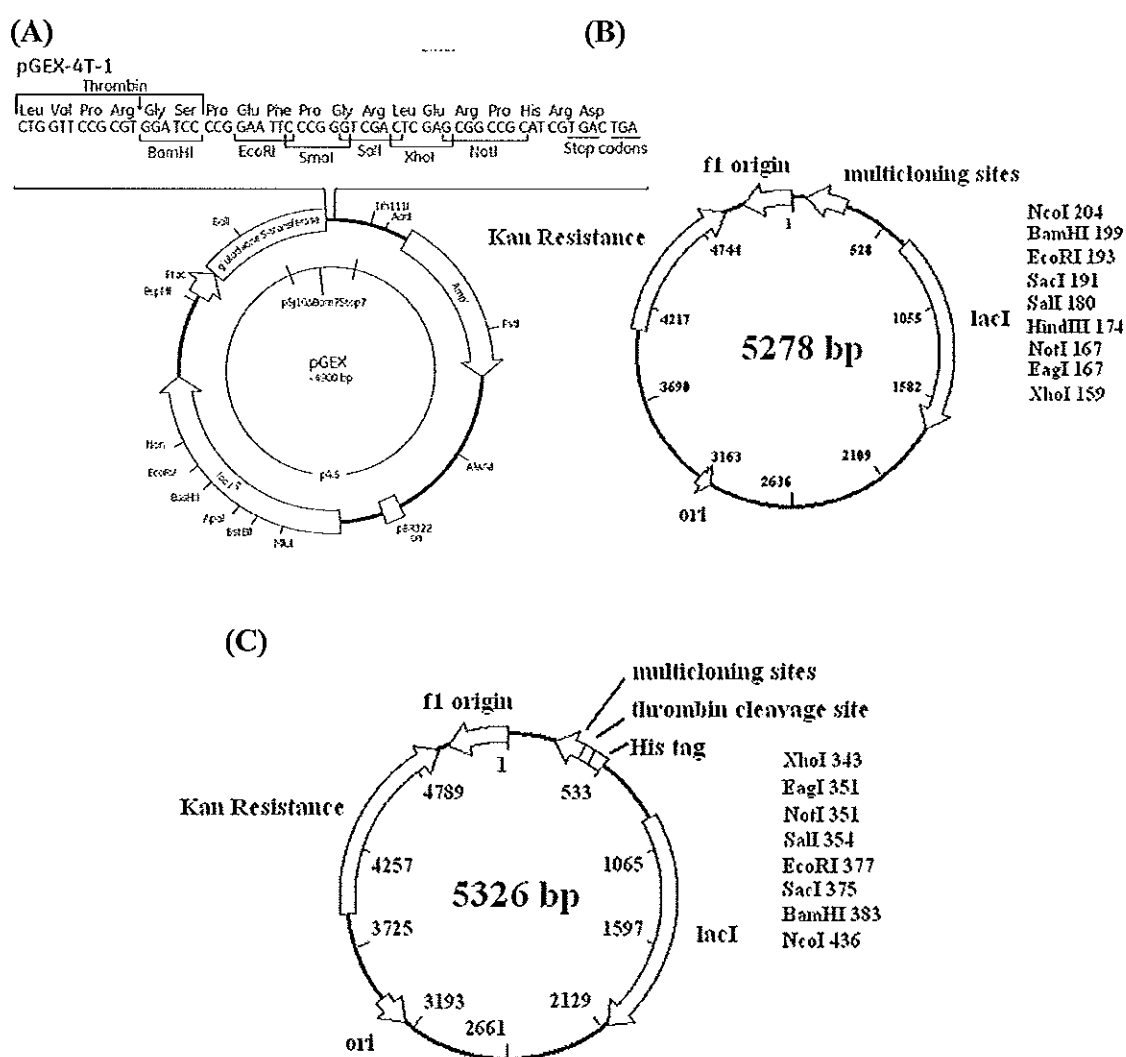


**Figure 20.** Schematic representations of the bacterial expression plasmids. (A) pGEX-4T1, (B) pET28a(+)] derivative without the His<sub>6</sub> fusion tag, and (C) pET28a(+)] derivatives with the His<sub>6</sub> fusion tag.

### 3.5 Site-directed mutagenesis of the BRCA1 RING domain

The missense mutations (D67A, D67E, D67Y, and C61G) were introduced to the BRCA1 RING domain using the QuikChange<sup>®</sup> site-directed mutagenesis kit (Stratagene). The basic procedure utilized a supercoiled double stranded DNA plasmid with an insert of interest [pET28(a+)-BRCA1(1-139) and pGEX-BRCA1(1-304)], and two synthetic oligonucleotide primers containing the desired mutation. The primers (Table 13), each complementary to the opposite strands of the plasmid, are extended during temperature cycling by using *PfuTurbo*<sup>®</sup> DNA polymerase that replicates both plasmid strands with high fidelity (Tables 14 and 15). Incorporation of the primers generates a mutated plasmid containing staggered nicks. Following temperature cycling, the PCR products were treated with *Dpn* I. The *Dpn* I endonuclease is specific for the methylated and hemimethylated DNA at the target sequence (5'-Gm<sup>6</sup>ATC-3'), and thus is used to digest the parental DNA template for selecting the synthesized mutant DNA. DNA isolated from almost all *E. coli* strains is dam-methylated, and therefore susceptible to *Dpn* I digestion. The nicked plasmid DNA, incorporating the desired mutations, is then transformed into *E. coli* XL1-Blue supercompetent cells that can repair the nicks. Briefly, 1 µl of the *Dpn* I-treated DNA was mixed with 50 µl of the supercompetant cells. The transformation reactions were heated at 42°C for 45 s, and then placed on ice for 2 min. After adding 0.5 ml of NZY<sup>+</sup> broth preheated to 42°C, the reactions were incubated at 37°C for 1 h with shaking. The reactions (250 µl) were poured on the LB-kanamycin agar plates, and then the transformation plates were incubated at 37°C for 16 h. The desired mutant plasmids were isolated, and verified by DNA sequencing.



**Table 13.** The oligonucleotide primers for site-directed mutagenesis.

Construct	Primer	Primer design (5' → 3')
BRCA1-D67A	forward	GTCCTTTATGTAAGAATGCTATAACCAAAAAGGAGCCTACA
	reverse	TGTAGGCTCCTTTTGGTTATAGCATTCTTACATAAAGGAC
BRCA1-D67E	forward	GTCCTTTATGTAAGAATGAGATAACCAAAAAGGAGCCTACA
	reverse	TGTAGGCTCCTTTTGGTTATCTCATTCTTACATAAAGGAC
BRCA1-D67Y	forward	CCTTTATGTAAGAATTATATAACCAAAAAGGAG
	reverse	CTCCTTTTGGTTATATAAATCTTACATAAAGG
BRCA1-C61G	forward	GAAAGGGCCTTCACAGGGTCCTTTATGTAAGAATG
	reverse	CATTCTTACATAAAGGACCCTGTGAAGGCCCTTTC

**Table 14.** The sample reaction for site-directed mutagenesis.

Components	Volume (μl)
10× reaction buffer	5
dsDNA template (5-50 ng)	0.5
oligonucleotide primer #1 (125 ng)	1.25
oligonucleotide primer #2 (125 ng)	1.25
dNTP mix	1
Quik Solution reagent	1.5
<i>PfuTurbo</i> DNA polymerase (2.5 U/μl)	1
ddH <sub>2</sub> O	to 51

**Table 15.** Thermal cycling condition for site-directed mutagenesis.

Segment	Cycles	Temperature	Time
1	1	95°C	30 sec
2	18	95°C	30 sec
		55°C	1 min
		68°C	1 min/kb of plasmid length

### **3.6 Verification of the recombinant plasmids by automated DNA sequencing**

The inserted *BRCA1*, *BARD1*, *ubiquitin*, and *UbcH5c* DNA fragments were verified by DNA sequencing using Big Dye Terminator Cycle Sequencing Ready Reaction Kit (Applied Biosystem). The reaction mixtures consisted of Big dye Terminator ready reaction mix (8  $\mu$ l), double strand DNA template (200-500 ng), and primer (3.2 pmol) in 20  $\mu$ l of total volume, and were placed in a thermal cycler, and run for 25 cycles of 96°C for 10 s, 50°C for 5 s, and 60°C for 4 min with an initial denaturation at 96°C for 1 min. The unincorporated Big Dye Terminator was removed by the addition of 75% isopropanol (80  $\mu$ l) that was subsequently left at room temperature for 15 min. The mixtures were spun at 14000xg for 20 min at room temperature, and the supernatant was discarded. Ethanol (70%) (250  $\mu$ l) was added, and the samples were spun at 14000xg for 5 min. After the supernatant was discarded, the samples were dried in a heat-block at 90°C for 1 min. The samples were resuspended in 6  $\mu$ l of the loading dye (deionized formamide and Blue dextran at the ratio of 1:5), heated at 90°C for 2 min, and then placed on ice immediately. One microliter of each sample was loaded into a separate lane of polyacrylamide gel, and run in a DNA sequencer. The sequence data were aligned to *BRCA1* (GenBank no. U14860), *BARD1* (GenBank no. NM000465), *ubiquitin* (GenBank no. NM021009), and *UbcH5c* (GenBank no. U39318) databases.

### **3.7 Expression and purification of the recombinant proteins**

All recombinant plasmids were transformed into *E. coli* BL21(DE3) for productions of the proteins. Transformed bacterial cells were grown in 1000 ml of Luria Broth medium, containing 100  $\mu$ g/ml ampicillin or 50  $\mu$ g/ml kanamycin with shaking at 37°C. Isopropyl- $\beta$ -D-thiogalactoside was added to a final concentration of 0.5 mM to induce the expression when the  $A_{600\text{ nm}}$  of the culture reached 0.5-0.6. Cells were allowed to grow for 12 h at 25°C after the induction, and harvested by centrifugation. Cell pellets were resuspended in 20 ml of lysis buffer [50 mM Tris

(pH 7.4), 50 mM NaCl, 10% glycerol, 10 mM DTT, 1% Triton X-100, 0.5% NP-40, 10 mM  $\beta$ -mercaptoethanol, and 1 mM PMSF], and then lysed by sonication (10 min with 60% amplitude, 9 s pulse on, and 4 s pulse off). Whole cell lysate was centrifuged at 13,000xg at 4°C for 30 min. The intact BRCA1 proteins (amino acid residues 1-139) were accumulated in the inclusion bodies. They were washed with 30 ml of lysis buffer, and subsequently centrifuged at 13,000xg at 4°C for 30 min. The inclusion bodies were solubilized with 30 ml of 6 M guanidine HCl in 50 mM Tris (pH 7.4), and 10 mM  $\beta$ -mercaptoethanol at room temperature for 3 h with stirring. The mixtures were centrifuged at 13000xg for 30 min at 10°C, and the supernatant was dialyzed overnight at 4°C against 0.1% acetic acid. The mixtures were then centrifuged at 13000xg for 30 min at 4°C, and the resulting supernatant was filtered through a 0.2  $\mu$ m cellulose acetate membrane. The filtrates were further purified using an analytical C4 reversed-phase column (Vydac protein C4 column; 4.6/250 mm dimensions with 5  $\mu$ m particle size) with a water/acetonitrile (ACN) gradient containing 0.1% trifluoroacetic acid. Protein solutions were eluted with a linear 40-60% ACN gradient at a rate of 0.35%/min. Purified protein was identified on 15% Coomassie blue-stained SDS-PAGE, and subsequently confirmed by sequencing the tryptic digested peptides. Glutathione-S-transferase (GST)-tagged proteins [GST-BRCA1(1-304) and GST-BARD1(26-327)] were freshly prepared by loading the soluble portions of cell lysates into the glutathione-agarose GSTrap column (1 ml) (Amersham Biosciences) with the slow rate of 0.3 ml/min. The bound proteins were washed with a 10 fold column volume of the washing buffer [50 mM Tris (pH 7.4), 50 mM NaCl, and 10 mM  $\beta$ -mercaptoethanol], and eluted with a buffer, containing 50 mM Tris (pH 7.4), 10 mM  $\beta$ -mercaptoethanol, and 20 mM reduced glutathione. The purified GST-tagged proteins were extensively dialyzed at 4°C against deionized water. His<sub>6</sub>-tagged proteins (His<sub>6</sub>-Ub and His<sub>6</sub>-UbCH5c) were purified using 1 ml of Ni<sup>2+</sup>-NTA beads (QIAGEN) by which the bound proteins were first washed with a 10 fold column volume of the binding buffer [50 mM Tris (pH 7.4), 50 mM NaCl, and

10 mM imidazole] before being eluted with the binding buffer containing 300 mM imidazole. Purified His<sub>6</sub>-Ub and His<sub>6</sub>-UbcH5c proteins were then dialyzed at 4°C against a buffer, containing 50 mM Tris (pH 7.0), 10 mM β-mercaptoethanol, and 10% glycerol. The amount of proteins was quantitated by the Bradford assay using BSA as a standard.

### **3.8 Gel-filtration chromatography**

Purified BRCA1(1-139) proteins from reversed-phase chromatography were lyophilized, and resuspended in 2 M guanidine HCl with three molar equivalent ratio of Zn<sup>2+</sup> to protein. Proteins (0.3 mM) were then applied on an analytical Superose 12 HR 10/30 column (Amersham Biosciences) using the 200 μl of sample loop, and the flow rate of 0.4 ml/min. The column was pre-equilibrated with 25 mM Tris (pH 7.0), 150 mM NaCl, and 10 μM ZnCl<sub>2</sub>, and calibrated using BSA (67 kDa), ovalbumin (45 kDa), chymotrypsinogen A (25 kDa), and ribonuclease A (13.7 kDa). The elution profiles were monitored at 212 nm.

### **3.9 Glutaraldehyde cross-linking**

Peak fractions from gel filtration column (typically 2 μM) were subjected to the cross-linking reaction in the presence of 0.001-0.05% glutaraldehyde (w/v) at ambient temperature. Reaction aliquots (20 μl) were removed at 0, 15, and 30 min after the addition of glutaraldehyde, quenched with an equal volume of SDS-loading dye (20 μl), and then heated at 95°C for 5 min. The reactions were visualized on 15% SDS-PAGE by silver staining.

### **3.10 Limited proteolysis and mass spectrometry**

Protein samples (30 μM) in the absence and presence of three molar equivalent ratio of Zn<sup>2+</sup> to protein were prepared in 10 mM cacodylate buffer (pH 6.8), and then mixed with either elastase or trypsin at the protein-protease ratio of 100-500:1 (w/w) at 37°C. Proteolysis of metal-free protein was also determined in the presence of 0.5 mM EDTA. Reaction aliquots at different time intervals (0, 0.25, 0.5, 1, 2, 3, 6, 12, and 24 h after the addition of protease) were quenched by adding an

equal volume of the SDS-loading dye. Samples were visualized on 15% SDS-PAGE by Coomassie blue staining. To determine the constituents of the digested products, the protein bands of interest from the SDS-PAGE gel were excised, in-gel alkylated with iodoacetamide, and digested with sequencing-grade trypsin (Promega). In-gel digestions of free BRCA1 and cisplatin-BRCA1 adducts for characterizing the binding sites of cisplatin were also performed with ignoring the modification by iodoacetamide. The peptide mixture was separated on a PepMap C18 column (75 $\mu$ m/150 mm dimensions with 3 $\mu$ m particle size) that connected to an UltiMate 3000 HPLC system (Dionex, Idstein, Germany), delivering a gradient of 4-50% ACN. Eluting peptides were ionized by electrospray ionization (ESI) and mass spectra were acquired with a QTRAP 4000 Mass Spectrometer (Applied Biosystems/MDS Sciex). MS/MS analyses were conducted using collision energy profiles chosen on the basis of the m/z value and the charge state of the parent ion. The Analyst/Bioanalyst software (version 1.4.1, Applied Biosystems) was used to process and submit the data to the MASCOT server (version 2.2, Matrix Science Ltd., London, UK) for in-house search against the SwissProt protein database. The mass tolerance of precursor ions and sequence ions was set to 0.4 Da. The searches included variable modifications of cysteine with propionamide and carbamidomethyl, and methionine oxidation.

### 3.11 Circular dichroism

Protein samples (10  $\mu$ M) were prepared in 10 mM cacodylate buffer (pH 6.8), according to Bradford assay using BSA as a standard. ZnCl<sub>2</sub> and cisplatin were prepared as 5 mM stock solutions in deionized water. Metal-dependent folding of the protein was monitored by acquiring CD spectra over a range of 200-260 nm using a Jasco J720 spectropolarimeter (Japan Spectroscopic Co. Ltd., Hachioji City, Japan) with a programable Peltier type cell holder that allows for the temperature control. Measurements of Zn<sup>2+</sup> and cisplatin binding were carried out at 20°C using a 0.1 cm quartz cuvette. The spectrum was the average of five separate spectra with a step size of 0.1 nm, a 2 s response time, and a 1 nm bandwidth. Data were baseline-

corrected by the subtraction of the data for cacodylate buffer. The secondary structures of proteins were predicted by the CONTIN program (Greenfield, 2006; Provencher and Glöckner, 1981). The effect of  $Zn^{2+}$  and cisplatin bindings on the protein stability was determined in the absence and presence of three molar equivalent ratio of  $Zn^{2+}$  to protein. CD experiments, involving thermal denaturation, were performed in three separate scans in the range from 15°C to 95°C at 208 nm with a heat rate of 1°C/min. Thermal renaturation (20°C after heating at 95°C) was also observed after the same length of time as for denaturation. The binding constant was determined using Eqn 1 (Engel, 1974):

$$\theta_{obs} = \theta_{max} [(1 + (KC/N) + KP)/(2KP) - \sqrt{(((1 + (KC/N) + KP)/(2KP))^2 - C/(NP))}] \quad (1)$$

in which  $\theta_{obs}$  is the observed ellipticity change at any concentration of metal,  $\theta_{max}$  is the ellipticity change when all of the protein binds metal, K is the binding constant, P is the protein concentration, C is the concentration of metal added, and N is the number of binding sites. The free energy of binding was given by Eqn 2.

$$\Delta G = -RT \ln k \quad (2)$$

in which  $\Delta G$  is the free energy, R is the gas constant of 1.987 cal mol<sup>-1</sup>, T is the temperature in Kelvin, and K is the binding constant.

### 3.12 X-ray absorption near-edge structure (XANES)

The absence of  $Zn^{2+}$  in protein sample was assessed by XANES. The excitation photon energy was scanned through the XANES energy range of the  $Zn^{2+}$  K-edge. The wildtype BRCA1(1-139) protein (168  $\mu$ M) in 10 mM cacodylate buffer (pH 6.8) was filled into a glass capillary with the diameter of 1 mm and the height of 2.5 cm. The data were collected on the Amptek XR-100 CR with a 17 mm<sup>2</sup> x 300  $\mu$ m Si-detector at beamline PSF-ID14.1, Berliner Elektronenspeicherring-Gesellschaft für Synchrotron-strahlung m.b.H. (BESSY, Berlin, Germany).

### 3.13 Three-dimensional structure modeling

The model structures of D67E and wild-type BRCA1 proteins were obtained using the automated protein homology-modeling server (SWISS-MODEL)

(Arnold *et al.*, 2006). The template used was the BRCA1 RING domain (PDB:1JM7). The predicted energy minimizations were -3423 and -3313 kJ/mol for wild-type and D67E BRCA1 protein models, respectively. The structures were visualized, and analyzed with the PyMOL program (<http://pymol.sourceforge.net>).

### **3.14 Preparation of the platinum-BRCA1 complexes**

Cisplatin, transplatin, carboplatin, and oxaliplatin were purchased from Sigma-Aldrich, and prepared as stock solutions (1-5 mM) in deionized water. For MS analyses, the purified BRCA1(1-139) proteins were incubated with the various concentrations of cisplatin at 37°C for 24 h before directly being subjected to mass spectrometer. For CD and *in vitro* ubiquitin ligase analyses, the purified BRCA1 proteins (10  $\mu$ M and 1.67  $\mu$ M, respectively) were mixed with the platinum compounds at concentration of 5-1000  $\mu$ M. The reaction mixtures were incubated in the dark for 24 h at 4°C to help to maintain BRCA1 activity and stability. Samples were subjected to extensive ultrafiltration using Macrosep centrifugal devices (Pall Life Sciences) to remove any unbound platinum. The amount of protein was then carefully determined by the Bradford assay, using BSA as standard.

### **3.15 *In vitro* ubiquitin ligase assay**

The ubiquitin ligase reactions (20 $\mu$ l) contained 20  $\mu$ M His<sub>6</sub>-Ub, 300 nM His<sub>6</sub>-E1, 5  $\mu$ M His<sub>6</sub>-UbcH5c, 2  $\mu$ g GST-BRCA1(1-304) or GST-BRCA1(1-304) adducts, and 2  $\mu$ g GST-BARD1(26-327) or GST-BARD1(26-327) adducts in a buffer [50 mM Tris (pH 7.5), 0.5 mM DTT, 5 mM ATP, 2.5 mM MgCl<sub>2</sub>, and 5  $\mu$ M ZnCl<sub>2</sub>]. Two separate reactions were incubated at 37°C for 3 h, and then terminated by adding an equal volume of SDS-loading dye and heating at 95°C for 5 min. The reactions were visualized on 8% SDS-PAGE by silver staining. The relative E3 ligase activity of BRCA1 adducts was quantified by normalizing the density of an apparent band of the ubiquitinated-protein conjugates to that of the parental BRCA1 as the control, using a Bio-Rad GS-700 Imaging Densitometer.

## CHAPTER 4

### RESULTS

#### 4.1 Expression and purification of the recombinant proteins

The BRCA1 RING domains, consisting of residues 1-139 [BRCA1(1-139)<sup>wt</sup> and BRCA1(1-139)<sup>D67E</sup>], were overexpressed in *E. coli* BL21(DE3) with the regulation of the inducible T7 promoter of the pET28a(+) derivative without His<sub>6</sub> tag. Because of the restriction sites used, the BRCA1 proteins contained the leading MGS (Met-Gly-Ser) residues derived from the plasmid. They were purified to apparent homogeneity by reversed phase chromatography (Figure 21).

Partial amino acid sequences of BRCA1 were verified by analyzing the peptides from a tryptic digestion with mass spectrometry (Figure 22). The experimentally obtained sequences corresponded to the N-terminal region of BRCA1. The GST-fused proteins, including the wild-type and mutant GST-BRCA1(1-304) proteins and the GST-BARD1(26-327) protein, were produced using the pGEX-4T1 system to improve protein solubility. Additionally, other His<sub>6</sub>-tagged proteins (His<sub>6</sub>-Ub and His<sub>6</sub>-UbcH5c) were overexpressed using the pET28a(+) derivative with His<sub>6</sub> tag. All GST- and His<sub>6</sub>-tagged proteins were purified by the immobilized glutathione and Ni<sup>2+</sup> affinity chromatography, respectively (Figure 23). The purified proteins were further used to characterize some specified properties in the following experiments.



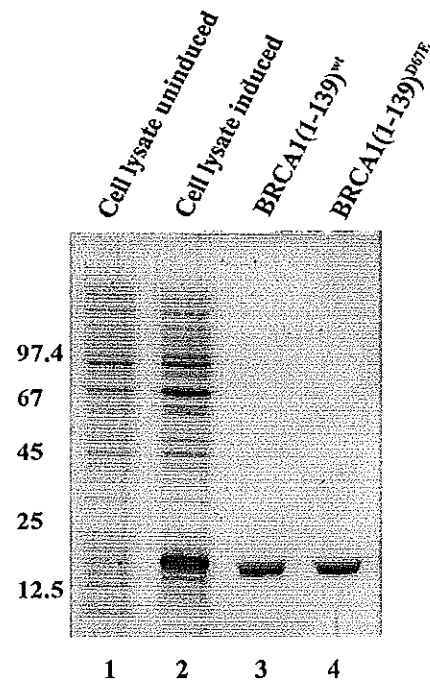


**Figure 21.** Expression and purification of the BRCA1 RING domain analyzed by 15% SDS-PAGE with Coomassie blue staining. Lane 1: whole-cell lysate uninduced; lane 2: BRCA1(1-139)<sup>wt</sup> whole-cell lysate after a 4 h induction; lane 3: purified BRCA1(1-139)<sup>wt</sup> and BRCA1(1-139)<sup>D67E</sup> proteins after reversed phase chromatography. The molecular mass of the wild-type and D67E BRCA1 proteins are 16301 and 16315 daltons, respectively.

```

1  MDLSALRVEE VQNVINAMQK ILECPICLEL IKEPVSTKCD HIFCKFCMLK 50
51  LLNQKKGPSQ CPLCKNDITK RSLQESTRFS QLVEELLKII CAFQLDTGLE 100
101 YANSYNFAKK ENNSPEHLKD EVSIIQSMGY RNRKRLLQ 139

```

**Figure 22.** Amino acid sequencing of the peptides after tryptic digestion. The BRCA1(1-139)<sup>wt</sup> protein band from Coomassie blue-stained SDS-PAGE was excised, alkylated with iodoacetamide, in-gel digested with trypsin, and then analysed by LC/ESI-MS/MS. Amino acid sequences of each tryptic peptide were shown as the italic bold letters. These corresponded to the N-terminal region of BRCA1. The Zn<sup>2+</sup>-binding sites were identified with the asterisk.

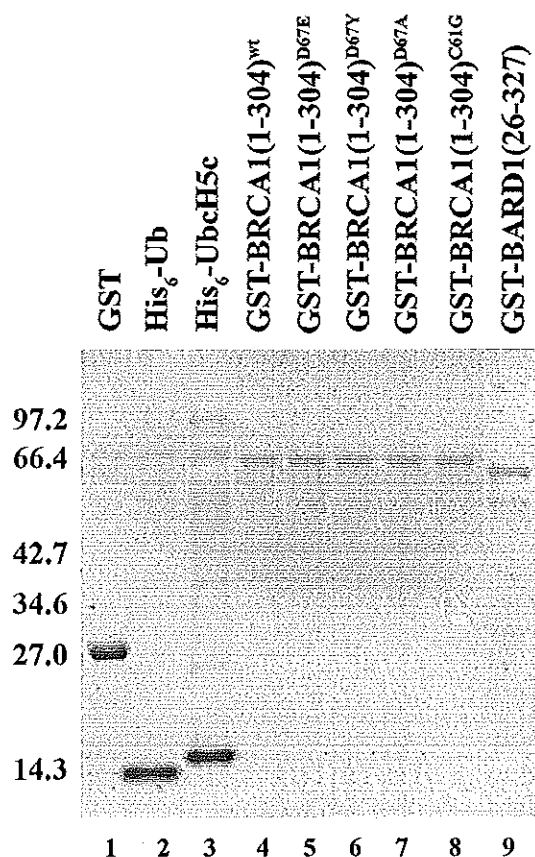


**Figure 23.** Purification of the affinity-tagged proteins. The GST, His<sub>6</sub>-Ub, His<sub>6</sub>-UbcH5c, GST-BRCA1(1-304)<sup>wt</sup>, GST-BRCA1(1-304)<sup>D67E</sup>, GST-BRCA1(1-304)<sup>D67Y</sup>, GST-BRCA1(1-304)<sup>D67A</sup>, GST-BRCA1(1-304)<sup>C61G</sup>, and GST-BARD1(26-327) proteins (2 μg; lane 1-9, respectively) were identified by 12% SDS-PAGE with Coomassie blue staining. The molecular mass marker (kDa) was positioned.

#### 4.2 Secondary structure and zinc(II)-binding of the D67E BRCA1 protein

Circular dichroism (CD) was used to examine the structural consequences of the D67E mutant and wild-type BRCA1 proteins upon Zn<sup>2+</sup>-binding. The mutant BRCA1(1-139) protein (10 μM) exhibited the CD spectral change in the presence of 5 μM and 10 μM Zn<sup>2+</sup> (Figure 24A). Interestingly, the CD spectra were identical in the presence of 20 μM, 30 μM, and 40 μM Zn<sup>2+</sup>, suggesting that Zn<sup>2+</sup>

saturated the mutant BRCA1 protein at the concentration of 20  $\mu\text{M}$ . Similarly, a change in the CD spectra was also observed for the wild-type protein (Figure 24B).

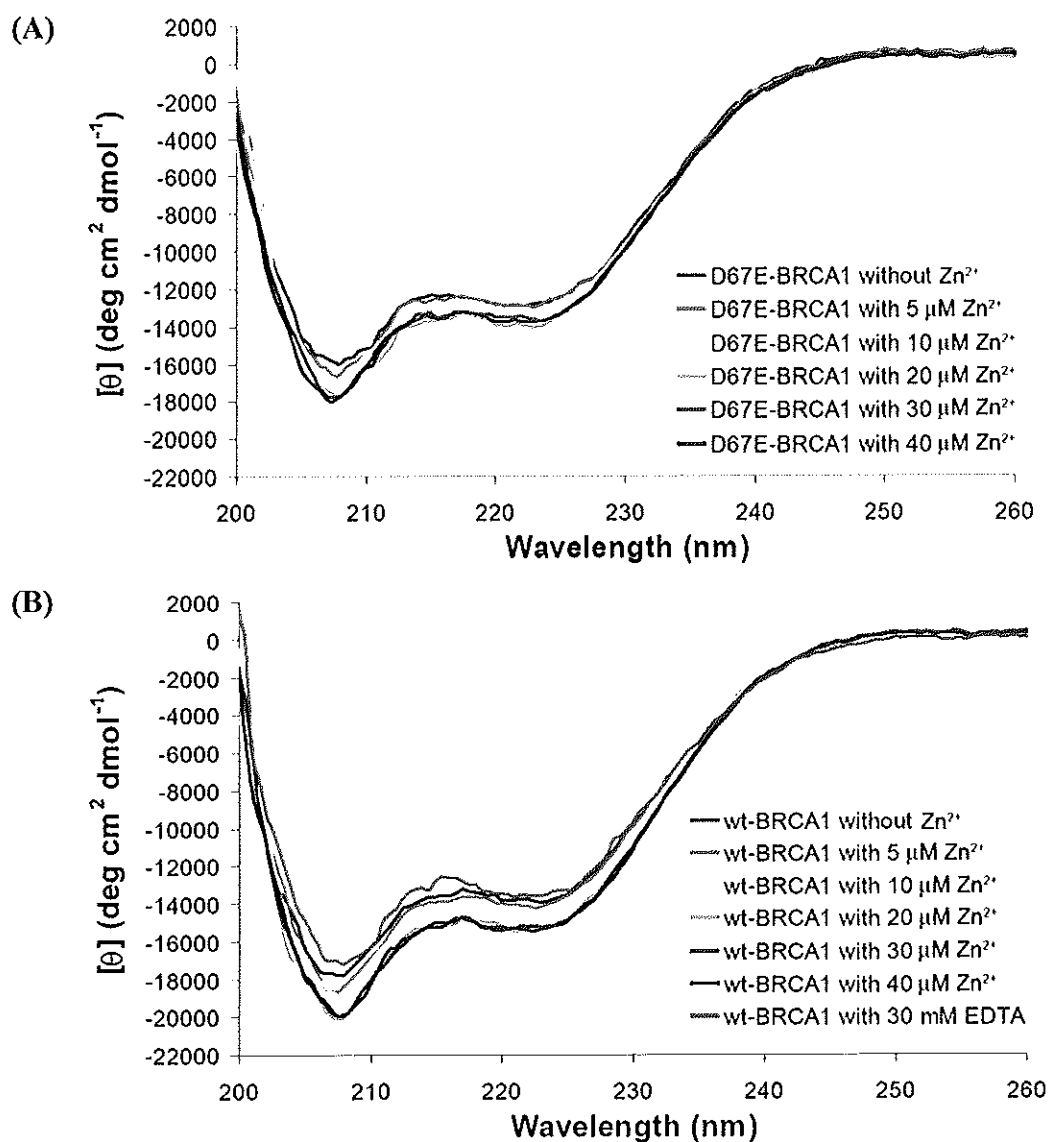


**Figure 24.** The CD spectra of the BRCA1 RING proteins. (A) The D67E and (B) wild-type BRCA1(1-139) proteins (10  $\mu\text{M}$ ) in the presence of 0, 5, 10, 20, 30, and 40  $\mu\text{M}$   $\text{Zn}^{2+}$  were used to monitor the zinc-dependent folding property of the BRCA1 RING domain. The wildtype protein with 30  $\mu\text{M}$  EDTA was also recorded. Values were given as the mean residue ellipticity. Samples were incubated with  $\text{Zn}^{2+}$  at 4°C for 24 h before CD measurement. The measurements were performed at 20°C with the scanning rate of 50 nm/min.

Based on the CONTIN program, the secondary structures of both proteins were predicted. In the absence of  $Zn^{2+}$ , there were 47% and 50%  $\alpha$ -helices, 12% and 24%  $\beta$ -sheets, 15% and 5%  $\beta$ -turns, and 26% and 22% disordered elements for the mutant and wild-type proteins, respectively. In the presence of 20  $\mu M$   $Zn^{2+}$ , structural changes were observed with 55% and 60%  $\alpha$ -helices, 8% and 4%  $\beta$ -sheets, 8% and 12%  $\beta$ -turns, and 29% and 24% disordered elements for such mutant and wild-type proteins, respectively. It indicated that the D67E mutation did not significantly perturb the native structure of the BRCA1 RING domain compared with the wild-type protein. In addition, the mutant protein still adopted a potentially preformed structure in the absence of  $Zn^{2+}$ , and was more folded upon  $Zn^{2+}$ -binding as judged by an increase in negative ellipticity at 208 and 220 nm. This was also supported by the coincidence of chromatographic elution profiles of both mutant and wild-type proteins that indicated the dimerization (Figure 25).

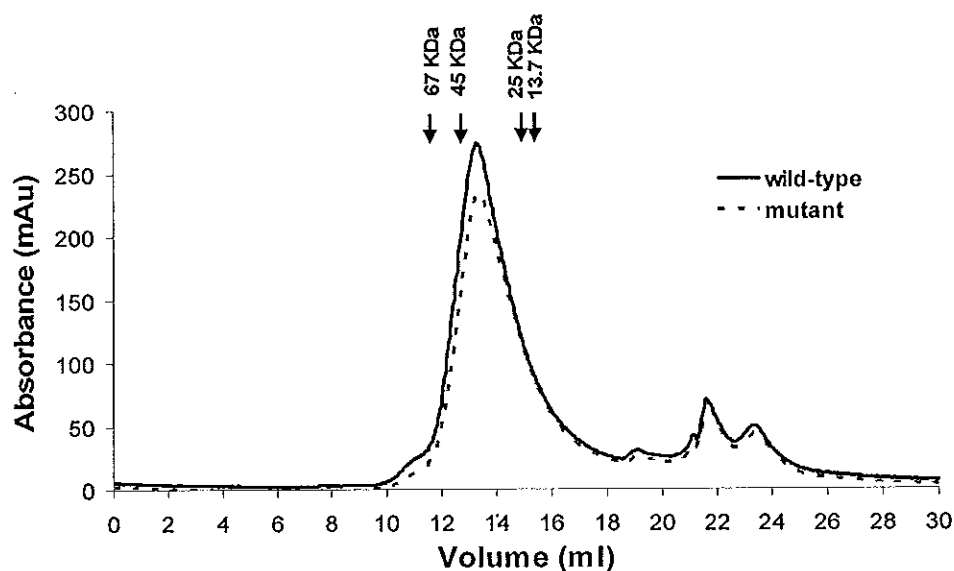


**Figure 25.** Gel-filtration chromatography of the BRCA1 RING domain. Elution profiles of the D67E (dash line), and wild-type (solid line) BRCA1(1-139) proteins were monitored at 212 nm. Positions for the protein standards were indicated by arrows. The predicted monomeric molecular mass based on the DNA sequence is 16315 and 16301 daltons for the D67E and wild-type BRCA1 proteins, respectively.

Moreover, the results from the glutaraldehyde cross-linking also confirmed that the D67E and wild-type BRCA1 proteins predominantly formed a dimer, although the higher order of oligomerization was also observed at the higher glutaraldehyde concentration and the prolonged incubation (Figure 26). The  $Zn^{2+}$ -binding constant of the mutant protein with a simple 1:2 (protein:metal) coordination model was  $2.91 \pm 0.20 \times 10^6 M^{-1}$ , and gave the free energy of binding ( $\Delta G$ ) of  $-8.66 \text{ kcal mol}^{-1}$  (Figure 27). These were almost identical to those of the wild-type protein with  $Zn^{2+}$  affinity of  $2.99 \pm 0.12 \times 10^6 M^{-1}$ , and a binding energy of  $-8.68 \text{ kcal mol}^{-1}$ . It indicated that the D67E mutation still retained  $Zn^{2+}$ -binding.

The absence of  $Zn^{2+}$  in protein samples was verified by recording the CD spectra in the presence of EDTA (Figure 24B). The result was similar to that of the protein without  $Zn^{2+}$ , and revealed 47%  $\alpha$ -helix, 29%  $\beta$ -sheets, 10%  $\beta$ -turn, and 15% disordered elements. Moreover, X-ray absorption near-edge structure (XANES) was used to assess the apo form of proteins. The excitation photon energy was scanned through the XANES energy range of the  $Zn^{2+}$  K-edge in which  $Zn^{2+}$  generally showed the characteristic edge at 9659 eV. Proteins in the presence of EDTA, and in the absence of  $Zn^{2+}$  revealed the identical profiles with no characteristic edge of  $Zn^{2+}$  (Figure 28). It implied that the protein samples did not contain  $Zn^{2+}$  at the detectable amount. On the other hand, the proteins in the presence of an equimolar ratio of  $Zn^{2+}$  to protein, revealing the characteristic edge of  $Zn^{2+}$  with an inflection point at 9662 eV represented a positive control.

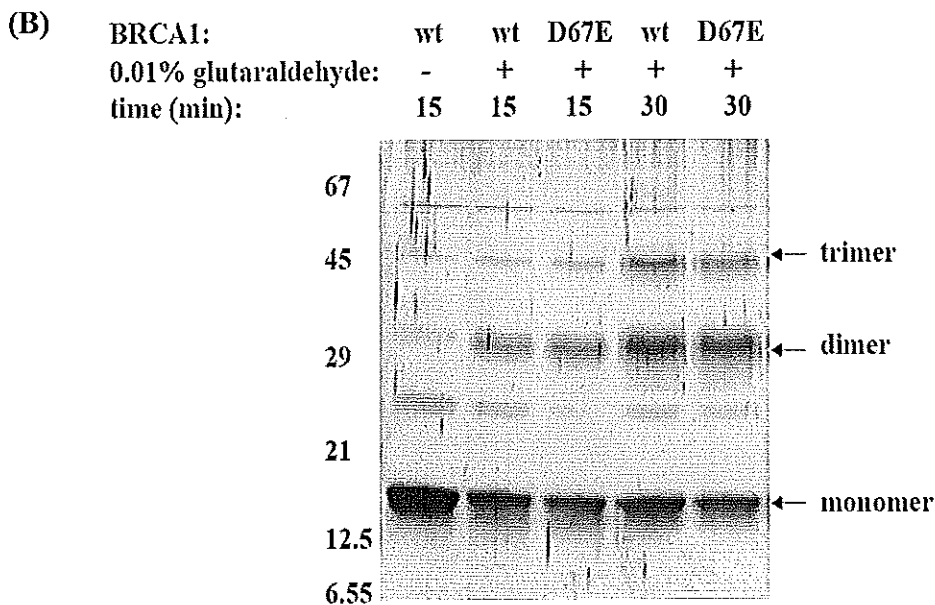
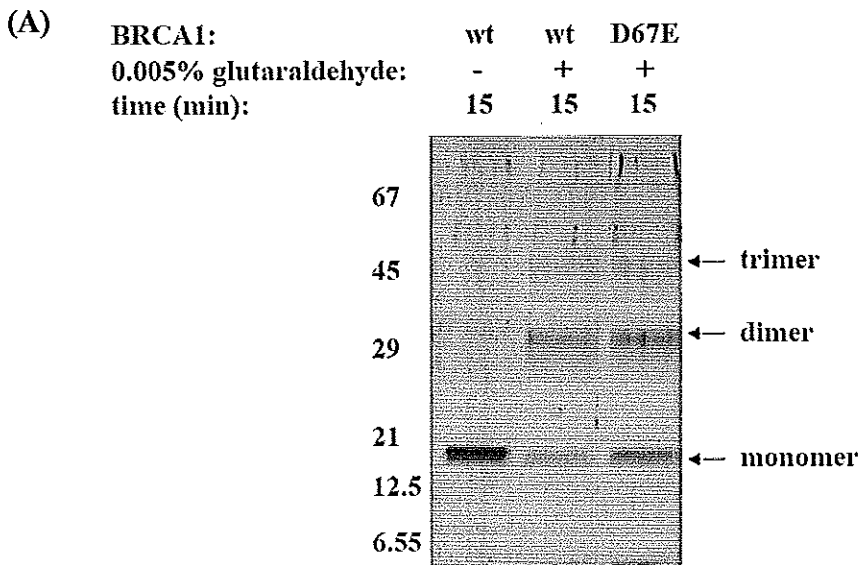


**Figure 26.** 15% SDS-PAGE of glutaraldehyde cross-linking. The BRCA1(1-139)<sup>wt</sup> and BRCA1(1-139)<sup>D67E</sup> proteins were incubated without (-) or with (+) 0.005% (A) and 0.01% (B) (w/v) glutaraldehyde at ambient temperature for 15 and 30 min. The predicted monomeric molecular mass based on the DNA sequence is 16301 and 16315 daltons for the wild-type and D67E BRCA1 proteins, respectively.

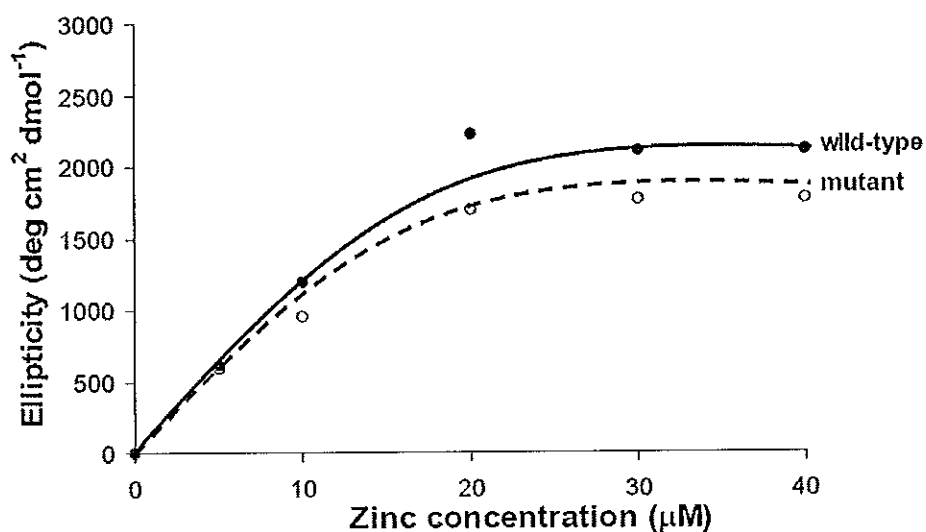


**Figure 27.** Titration curves of  $Zn^{2+}$ -binding to the BRCA1 RING proteins. Changes in ellipticity at 208 nm with increasing  $Zn^{2+}$  concentrations of the D67E mutant (dash line), and wild-type BRCA1(1-139) proteins (solid line) were plotted. The binding constants were  $2.91 \times 10^6$  and  $2.99 \times 10^6 M^{-1}$  for the mutant and wild-type proteins, respectively.

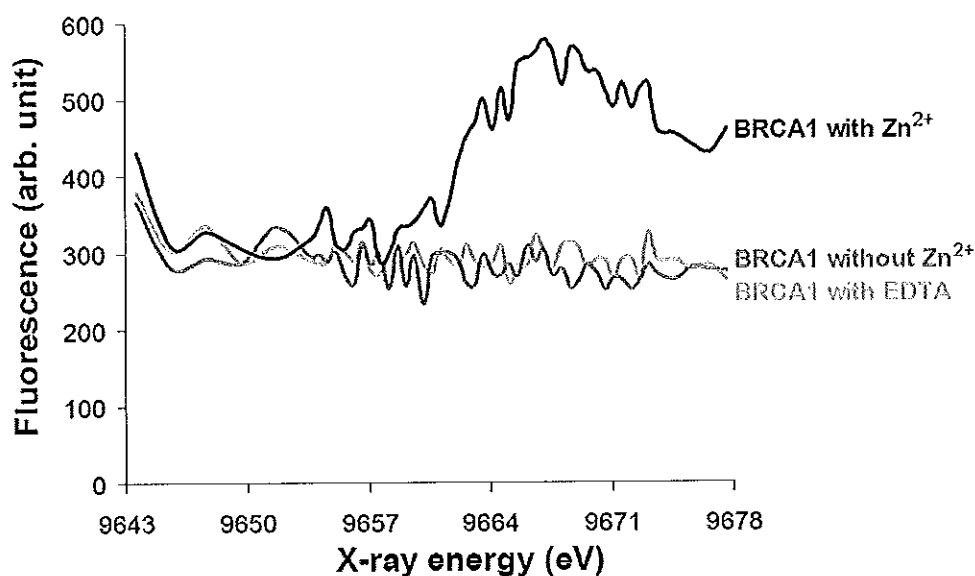


**Figure 28.** X-ray absorption near-edge structure (XANES) of the wild-type BRCA1(1-139) RING proteins. Samples were incubated without  $Zn^{2+}$ , with an equimolar ratio of  $Zn^{2+}$  to protein, and with 10 mM EDTA at 4°C for 24 h before XANES measurement.

### 4.3 Proteolytic resistance of the D67E BRCA1 mutation

Limited proteolysis was used to probe the structural consequences of the BRCA1 mutations upon  $Zn^{2+}$ -binding. The D67E mutant BRCA1(1-139) protein without  $Zn^{2+}$  or in excess of EDTA was rapidly degraded after the addition of elastase (Figure 29A). Two residual fragments were apparent, and the examination by in-gel tryptic digestion with mass spectrometry revealed the identity of the residues 1-88 and 8-38 which possessed only the minimal RING domain. Similar results were obtained with trypsin digestion (Figure 29B). The results suggested that two long helices (residues 8-22 and 81-96) of the BRCA1 protein were potentially involved in the proteolytic prevention of the RING structure in the absence of  $Zn^{2+}$  although the BRCA1 protein without  $Zn^{2+}$  was globally flexible with slightly or no protease-resistance. On the other hand, the mutant protein was rather resistant to proteolysis throughout the time course in the presence of  $Zn^{2+}$  (Figures 29C and 29D). It indicated that  $Zn^{2+}$  caused the structure of the BRCA1 protein to be more folded or rigid with reduced proteolytic susceptibility throughout its C-terminal portion. Similar limited proteolysis profiles were also observed for the wild-type BRCA1 protein (Figure 30). It indicated that the D67E mutation maintained  $Zn^{2+}$ -binding, and barely perturbed the native global structure of the BRCA1 RING domain.



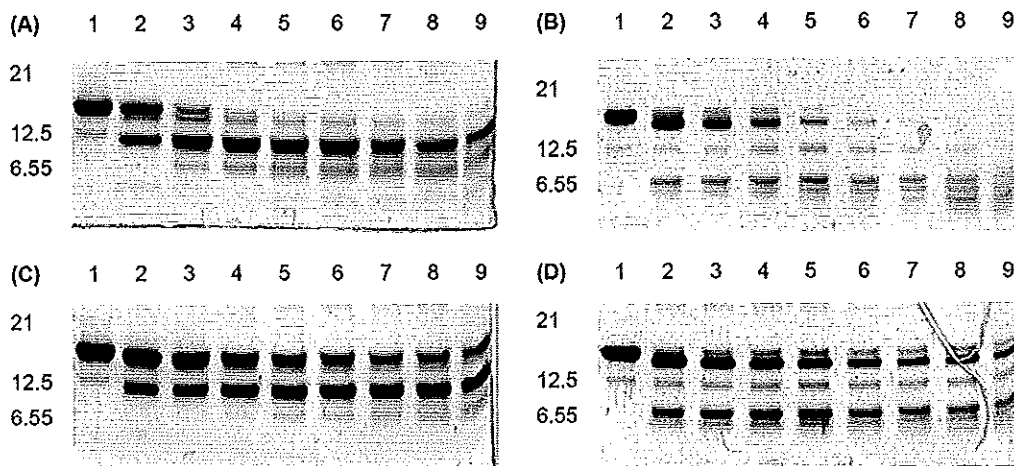


**Figure 29.** Limited proteolysis of the D67E BRCA1 protein. Purified D67E BRCA1(1-139), without (A and B) and with (C and D)  $Zn^{2+}$ , were incubated with elastase (A and C) or trypsin (B and D) at the protein-protease ratio of 100-200:1 (w/w). Reaction aliquots were removed at 0, 0.25, 0.5, 1, 2, 3, 6, 12, and 24 h after the addition of protease (lanes 1-9, respectively), and then identified on 15% Coomassie blue-stained SDS-PAGE. The molecular mass marker (kDa) was positioned.

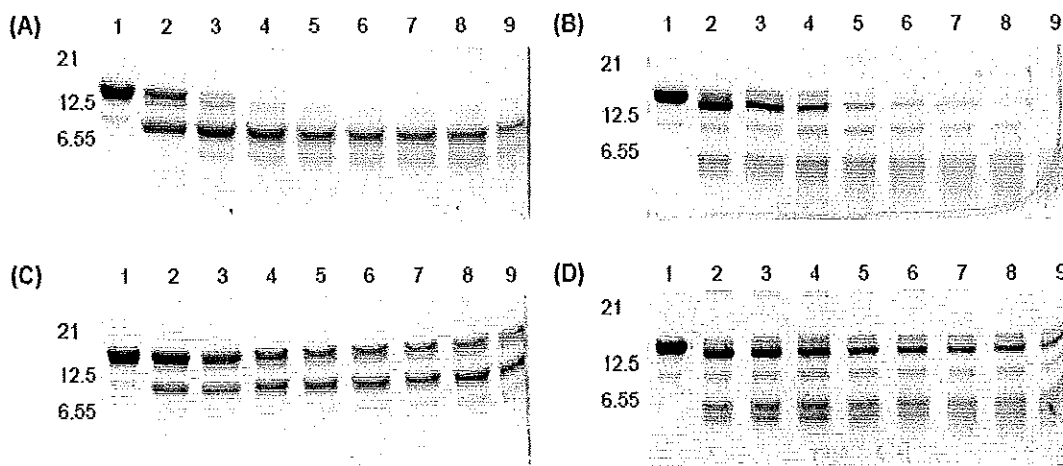


**Figure 30.** Limited proteolysis of the wild-type BRCA1 protein. Purified wild-type BRCA1(1-139), without (A and B) and with (C and D)  $Zn^{2+}$ , were incubated with elastase (A and C) or trypsin (B and D) at the protein-protease ratio of 100-200:1 (w/w). Reaction aliquots were removed at 0, 0.25, 0.5, 1, 2, 3, 6, 12, and 24 h after the addition of protease (lanes 1-9, respectively), and then identified on 15% Coomassie blue-stained SDS-PAGE. The molecular mass marker (kDa) was positioned.

#### 4.4 Thermal stability of the D67E BRCA1 mutation

Thermal unfolding was monitored by CD to determine the stability of the BRCA1 RING domain. The D67E mutant and wild-type BRCA1(1-139) proteins in the absence and presence of  $Zn^{2+}$  gave identical changes in CD spectra with an increase in ellipticity when the temperature was raised from 15°C to 95°C (Figures 31 and 32). It indicated that the folded proteins gradually lost their ordered structures upon thermal denaturation. However, the unfolding/refolding of protein was irreversible (20°C after 95°C). The irreversibility was caused by the aggregation of the heat-unfolded protein during denaturation. As a result, no thermodynamic parameters could be analyzed. The thermal unfolding curves obtained were used for comparison of protein stabilities (Figure 33). The unfolding transition temperatures ( $T_m$ ) in the absence and presence of  $Zn^{2+}$  were  $77.6 \pm 0.2^\circ\text{C}$  and  $85.5 \pm 0.1^\circ\text{C}$  for the wild-type, and  $76.0 \pm 0.3^\circ\text{C}$  and  $82.6 \pm 0.2^\circ\text{C}$  for the mutant D67E BRCA1(1-139) proteins, respectively. It was likely that the  $Zn^{2+}$ -bound proteins were more thermostable by about 8°C than the  $Zn^{2+}$ -free form. The stability was apparently attributed to the cooperative  $Zn^{2+}$  coordination at the metal-binding sites. However, the D67E mutant appeared to be 3°C less thermostable than the wild-type protein as indicated by a broader transition and a lower melting temperature.

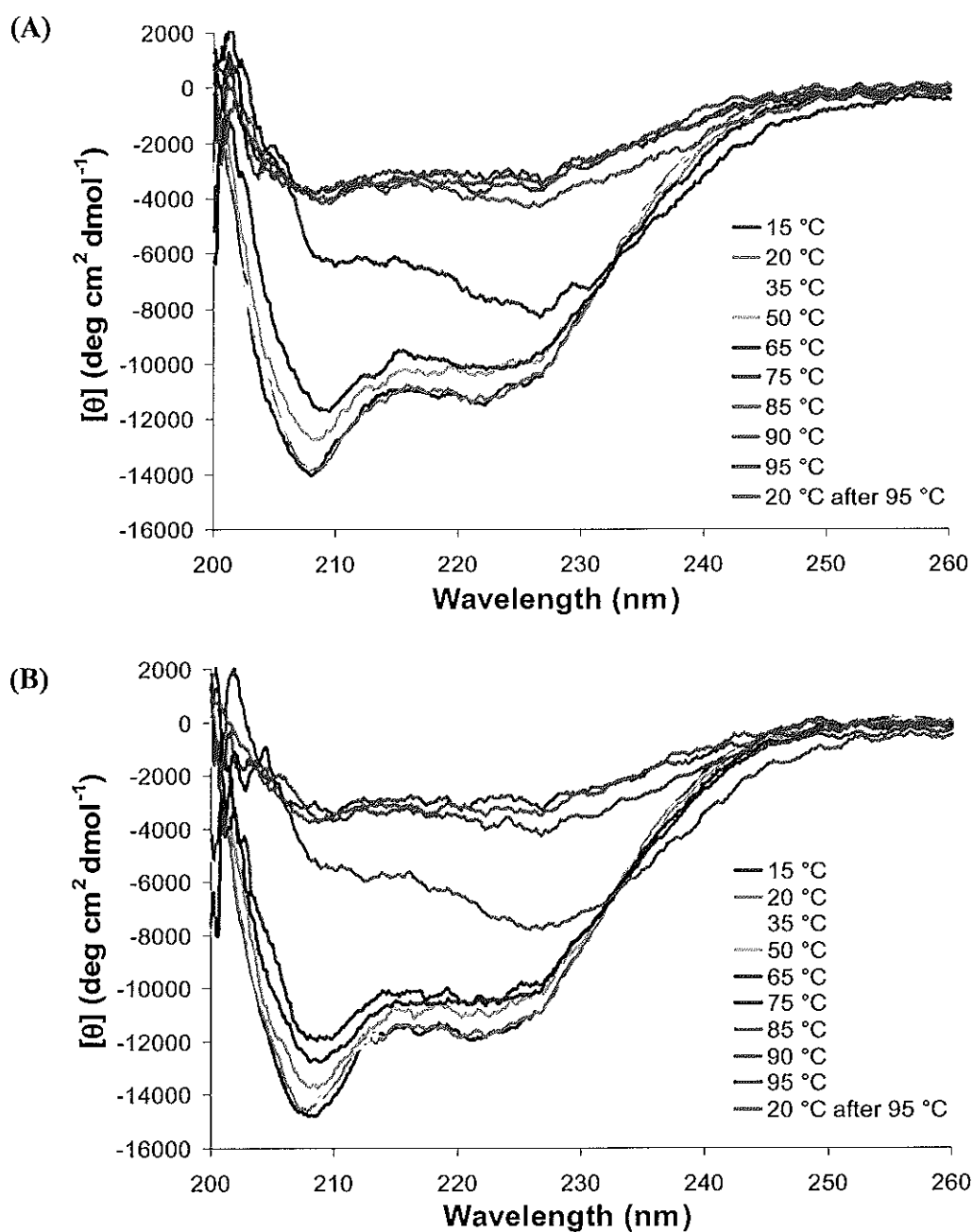


**Figure 31.** Thermal transition of the D67E BRCA1 protein. Thermal denaturations of 10  $\mu\text{M}$  D67E BRCA1(1-139), (A) in the absence of  $\text{Zn}^{2+}$  or (B) in the presence of 30  $\mu\text{M}$   $\text{Zn}^{2+}$ , were monitored by CD at defined temperatures. Samples were incubated at 4°C for 24 h before CD measurement. The measurements were performed from 15°C to 95°C with a heating rate of 1°C/min. After heating at 95°C, the measurement at 20°C was also performed. The CD spectra were plotted between wavelength and mean residue ellipticity.

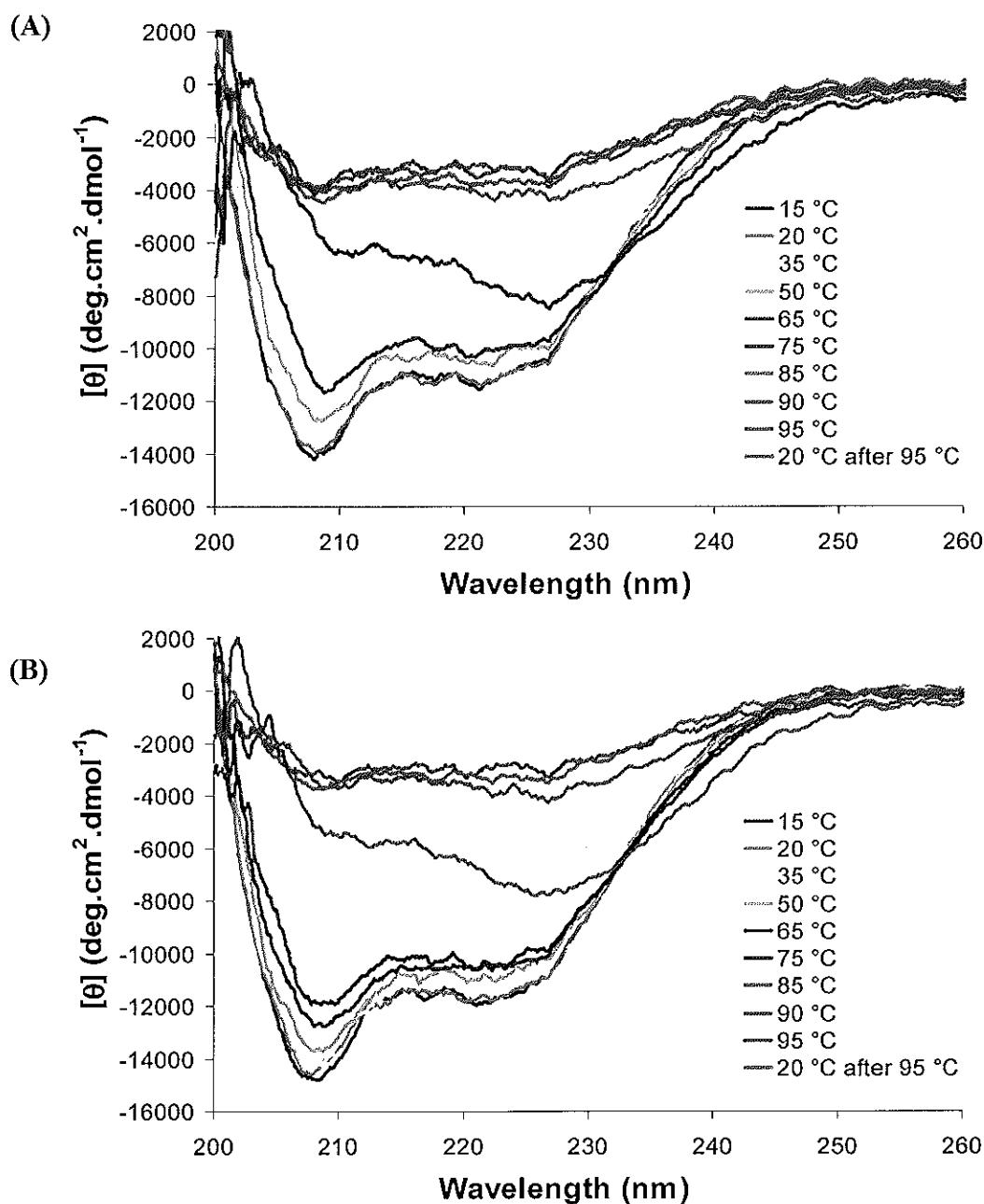


**Figure 32.** Thermal transition of the wild-type BRCA1 protein. Thermal denaturations of 10  $\mu\text{M}$  wild-type BRCA1(1-139), (A) in the absence of  $\text{Zn}^{2+}$  or (B) in the presence of 30  $\mu\text{M}$   $\text{Zn}^{2+}$ , were monitored by CD at defined temperatures. Samples were incubated at 4°C for 24 h before CD measurement. The measurements were performed from 15°C to 95°C with a heating rate of 1°C/min. After heating at 95°C, the measurement at 20°C was also performed. The CD spectra were plotted between wavelength and mean residue ellipticity.

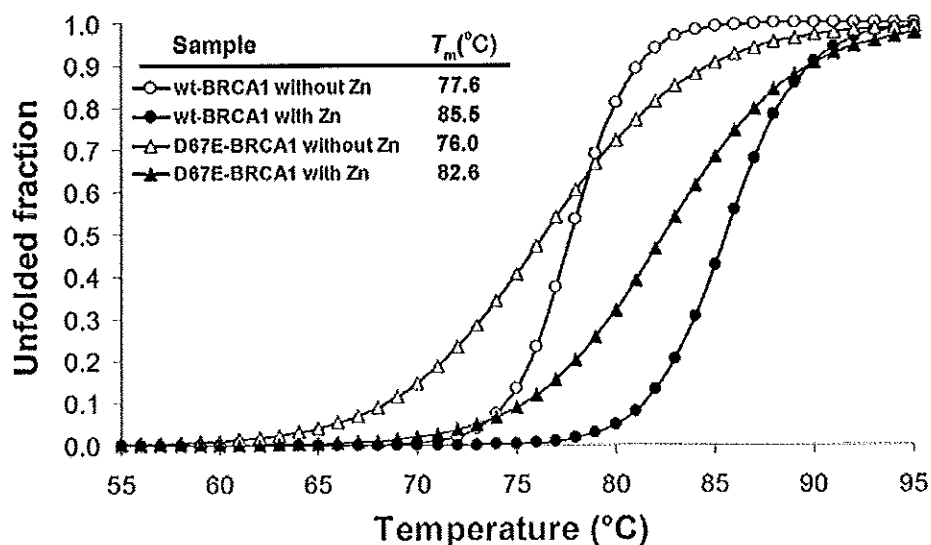


**Figure 33.** Thermal unfolding curve of the BRCA1 RING domains. The wild-type (wt) and D67E BRCA1(1-139) proteins (10  $\mu$ M) were incubated without or with 30  $\mu$ M  $Zn^{2+}$  at 4°C for 24 h before CD measurement. Samples were heated from 15°C to 95°C with a rate of 1°C/min, and the CD signals at 208 nm were measured. The unfolded fraction as a function of temperature was plotted.

#### 4.5 *In vitro* ubiquitin ligase activity of the D67E BRCA1 protein

Previous studies demonstrated that BRCA1 and BARD1 formed a stable heterodimeric complex through their RING domains. The BRCA1 and BARD1 RING complex showed an enzymatic activity of E3 ubiquitin ligase, promoting the formation of high molecular weight polyubiquitin species. The BRCA1(1-139) and BRCA1(1-304) proteins were compared for their capability of ubiquitination. The extended BRCA1 RING domain exhibited a higher activity of ubiquitin ligase, suggesting that the sequences outside the minimal RING domain of BRCA1 were required for an efficient activity (Figure 34). The apparent ubiquitinated products, migrating at ~70, 80, and 212 kDa, were likely to be the free ubiquitin polymer or autoubiquitinated BRCA1 or BARD1 conjugates, respectively (Figure 34, filled diamond) (Chen *et al.*, 2002; Nishikawa *et al.*, 2004; Wu-Bear *et al.*, 2010).

Individual GST protein as a negative control did not contribute to the activity. Therefore, GST-BRCA1(1-304) was further used for the ubiquitin ligase reactions. The reaction incubation of 3 h apparently showed the ubiquitinated products (Figure 35), and the BRCA1-directed ubiquitination was ATP-dependent (Figure 36). Furthermore, the isolated BRCA1 protein showed some activity, whereas in the presence of BARD1 it displayed the greater activity than an individual BRCA1 or BARD1 subunit (Figure 36).

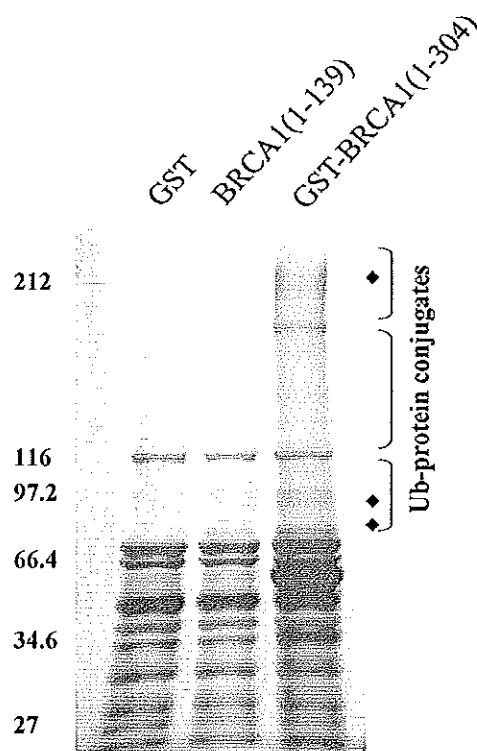


**Figure 34.** The extended BRCA1 RING domain exhibited the higher ubiquitination. The ubiquitin ligase reactions, containing 20  $\mu$ M His<sub>6</sub>-Ub, 300 nM His<sub>6</sub>-E1, 5  $\mu$ M His<sub>6</sub>-UbcH5c, 2  $\mu$ g BRCA1(1-139) or 2  $\mu$ g GST-BRCA1(1-304), and 2  $\mu$ g GST-BARD1(26-327), were incubated at 37°C for 3 h. The samples were terminated by adding an equal volume of SDS-loading dye, and heating at 95°C for 5 min. The samples were then resolved on 8% silver-stained SDS-PAGE. The GST protein (2  $\mu$ g) was used as a negative control. The apparent ubiquitinated products were indicated by filled diamond.

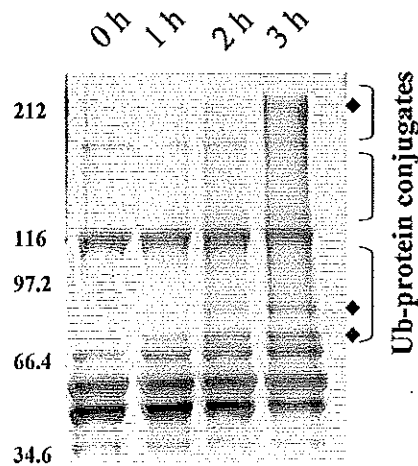


**Figure 35.** Time-dependence of the ubiquitination reaction. The ubiquitin ligase reactions, containing 20  $\mu$ M His<sub>6</sub>-Ub, 300 nM His<sub>6</sub>-E1, 5  $\mu$ M His<sub>6</sub>-UbcH5c, 2  $\mu$ g GST-BRCA1(1-304), and 2  $\mu$ g GST-BARD1(26-327), were incubated for various length of time (0, 1, 2, and 3 h) at 37°C. The samples were terminated by adding an equal volume of SDS-loading dye, and heating at 95°C for 5 min. The samples were then resolved on 8% silver-stained SDS-PAGE.

ATP	-	+	+	+	+	+	+	+
Ub	+	-	+	+	+	+	+	+
E1	+	+	-	+	+	+	+	+
UbcH5c	+	+	+	-	+	+	+	+
BRCA1	+	+	+	+	-	-	+	+
BARD1	+	+	+	+	-	+	-	+

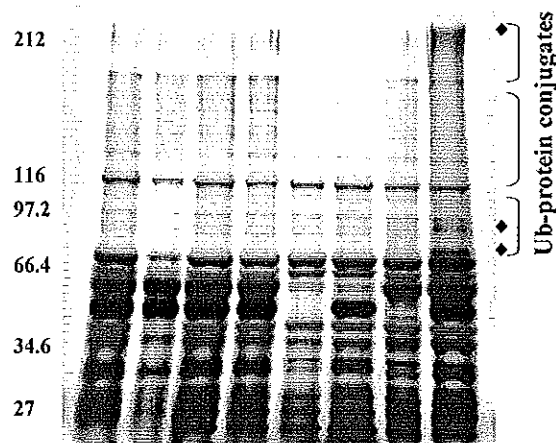


**Figure 36.** *In vitro* ubiquitination. The reactions, lacking a defined reactant, were incubated at 37°C for 3 h, and assayed for the ubiquitin ligase activities. The samples were terminated by adding an equal volume of SDS-loading dye, and heating at 95°C for 5 min. The samples were then resolved on 8% silver-stained SDS-PAGE.

In order to determine the functional consequences of the mutations on the BRCA1 RING domain, the breast cancer-predisposing mutation of the second Zn<sup>2+</sup>-binding residue (C61G) was used as a negative control. The C61G BRCA1 mutation completely abolished the ubiquitin ligase activity (Figure 37). Moreover, the familial D67E and the designed D67A BRCA1 mutations still maintained the ubiquitination activity identically to the wild-type protein, whereas the D67Y mutation partially abrogated this activity (Figure 37).

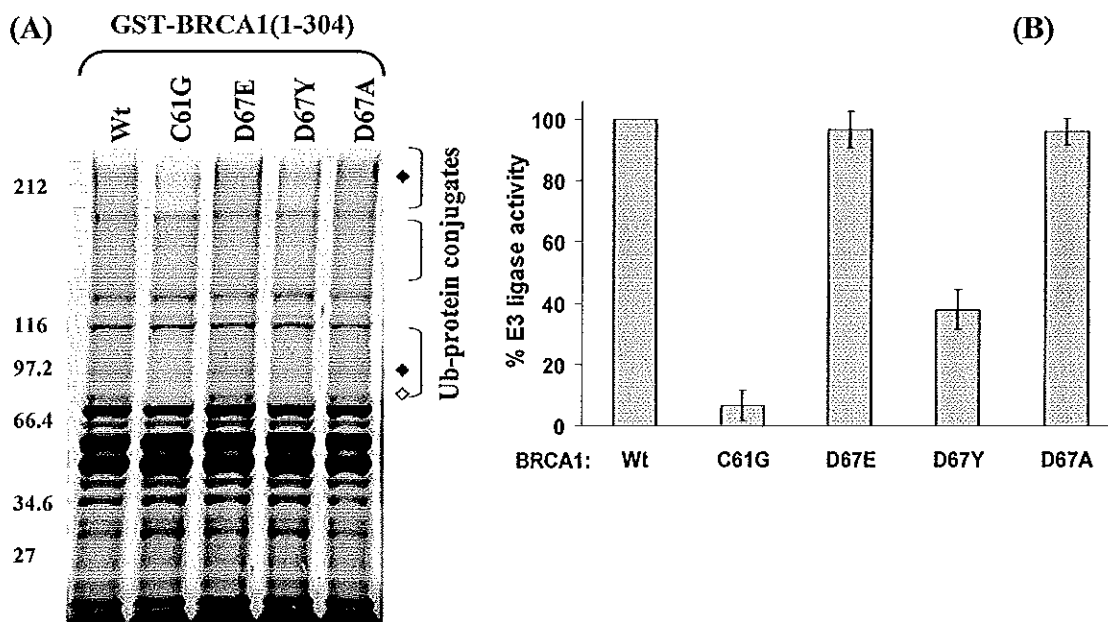
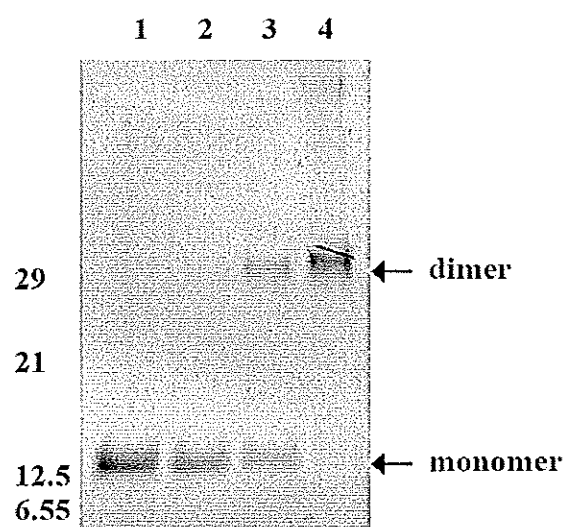


**Figure 37.** (A) *In vitro* ubiquitin ligase activity of the mutant BRCA1 RING proteins. The mutant BRCA1 proteins (C61G, D67E, D67Y, and D67A) were assayed for the ubiquitin ligase activity compared to the wild-type protein. The ubiquitin ligase reactions, containing 20  $\mu$ M His<sub>6</sub>-Ub, 300 nM His<sub>6</sub>-E1, 5  $\mu$ M His<sub>6</sub>-UbcH5c, 2  $\mu$ g GST-BRCA1(1-304), and 2  $\mu$ g GST-BARD1(26-327), were incubated at 37°C for 3 h. The samples were terminated by adding an equal volume of SDS-loading dye, and heating at 95°C for 5 min. The samples were then resolved on 8% silver-stained SDS-PAGE. (B) An apparent ubiquitinated product as indicated by opened diamond from the two separate reactions was quantified by Bio-Rad GS-700 Imaging Densitometer. The relative E3 ligase activity (%) was plotted against each BRCA1 RING variant.

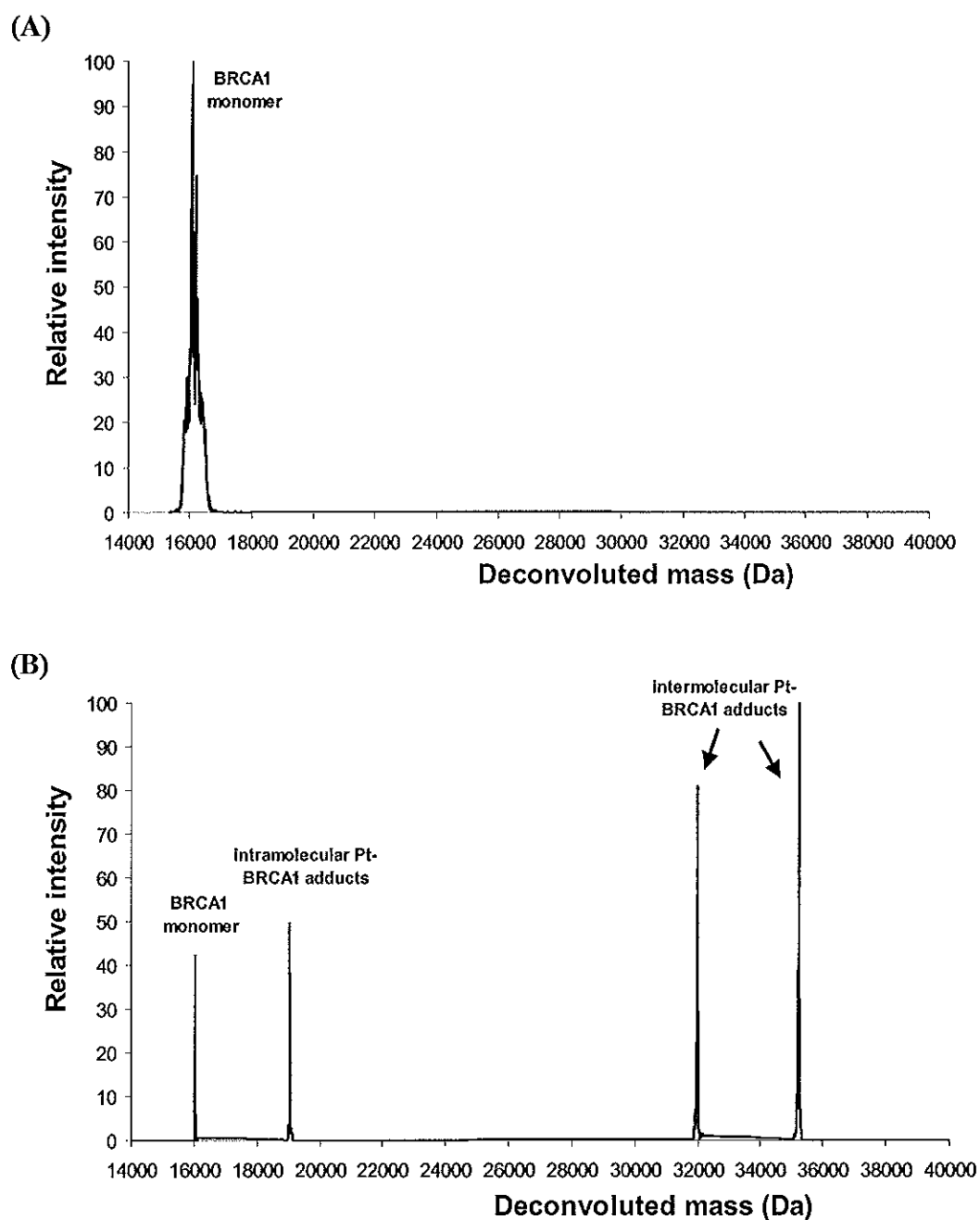


#### 4.6 Cisplatin binding to the BRCA1 RING domain

It was well established that cisplatin induced the bifunctional adducts through the intermolecular crosslinks of some proteins (Ivanov *et al.*, 1998). The mono- and trifunctional protein adducts also occurred by the intramolecular crosslinks (Peleg-Shulman *et al.*, 2002). Thus, the types of adduct formation by cisplatin are distinctive and dependent on the accessibility of platinum center and protein side-chains. The BRCA1 RING domain formed intermolecular crosslinks caused by cisplatin, and the high amount of crosslinks was accompanied by an increase in cisplatin concentration (Figure 38). This result was further verified by mass spectrometric analysis, suggesting favourably intramolecular and intermolecular BRCA1 adducts (Figure 39).



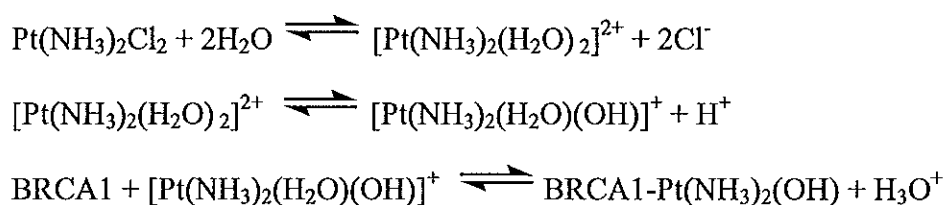
**Figure 38.** 15% SDS-PAGE of the cisplatin-BRCA1 intermolecular crosslinks. The BRCA1(1-139) protein (10  $\mu\text{M}$ ) was incubated with a number of cisplatin concentrations in the dark at 37°C for 24 h. Lane 1: protein without cisplatin ; lane 2-4: proteins with 10, 100, and 1000  $\mu\text{M}$  cisplatin, respectively.



**Figure 39.** Mass spectrometric analyses of the cisplatin-BRCA1 adducts. (A) BRCA1(1-139) proteins (15  $\mu$ M) or (B) cisplatin-BRCA1(1-139) adducts (1:1) were incubated in the dark at 37°C for 24 h. Samples were directly subjected to an ESI mass spectrometer, and the deconvoluted spectra were given.

Although cisplatin has been demonstrated to induce protein dimerization and perturbed some protein structures, the secondary structure of the BRCA1 RING domain in the apo-form was maintained and underwent more folded structural rearrangement after increasing cisplatin concentrations as judged by an increase in negative CD spectra at 208 and 220 nm (Figure 40A). It was possible that cisplatin might bind to the unoccupied  $Zn^{2+}$ -binding sites and caused the structural changes from 50%  $\alpha$ -helix, 9%  $\beta$ -sheets, 14% turn, and 26% disordered element to 60%  $\alpha$ -helix, 2%  $\beta$ -sheets, 15% turn, and 24% disordered element, respectively. The binding constant of the *in vitro* platination was  $3.00 \pm 0.11 \times 10^6 M^{-1}$ , and the free energy of binding ( $\Delta G$ ) was  $-8.68 \text{ kcal mol}^{-1}$  (Figure 41). In addition, CD spectra of BRCA1 pre-incubated with  $Zn^{2+}$  gave the identical profiles, suggesting that cisplatin could interact with other residues rather than the  $Zn^{2+}$ -binding sites and barely affected the overall conformation of  $Zn^{2+}$ -bound BRCA1 (Figure 40B).

In order to locate the binding site of cisplatin on the BRCA1(1-139) protein, in-gel tryptic digestion of the free BRCA1 and the cisplatin-BRCA1 adducts (molar ratio 1:1) were subjected to analysis by LC-MS. The result revealed a unique fragment ion of  $656.29^{2+}$  obtained only from the cisplatin-BRCA1 adduct digests (Figure 42). Tandem mass spectrometric analyses (MS/MS) of the  $656.29^{2+}$  ion (measured mass 1310.57 Da) indicated that the ion arose from  $[Pt(NH_3)_2(OH)]^+$  (theoretical mass 245.99 Da) that attached to a BRCA1 peptide  $^{111}ENNSPEHLK^{119}$  (theoretical mass 1066.44 Da) with a mass difference of 0.86 (Figure 43). Coordination of water to cisplatin lowers its  $pK_a$  ( $pK_{a1}$  5.37 and  $pK_{a2}$  7.21), giving hydroxo forms (Berners-Price *et al.*, 1992). This product potentially reacted with BRCA1 and yielded BRCA1- $Pt(NH_3)_2(OH)$  as described by the following reactions.



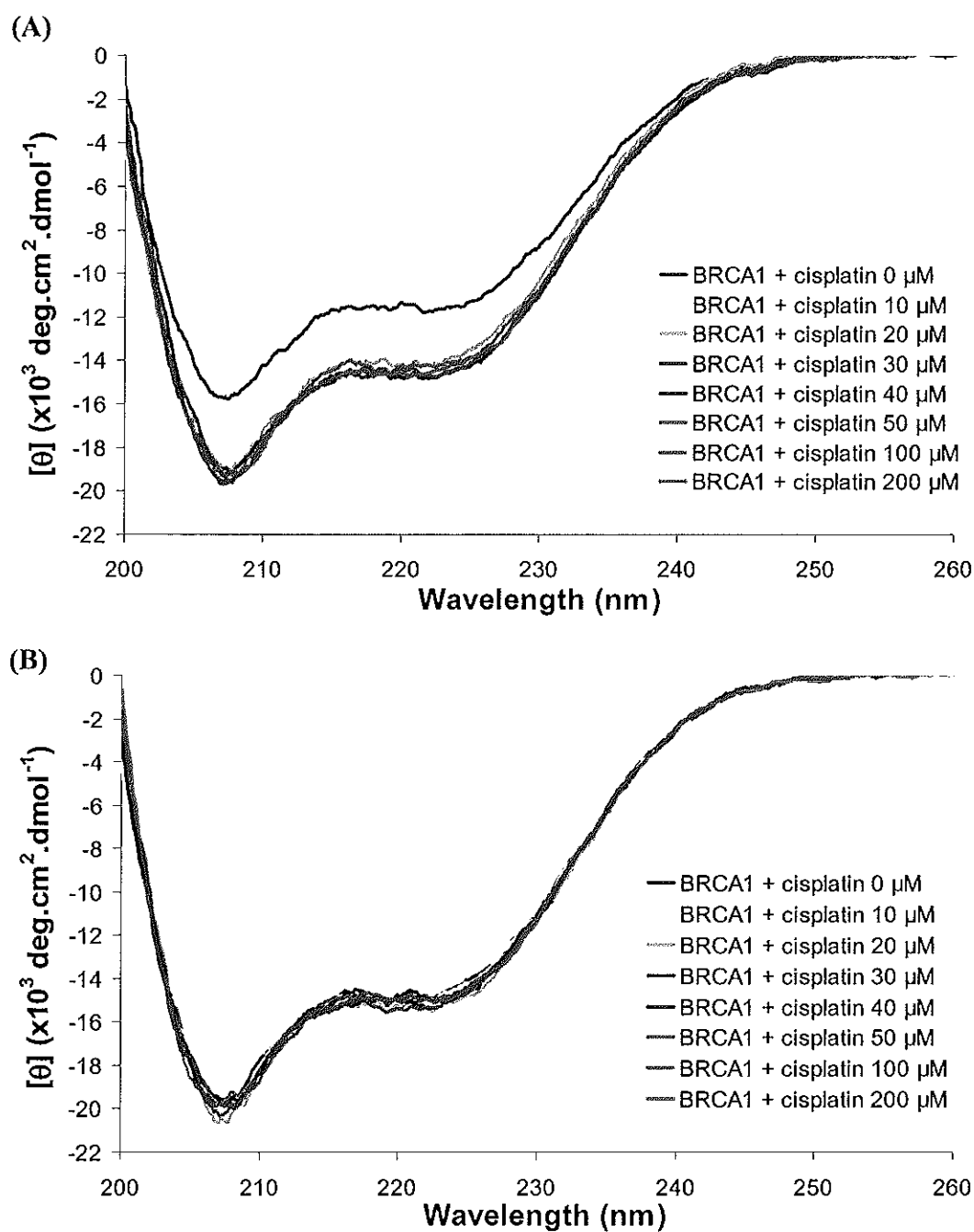


**Figure 40.** The CD spectra of the cisplatin-BRCA1 adducts. BRCA1(1-139) proteins (10  $\mu\text{M}$ ) without  $\text{Zn}^{2+}$  (A) and with pre-incubation of 3 molar equivalent ratio of  $\text{Zn}^{2+}$  to protein (B) were mixed by a number of cisplatin concentrations. Samples were incubated in the dark at ambient temperature for 24 h before CD measurement at  $20^\circ\text{C}$  with the scanning rate of 50 nm/min. The mean residue ellipticity and wavelength ranging from 200 nm to 260 nm were plotted.

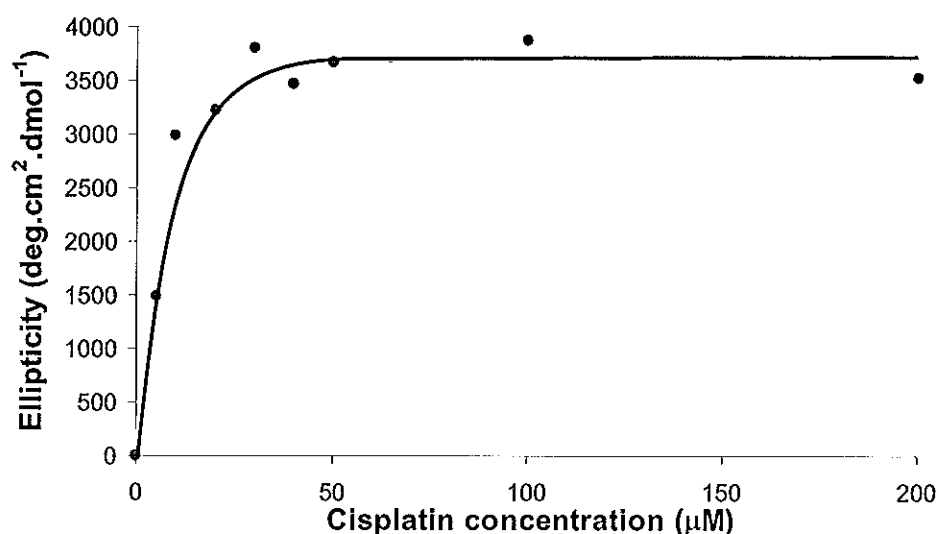


**Figure 41.** Titration curve of cisplatin binding to the BRCA1(1-139) protein. Changes in ellipticity of protein at 208 nm with increasing cisplatin concentrations were plotted. The calculated binding constant using equation (1) (chapter 3, materials and methods) was  $3.00 \pm 0.11 \times 10^6 \text{ M}^{-1}$ .

The product-ion spectrum of the  $656.29^{2+}$  ion revealed the sequence ions ( $b_2^+$ ,  $[b_3-H_2O]^+$ ,  $[b_4-H_2O]^+$ ,  $[b_6-H_2O]^+$ ,  $[b_7-H_2O]^+$ ,  $b_7^+$ ,  $[b_8-H_2O]^+$ ,  $b_8^+$ , and  $y_2^+$ ) that corresponded to the peptide Glu111-Lys119 of BRCA1 (Figure 43). The observed  $1165.53^+$  and  $1293.57^+$  ions were the platinum-bound  $b_8^+$  (theoretical  $m/z$   $1166.39^+$ ) and  $b_9^+$  (theoretical  $m/z$   $1294.43^+$ ), respectively, whereas the  $656.28^+$  ion was assigned as the platinum-free  $b_6^+$  ion with losing a water molecule (theoretical  $m/z$   $653.26^+$ ). It was speculated that cisplatin interacted with the counterpart of the  $b_6^+$  ion (His117-Lys119). The  $641.32^+$  ion was the platinum-containing  $y_3^+$  ion (theoretical  $m/z$   $642.24^+$ ), and the  $260.19^+$  ion was the platinum-free  $y_2^+$  ion (theoretical  $m/z$   $260.20^+$ ). The difference in  $m/z$  (381.13 Da) indicated the binding of cisplatin to His117 (theoretical  $m/z$  382.05 Da).

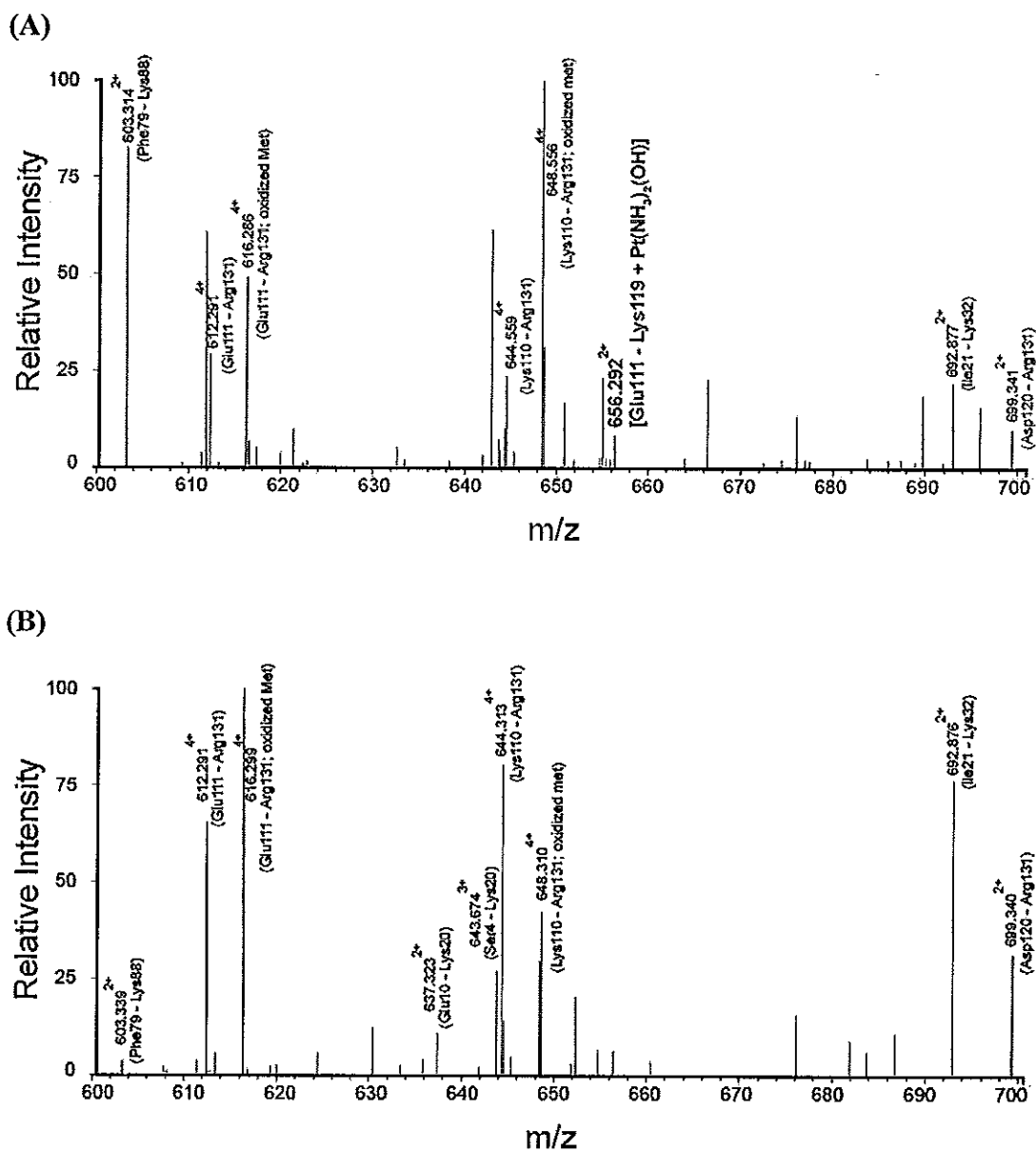


**Figure 42.** Mass spectrometric analyses of the cisplatin-BRCA1(1-139) adduct digests. In-gel tryptic digestion of (A) the cisplatin-BRCA1 adducts (molar ratio 1:1), and (B) free BRCA1 were subjected to analysis by LC-MS. A unique fragment ion of 656.29<sup>2+</sup> only derived from the cisplatin-BRCA1 adduct digests presented a platinum-containing peptide.

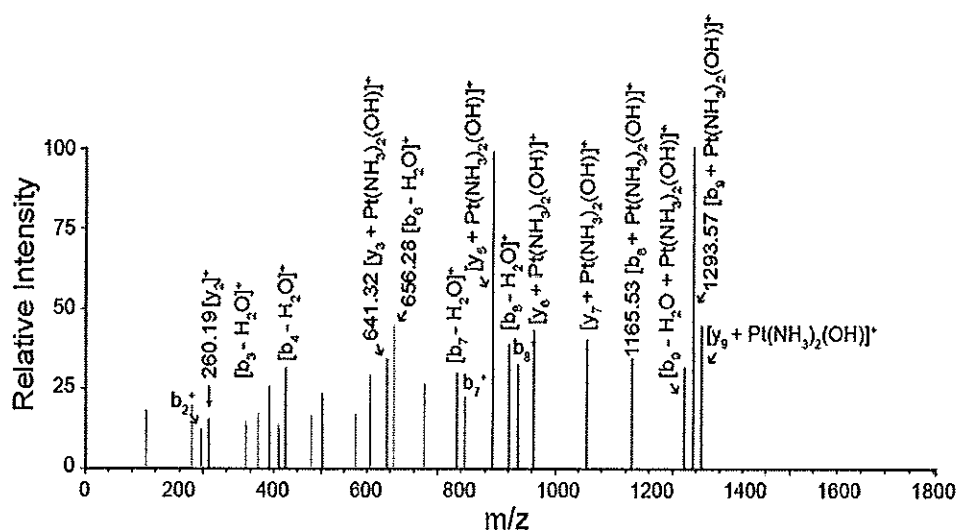
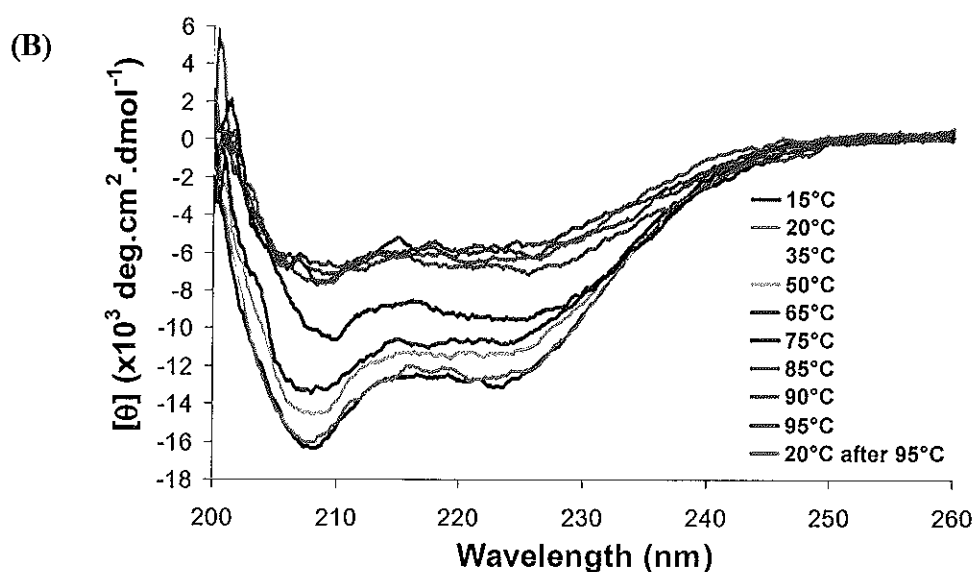
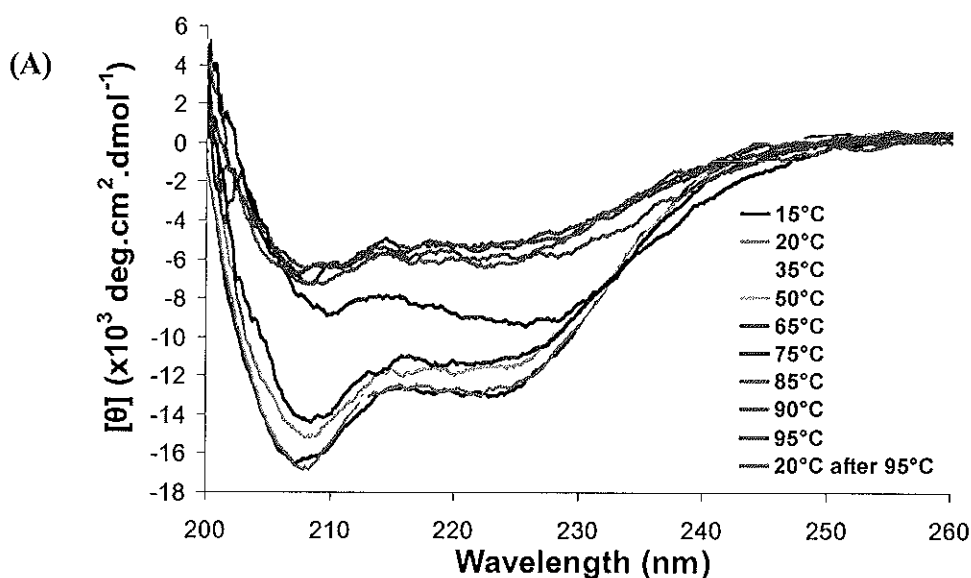


**Figure 43.** The product-ion spectrum of the MS/MS analysis for the  $656.29^{2+}$  ion. It indicated that  $[\text{Pt}(\text{NH}_3)_2(\text{OH})]^+$  attached to a peptide  $^{111}\text{ENNSPEHLK}^{119}$  of BRCA1.

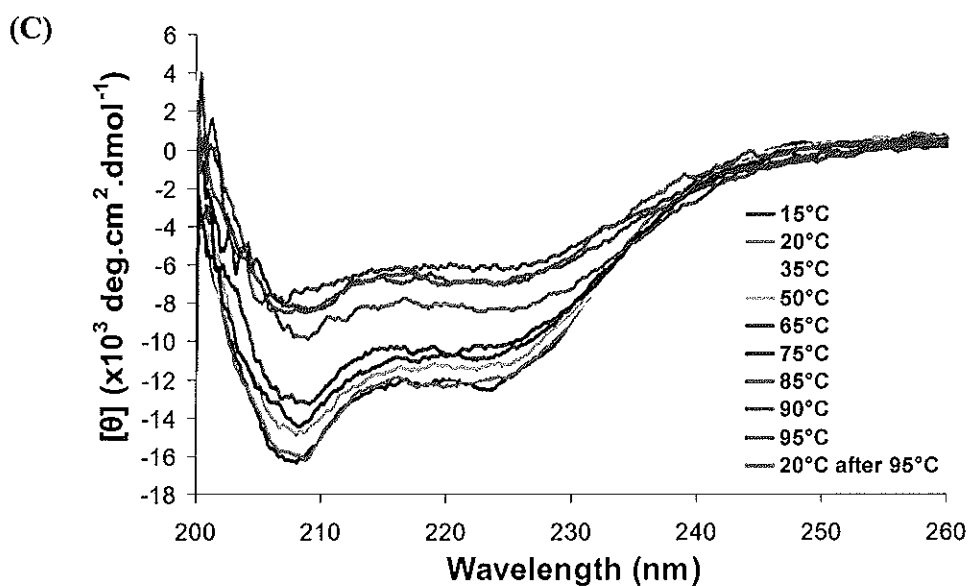
#### 4.7 Thermal stability of the cisplatin-BRCA1 adducts

Thermal denaturation was monitored by CD to follow heat-induced unfolding which determined the effect of cisplatin binding on the stability of the BRCA1 RING domain. The BRCA1(1-139) protein pre-incubated with or without  $\text{Zn}^{2+}$  was incubated with cisplatin, and CD spectra showed the identical changes with an increase in ellipticity when the temperature was raised from  $15^\circ\text{C}$  to  $95^\circ\text{C}$  (Figures 44 and 45). It indicated that the folded proteins gradually lost the extent of the ordered structures. When cooling to  $20^\circ\text{C}$  after being heated at  $95^\circ\text{C}$ , CD spectrum was partially recovered, indicating an incomplete reversibility of the unfolding/refolding process. Furthermore, the thermal denaturation curves were used to compare the stabilities among the platinated proteins and the melting temperatures ( $T_m$ ) were summarized in the inset (Figure 46). The results showed that the melting temperatures of the BRCA1(1-139) proteins were about  $74^\circ\text{C}$  and  $83^\circ\text{C}$  in the absence and presence of  $\text{Zn}^{2+}$ , respectively. This suggested that the BRCA1 RING domain was more thermostable by about  $9^\circ\text{C}$  upon  $\text{Zn}^{2+}$ -binding. Thus, it supported the important role of  $\text{Zn}^{2+}$  in the determination and stabilization of the local secondary structure in the

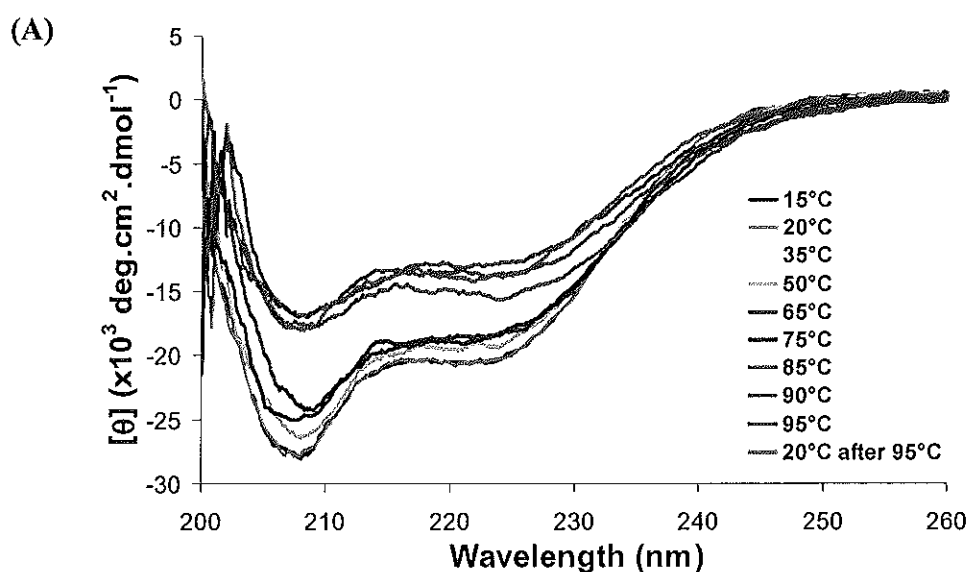
RING domain. It was notable that cisplatin at the concentration of 10  $\mu\text{M}$  exhibited the similar melting temperatures as those observed for  $\text{Zn}^{2+}$  binding to the BRCA1 RING domain. However, higher melting temperatures were observed at a 10-fold concentration of cisplatin (100  $\mu\text{M}$ ). These data suggested that cisplatin binding to the BRCA1 RING domain conferred an enhanced thermostability by 13°C. Resistance to thermal denaturation of the cisplatin-modified BRCA1 RING domain might result from the favourably intramolecular and intermolecular crosslinks driven by the free energy.







**Figure 44.** Thermal transition of the cisplatin-BRCA1 adducts in the absence of  $Zn^{2+}$ . The BRCA1(1-139) proteins ( $10 \mu M$ ) without  $Zn^{2+}$  were mixed with a number of cisplatin concentrations [ $0 \mu M$  for (A),  $10 \mu M$  for (B), and  $100 \mu M$  for (C)]. Samples were incubated in the dark at ambient temperature for 24 h. The measurements were performed from  $15^\circ C$  to  $95^\circ C$  with a heating rate of  $1^\circ C/min$ . After heating at  $95^\circ C$ , the measurement at  $20^\circ C$  was also performed. The CD spectra were plotted between mean residue ellipticity and wavelength.



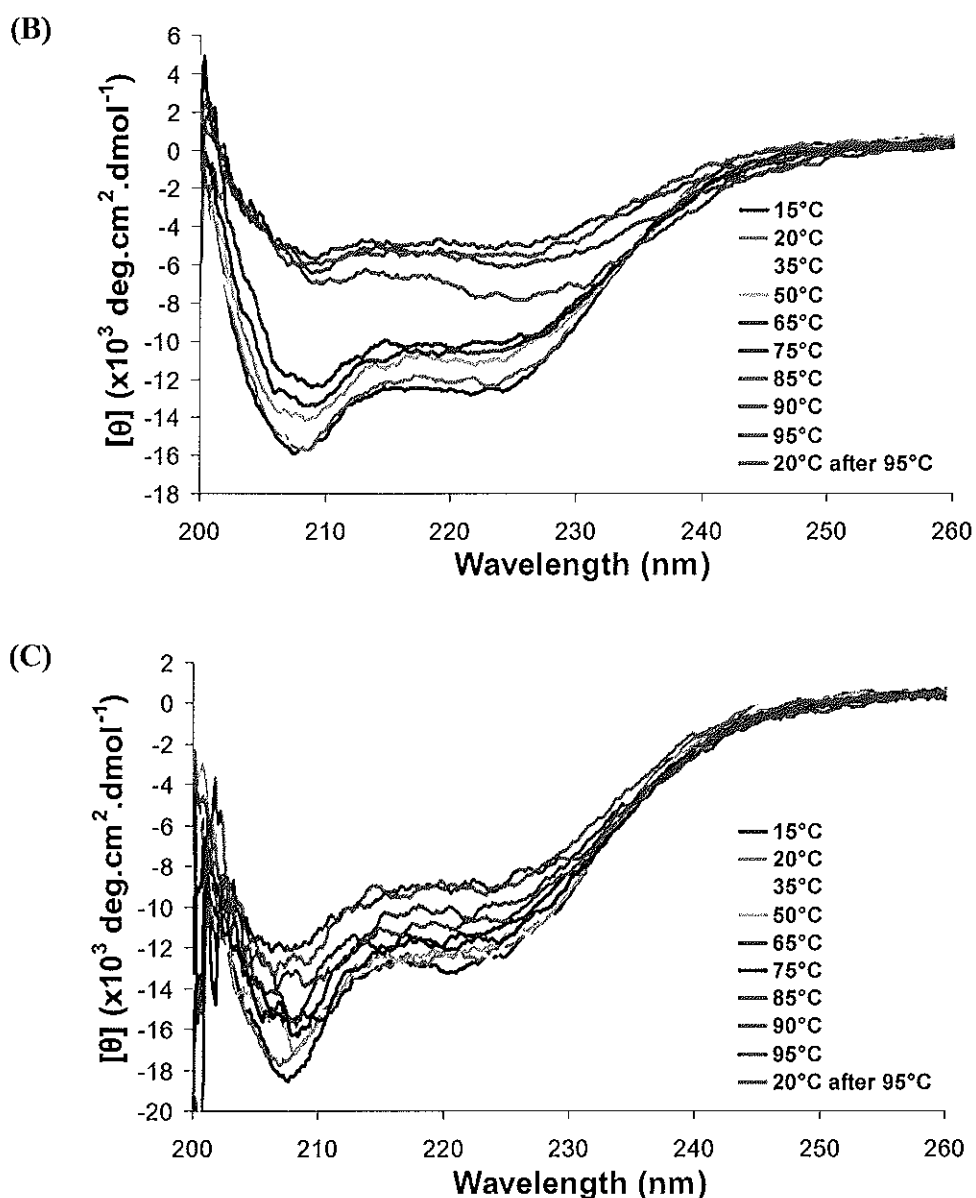


**Figure 45.** Thermal transition of the cisplatin-BRCA1 adducts in the presence of  $\text{Zn}^{2+}$ . The BRCA1(1-139) proteins ( $10 \mu\text{M}$ ) with pre-incubation of 3 molar equivalent ratio of  $\text{Zn}^{2+}$  to protein were mixed with a number of cisplatin concentrations [ $0 \mu\text{M}$  for (A),  $10 \mu\text{M}$  for (B), and  $100 \mu\text{M}$  for (C)]. Samples were incubated in the dark at ambient temperature for 24 h. The measurements were performed from  $15^\circ\text{C}$  to  $95^\circ\text{C}$  with a heating rate of  $1^\circ\text{C}/\text{min}$ . After heating at  $95^\circ\text{C}$ , the measurement at  $20^\circ\text{C}$  was also performed. The CD spectra were plotted between mean residue ellipticity and wavelength.

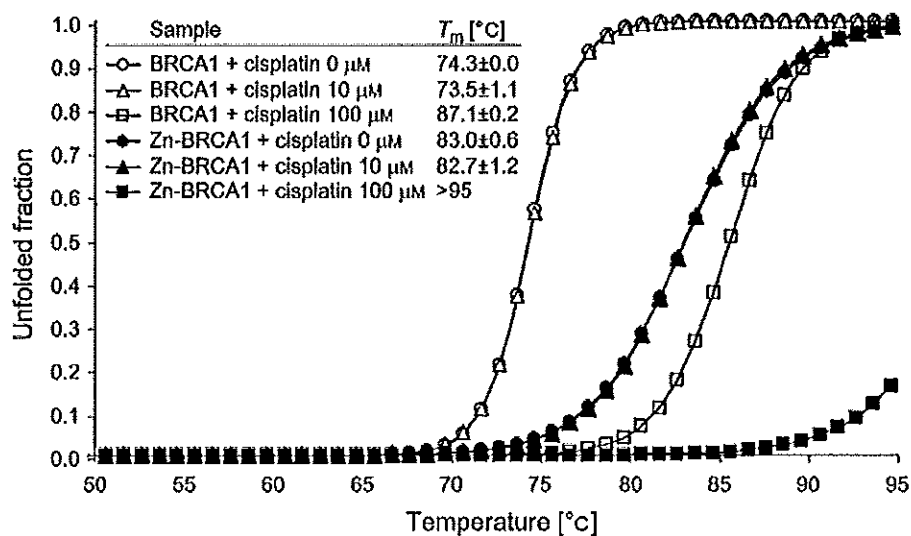


**Figure 46.** Thermal denaturation curves of the cisplatin-BRCA1 adducts. The BRCA1(1-139) protein (10  $\mu\text{M}$ ) without  $\text{Zn}^{2+}$  and with pre-incubation of 3 molar equivalent ratio of  $\text{Zn}^{2+}$  to protein were mixed with various concentrations of cisplatin (0, 10, and 100  $\mu\text{M}$ ). Samples were incubated in the dark at ambient temperature for 24 h before CD measurement. The CD signals at 208 nm were measured, and the unfolded fraction as a function of temperature was plotted.

#### 4.8 *In vitro* ubiquitin ligase activity of the cisplatin-BRCA1 adducts

To gain further insights into the functional consequence of the platinated BRCA1, the BRCA1 RING protein [GST-BRCA1(1-304)] was platinated *in vitro* by cisplatin, transplatin, carboplatin, and oxaliplatin at various concentrations. The results showed that the relative E3 ligase activity was inversely proportional to the concentration of the platinum complexes (Figure 47). An increase in platinum concentration was accompanied by a high amount of BRCA1 adducts and a low amount of native BRCA1 protein as described previously (Figure 38). To address whether the inhibition of the E3 ligase activity resulted from the formation of BRCA1 adducts or a reduced amount of the BRCA1 subunit, a ten-fold excess amount of the platinated BRCA1 was assayed for the E3 ligase activity. The result demonstrated that

the platination of BRCA1 was indeed involved in the inhibition of the E3 ligase activity (lane 3, Figure 48). In a similar way, the platinum-BARD1 adducts failed to exhibit any E3 ligase activity (lanes 4 and 5, Figure 48).

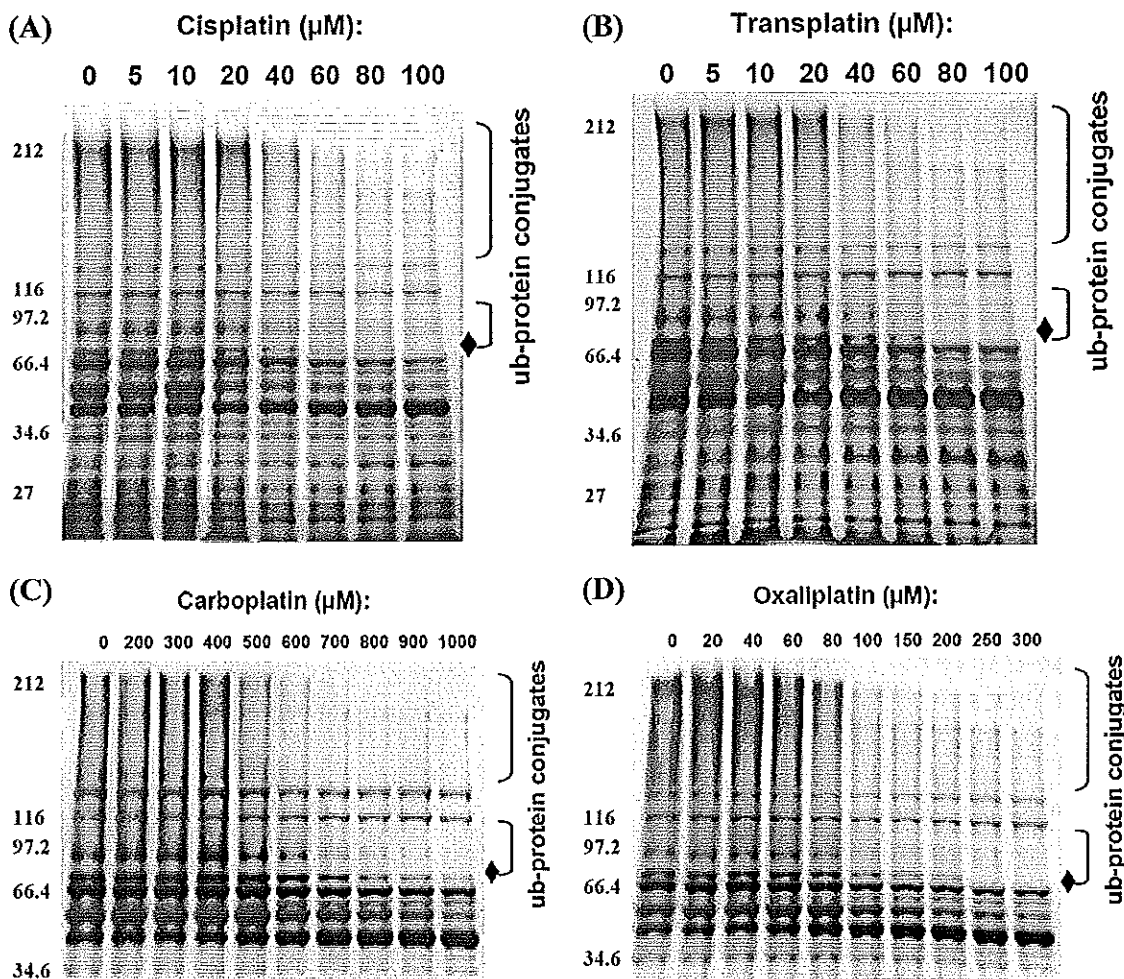


**Figure 47.** *In vitro* ubiquitin ligase activity of the platinum-BRCA1 complexes. Two  $\mu\text{g}$  of the platinum-BRCA1 adducts with a number of defined concentrations of cisplatin (A), transplatin (B), carboplatin (C), and oxaliplatin (D) was assayed for the ubiquitin ligase activity. An apparent ubiquitinated product (as indicated by filled diamond) was markedly reduced as the concentration of platinum increased.

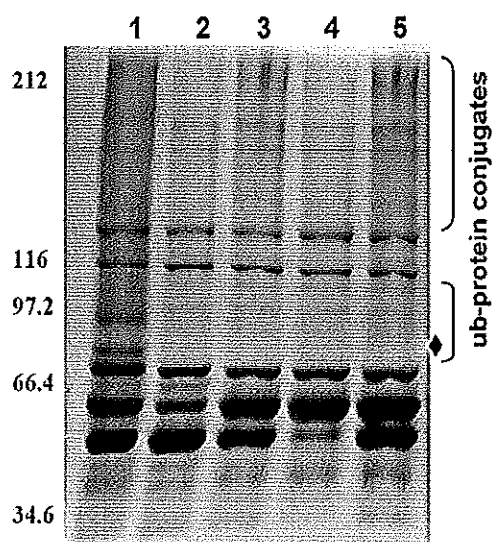


**Figure 48.** *In vitro* ubiquitin ligase activity of the platinum-BRCA1 or platinum-BARD1 complexes. Lane 1: complete E3 ligase reaction with 2  $\mu$ g native BRCA1, lane 2: reaction of 2  $\mu$ g BRCA1 adduct with 100  $\mu$ M cisplatin, lane 3: reaction of 20  $\mu$ g BRCA1 adduct with 100  $\mu$ M cisplatin, lane 4: reaction of 2  $\mu$ g BARD1 adduct with 100  $\mu$ M cisplatin, and lane 5: reaction of 20  $\mu$ g BARD1 adduct with 100  $\mu$ M cisplatin. An apparent ubiquitinated product (as indicated by filled diamond) was markedly reduced as the concentration of cisplatin increased (Figure 45A).

Transplatin, a clinically ineffective *trans*-platinum complex, was the most promising agent to completely abolish the E3 ligase activity at its effective concentration of 80  $\mu$ M compared to cisplatin and oxaliplatin (100 and 250  $\mu$ M, respectively) (Figure 49). Under the same experimental condition, the partial E3 ligase activity was still observed for the carboplatin-BRCA1 adducts at concentrations that exceeded 1000  $\mu$ M. The E3 ligase activity was reduced by half at concentrations of 53  $\mu$ M for transplatin, 60  $\mu$ M for cisplatin, 150  $\mu$ M for oxaliplatin, and 780  $\mu$ M for carboplatin, respectively (Figure 49). As a result, the reactivity of the platinum complexes towards the BRCA1 RING domain was decreased in the following order: transplatin > cisplatin > oxaliplatin > carboplatin.

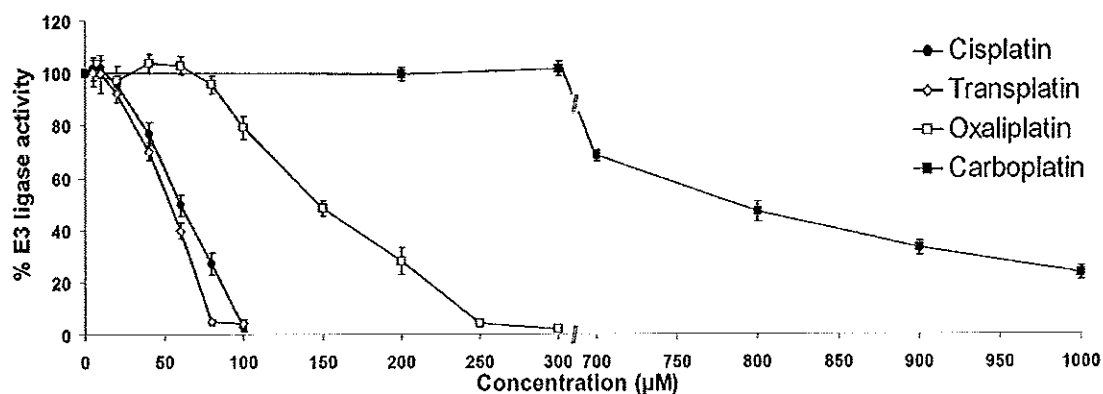


**Figure 49.** Inhibition of the BRCA1 E3 ligase activity by the platinum complexes. The apparent ubiquitinated products (as indicated by filled diamond) in gels shown in Figure 45 were quantified by Bio-Rad GS-700 Imaging Densitometer. The relative E3 ligase activity of BRCA1 adducts (%) was plotted as a function of the concentration of the platinum complexes.

## CHAPTER 5

### DISCUSSION

#### 5.1 The structural consequence of the D67E BRCA1 mutation

Numerous studies of BRCA1 have revealed its involvement in genomic stability maintenance. The malfunction of this protein reportedly results from mutations at the N-terminus of Zn<sup>2+</sup> finger RING domain. In particular, cancer-predisposing site II substitution mutations at position 39, 61, and 64, which potentially impaired Zn<sup>2+</sup> coordination, have been shown to disrupt the RING integrity and protein functions (Brzovic *et al.*, 1998; Brzovic *et al.*, 2003; Hansen *et al.*, 2009; Szabo *et al.*, 2004). The presence of two long helices (residues 8-22 and 81-96), and a central helix (residues 4-53) in the RING structure mostly contributed to the CD signals (Brzovic *et al.*, 2001). The CD spectra revealed that both the D67E mutant and wild-type BRCA1 RING domains predominantly adopted the helical structures in the apo form, and showed additional folded structures in the holo form. As a result, the mutation barely perturbed the native global structure of the BRCA1 RING domain, and assumed a preformed structure in the apo form. Not only was the structure more folded upon Zn<sup>2+</sup>-binding, but the mutant and wild-type BRCA1 RING domains, coordinating with Zn<sup>2+</sup> ions with an almost identical Zn<sup>2+</sup> affinity ( $2.91 \times 10^6 \text{ M}^{-1}$  and  $2.99 \times 10^6 \text{ M}^{-1}$ , respectively), also appeared to be resistant to proteolysis. Additionally, the Zn<sup>2+</sup>-bound forms of the proteins were more stable toward thermal denaturation than the Zn<sup>2+</sup>-free forms. An enhanced stability was apparently provided by the coordinating Zn<sup>2+</sup> that contributed to the proper RING integrity of BRCA1. This was also consistent with the Zn<sup>2+</sup> finger DNA-binding domain (DBD) of p53 whose apoDBD was still folded but it was significantly less stable than the holo form ( $\Delta G^\circ = 6$  and  $10 \text{ kcal mol}^{-1}$  for the apoDBD and holoDBD, respectively) (Loh, 2010;

Xue *et al.*, 2009). Although the melting temperatures of the BRCA1 RING domains were high and far from the physiological condition (about 76-85°C), they were consistent with the previous studies, showing that Zn<sup>2+</sup> finger domain formed the thermostable structure (Arnold and Zhang, 1994; Frankel *et al.*, 1987; Matthews *et al.*, 2000).

However, the mutant protein was slightly less thermostable than the wild-type protein. A structural model of the D67E BRCA1 mutation suggested a potential salt bridge between side-chains of Lys38 and Glu67. The local conformation at position 39 was slightly altered in order to accommodate the salt bridge, as indicated by changes in dihedral angles ( $\Delta\phi = -1.5^\circ$ ,  $\Delta\psi = 4.2^\circ$ ,  $\Delta\omega = 1.7^\circ$ ; Figure 50). The salt bridge would mask the negative surface charge that could disrupt the local interaction with solvent (Figure 51). The altered interactions between surface residues and solvent could be related to such a protein instability (Pjura and Matthews, 1993; Xu *et al.*, 2001). Reduced thermal stability in the D67E BRCA1 might reflect an alteration in the microenvironment at the mutation site necessary for protein interactions to cause tumor suppression.

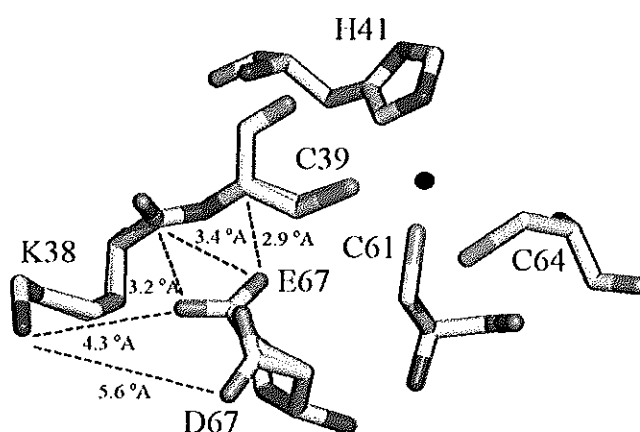


**Figure 50.** Superposition of the model structures in the Zn<sup>2+</sup>-binding site II. The wild-type and D67E BRCA1 RING domains were simulated using the automated protein structure homology-modeling server (SWISS-MODEL). The BRCA1 RING domain (PDB:1JM7) was used as template. The sphere specified the Zn<sup>2+</sup> position, and the number represented the interatomic distance.



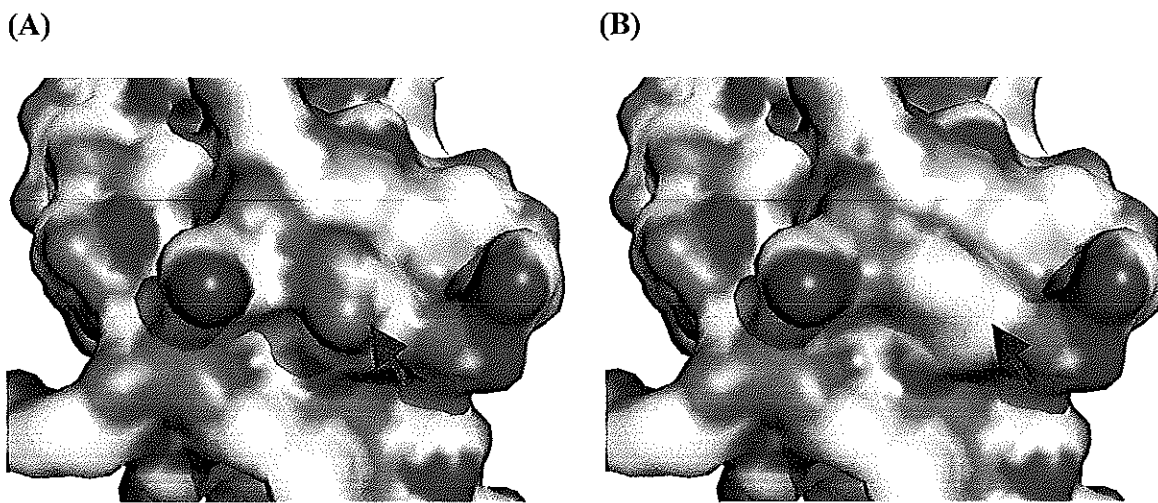


**Figure 51.** Surface representation of the model structures of (A) the wild-type and (B) D67E BRCA1 RING domains. Negatively charged surfaces were shown in red, and positively charged surfaces were shown in blue. The arrow indicated the position 67.

## 5.2 The functional consequence of the D67E BRCA1 mutation

The present study here and elsewhere revealed that the BRCA1 and BARD1 RING complex exhibited an enhanced E3 ubiquitin ligase activity compared to BRCA1 or BARD1 protein alone. The interaction between both proteins, which mutually stabilized each other and dictated a suitable BRCA1 conformation for its binding to a ubiquitin-conjugating enzyme (E2), conferred the maximal ubiquitination function (Brzovic *et al.*, 2006; Mallery *et al.*, 2002). The flanking sequences proximal to the minimal RING domain of BRCA1 required for the ubiquitin ligase activity, suggesting that they might contain the catalytic residues involved and contributed to an active conformation necessary for ubiquitin polymerization (Mallery *et al.*, 2002). To further investigation whether the D67E mutant was capable of polymerizing ubiquitin, the cancer-predisposing C61G BRCA1 mutant was used for comparison. The C61G mutation, that was shown to disrupt the BRCA1 RING structure and the BARD1 and E2 bindings, exhibited the defective ubiquitin ligase activity (Morris *et*

*al.*, 2006; Nishikawa *et al.*, 2004). It indicated that both the proximity effects of the bound substrates and the catalysis were required for full activity to be exerted. The result presented herein revealed that the D67E and D67A BRCA1 mutants still retained their E3 ligase activities, implying that the mutations did not perturb the native BRCA1 RING structure and function. It was in agreement with the findings of a previous study, demonstrating that these mutations retained the ability of proper binding to BARD1 and E2, and thus could mediate the ubiquitin ligase activity (Morris *et al.*, 2006). The partial E3 ligase activity was observed for the D67Y BRCA1 mutant. It suggested that the large hydrophobic side-chain of tyrosine in the second Zn<sup>2+</sup>-binding loop might affect protein interface and then impaired the BRCA1 function.

Recently, it has been reported that the D67E protein inhibited the estrogen signaling similar to the wild-type protein (Pongsavee *et al.*, 2009). Therefore, the substitution of aspartic acid with glutamic acid at position 67 of the BRCA1 RING domain might appear to be a neutral or mild cancer-risk modifier of other defective mechanisms that underlie the BRCA1 mutation-related breast cancer. Recently, the complex of the BRCA1 and BARD1 RING domain has been shown to regulate estrogen signaling through the ubiquitination-mediated estrogen receptor  $\alpha$  (ER $\alpha$ ) degradation (Eakin *et al.*, 2007). The truncated BARD1 isoforms, which lack the RING domain and the ubiquitin ligase activity, were found to be up-regulated in cancerous cells (Li *et al.*, 2007; Tsuzuki *et al.*, 2006). This could compromise the stability of BRCA1 and the functions of the BRCA1-BARD1 complex by interacting with ER $\alpha$  and inhibiting its degradation (Dizin and Irminger-Finger, 2010). The ER $\alpha$  stabilization and activation by BARD1 isoforms might play a pivotal role in the breast carcinogenesis. In addition, BAP1 (BRCA1-associated protein 1) has been hypothesized to increase its stability by deubiquitination or to serve some signaling for BRCA1 and other substrates that may bind to BRCA1. Mutations on BRCA1 at the Zn<sup>2+</sup>-binding sites and its vicinity have been shown to disrupt the BAP1

interaction, and potentially promote the unregulated cell growth (Jensen *et al.*, 1998). Alteration in this function by mutations on BRCA1 would destabilize the proteins by the proteasome-dependent degradation (Orlowski and Dees, 2003; Varshavsky, 2008). Cyclin D1 is also a considerable factor in breast carcinogenesis. It is defined as an oncoprotein that increases cell proliferation by phosphorylating the retinoblastoma protein. It was overexpressed in human breast cancer, and associated with a poor prognosis in ER $\alpha$  positive cases (Kenny *et al.*, 1999; Pestell *et al.*, 1999). Cyclin D1 competed with the BRCA1 RING protein for ER $\alpha$  binding in the same region, and reversed the BRCA1-mediated repression of estrogen signaling that played a role in the growth and development of breast cancer (Gudas *et al.*, 1995; Wang *et al.*, 2005). Moreover, cyclin D1 in combination with CDK4 phosphorylated BRCA1 at serine 632. This event inhibited the ability of the BRCA1-mediated DNA-binding and its recruitment to some particular promoters of the cell-cycle regulatory genes for aiding in carcinogenesis (Kehn *et al.*, 2007). More recently, HERC2 protein, which is an E3 ubiquitin ligase and implicated in DNA damage repair, was identified to interact with the BRCA1 RING domain through its C-terminal HECT-containing motif (Wu *et al.*, 2010). The HERC2 protein could ubiquitinate and target BRCA1 for degradation, and its effect was blocked by BARD1 binding. This suggested that BRCA1 protein stability was tightly regulated by at least two proteins (BARD1 and HERC2), and that this regulation was important for BRCA1 tumor suppression function especially through G2-M cell cycle checkpoint. Interestingly, the HERC2 expression was found at the detectable levels in approximately half of the breast cancer cases, and thus it potentially played a role in breast carcinogenesis (Wu *et al.*, 2010). Therefore, the D67E BRCA1 mutation investigated in the present study might be a cancer-risk modifier potentially by modulating the binding and activity of HERC2.

### 5.3 The interaction between the anticancer drug cisplatin and the BRCA1 RING domain

The interactions of some proteins with cisplatin have extensively been investigated, and the cisplatin-protein adducts are divergent in the formations and functions. For instance, the platination of human serum albumin caused the partial unfolding of the protein structure at high drug concentration and induced intermolecular crosslinks (Ivanov *et al.*, 1998; Neault and Tajmir-Riahi, 1998). A few types of intramolecular crosslinks were also occurred in ubiquitin adducts (Peleg-Shulman *et al.*, 2002). The loss of activity in protein aggregation prevention of the C-terminal heat shock protein 90 was reported as the consequence of cisplatin binding but it did not show any conformational change (Ishidaa *et al.*, 2008). In the present study, the interaction between cisplatin and BRCA1 was investigated with respect to protein conformation and thermal denaturation. The cisplatin-modified BRCA1 RING domain revealed the formations of the favourably intramolecular and intermolecular protein adducts. Binding of cisplatin to the apo-form of BRCA1 potentially at the vacant  $Zn^{2+}$ -binding sites caused more folded structural rearrangement. However, cisplatin did not perturb the global conformation of the holo-form of the BRCA1 RING protein. It implied that cisplatin interacted with the other residues beyond the  $Zn^{2+}$ -binding sites. Tandem mass spectrometric analyses (MS/MS) indicated that the formation of the monofunctional adduct with  $[Pt(NH_3)_2(OH)]^+$  occurred at the BRCA1 peptide  $^{111}ENNSPEHLK^{119}$ . The protonation of Lys119 at neutral pH and the preference of aquated cisplatin for His based on a dipeptide His-Ser model also supported our result that His117 was the primary platinum-binding site (Zhao and King, 2010). Although the hydroxo form in the adduct complex is generally less reactive than the aqua form, its existence may be essential for interaction with the other nucleophiles as it shows the significant reactivity towards thiol groups (El-Khateeb *et al.*, 1999).

The platinum binding to BRCA1 gave the binding constant of  $3.00 \times 10^6 \text{ M}^{-1}$ , equivalent to that of  $\text{Zn}^{2+}$  binding ( $2.99 \times 10^6 \text{ M}^{-1}$ ). The calculated free energy of cisplatin and  $\text{Zn}^{2+}$  bindings were almost identical at about  $-8.68 \text{ kcal mol}^{-1}$ , suggesting the similar thermodynamic contribution of the metal-induced protein folding in the RING domain to drive protein folding, dimerization, and thermostability of BRCA1. The comparison of those two binding constants was not straightforward as described in a previous study, demonstrating the affinity of  $\text{Zn}^{2+}$  and cisplatin to a short  $\text{Zn}^{2+}$  finger peptide of 31 mers in the different fashion (Bose *et al.*, 2005).  $\text{Zn}^{2+}$ -binding to such a peptide employed the stepwise coordination by four cysteines with the binding constant of  $3.91 \times 10^4 \text{ M}^{-1}$ , whilst the platinum binding involved the coordination by two cysteines with the affinity of  $8.80 \times 10^4 \text{ M}^{-1}$ . However, the binding constant of the platinum atom to a larger  $\text{Zn}^{2+}$  finger protein was suggested to be much higher due to the other favourable binding sites beyond the  $\text{Zn}^{2+}$ -binding residues of protein. Moreover, a short synthetic peptide, containing a minimal BRCA1 RING domain, exhibited the  $\text{Co}^{2+}$ -binding constants ranging from  $1.26 \times 10^5 \text{ M}^{-1}$  to  $3.85 \times 10^7 \text{ M}^{-1}$  (Roehm and Berg, 1997). Generally, the binding specificity of a  $\text{Zn}^{2+}$ -binding peptide for  $\text{Co}^{2+}$  was 2-4 orders of magnitude lower than that for  $\text{Zn}^{2+}$  (Krizek *et al.*, 1993; Magyar and Godwin, 2003). Our observed binding constants were therefore consistent with those studies, and showed approximately a 34-fold higher platinum affinity than that observed for the short  $\text{Zn}^{2+}$  finger peptide of 31 mers ( $3.00 \times 10^6 \text{ M}^{-1}$  compared to  $8.80 \times 10^4 \text{ M}^{-1}$ ), implying the overall influence of the adjacent residues of the RING protein on the metal affinity (Bose *et al.*, 2005). Furthermore, the increased thermostability of the cisplatin-BRCA1 adducts by  $13^\circ\text{C}$  was observed, and it was probably resulted from the thermodynamically stabilizing contribution of the intramolecular and intermolecular crosslinks (Byrne and Stites, 1995). The mechanism by which such a crosslink stabilized the protein was widely thought to involve a reduction in the chain flexibility and the entropy of the denatured state (Kuroki *et al.*, 1992; Muheim *et al.*, 1993; Vaz *et al.*, 2006).

#### 5.4 The BRCA1 E3 ligase activity inactivated by the platinum-based drugs

The results presented herein revealed that the BRCA1-mediated ubiquitin ligase activity was inversely proportional to the concentration of the platinum complexes, and that the reactivity of the platinum complexes towards the BRCA1 RING domain was decreased in the following order: transplatin > cisplatin > oxaliplatin > carboplatin. The geometry and the properties of both the leaving and the non-leaving groups of the platinum complexes seemed to play essential roles in controlling the reactivity towards BRCA1. The activation of the platinum complexes occurs when the leaving group either chloride or oxygen is replaced by water before the interaction with the nucleophilic groups of the protein side-chains. The chelation effect and steric hindrance by the bulky leaving ligand of cyclobutane-1,2-dicarboxylic acid results in a much slower hydrolysis rate ( $5.00 \times 10^{-9} \text{ s}^{-1}$  for carboplatin vs  $1.62 \times 10^{-5} \text{ s}^{-1}$  for cisplatin), and indicates that there is a very low reactivity of carboplatin to BRCA1 (Davies *et al.*, 2000; Frey *et al.*, 1993; Pavelka *et al.*, 2007). The chloro leaving groups in both cisplatin and transplatin readily undergo hydrolysis in water, and this results in a higher reactivity. The displacement of two chlorides in the *trans* configuration of transplatin is the easiest process compared to that of cisplatin. Transplatin is, therefore, the most effective compound in inhibiting the E3 ligase activity. Similar to a previous report, we suggest that the *cis/trans* geometry plays an important role in the reactivity and interaction with proteins (Trynda-Lemiesz *et al.*, 1999). In addition, oxaliplatin exhibits a moderate reactivity towards BRCA1 because the hydrolysis rate of the oxalate exchangeable group ( $1.20 \times 10^{-6} \text{ s}^{-1}$ ) is intermediate between those reported for cisplatin and carboplatin under similar conditions (Jerremalm *et al.*, 2002). The five-membered chelation and the steric hindrance of the diamminecyclohexane non-leaving moiety at the platinum center of oxaliplatin are believed to be unhydrolyzable, and resulted in its significant stability (Lucas *et al.*, 2009). This result was consistent with previous studies that

have demonstrated a similar reactivity of the platinum complexes to a number of oligonucleotides and proteins such as ubiquitin, human serum albumin, and a human copper transporter 1 (Casini *et al.*, 2009; Groessl *et al.*, 2010; Trynda-Lemiesz *et al.*, 1999; Wu *et al.*, 2009).

This study has revealed the inactivation of a BRCA1 function by the platinum complexes. It could raise the possibility of utilizing the BRCA1 RING domain as a potentially molecular target for platinum-based agents in cancer chemotherapy. There are some considerations with regards to the cellular activity of cisplatin or the platinum-based agents. Cisplatin can interact nonspecifically with the cellular proteins. Nucleophilic thiol proteins such as glutathione and metallothioneins are capable of binding to cisplatin before reaching the cellular targets. The intracellular concentration of glutathione is as high as 10 mM, and it correlates to cisplatin resistance by which 1 mol of platinum binds to 2 mol of glutathione with the rate constant of  $8.45 \times 10^{-2} \text{ M}^{-1} \text{ s}^{-1}$  (Miao *et al.*, 2005; Petrović *et al.*, 2007). Moreover, the increased levels of metallothioneins have been found in some cisplatin-resistant cells (Ebadi and Iversen, 1994). The stoichiometry of the cisplatin-metallothionein (7:1) complex is established with a significantly high association constant of  $2.3 \times 10^{23} \text{ M}^{-1}$  (Zhang *et al.*, 1997). The high abundance and affinity to platinum of both two proteins in cells can compete with the BRCA1 RING protein for cisplatin binding. To avoid cisplatin inactivation, some specific enzyme inhibitors for the biosynthesis of glutathione and metallothioneins have been used (Saga *et al.*, 2004). Alternatively, a new generation of the platinum-based drug such as picoplatin currently in phase III trial is promising in cancer treatment because of its steric hindrance around the platinum center that reduces the drug inactivation by these thiol-containing molecules (Eckardt *et al.*, 2009; Holford *et al.*, 1998). The *trans*-platinum compounds or other metal-based drugs are also more pronounced to selectively target and inhibit the activity of the  $\text{Zn}^{2+}$  finger domain (Aris and Farrell, 2009; de Paula *et al.*, 2009). Additionally, novel drug delivery systems such as liposomes, dendrimers,

polymers, and nanotubes are now of great interest. They have shown promise for the improved delivery of platinum compounds to cancerous cells with the reduced toxicity and drug inactivation and the extended drugs circulation half-life (Aryal *et al.*, 2010; Boulikas, 2009; Dhar *et al.*, 2008; Lee *et al.*, 2005; Stathopoulos *et al.*, 2010). The attachment of small molecules with biological significance to platinum complexes in the form of platinum (II) and platinum (IV) also allows for targeted delivery (Choy *et al.*, 2008; Dhar and Lippard, 2009; Harper *et al.*, 2010; van Rijt and Sadler, 2009). Taken together, the developments of new metal-based anticancer agents and novel combination of the current chemotherapeutic drugs, that specifically target the BRCA1 RING domain and disrupt its E3 ligase activity, gain much attention for significantly improving the efficacy of the anticancer drugs in cancer therapy.



## CHAPTER 6

### CONCLUSION

The present study is aimed to characterize the structural and functional significances of the D67E mutation in the BRCA1 RING domain by which this conservative missense substitution is probably a founder mutation that was solely identified in Thai breast cancer patients. The outcome of the studies would provide the insights into the molecular mechanisms, underlying the BRCA1 mutation-related breast and ovarian cancers. The structural investigation confirmed that the D67E BRCA1 mutation predominantly adopted the helical structures in the apo form, and showed additional folded structures in the holo form. Although the mutation retained the affinity of  $Zn^{2+}$ -binding, the D67E BRCA1 protein was 3°C less stable than the wild-type protein towards thermal denaturation. The result from the structural modeling suggested potential alteration in the interactions between the BRCA1 surface residues and solvent that would be related to a protein instability. An enzymatic activity of E3 ubiquitin ligase is observed in the BRCA1 RING domain by which the E3 ligase activity plays diverse roles for tumor suppression function. It is of interest to elucidate the functional consequences of the BRCA1 mutations on the ubiquitination. It revealed that the D67E mutant still maintained the E3 ligase activity identically to the wild-type protein, while the C61G mutant that was represented as a negative control had the defective activity. Therefore, the substitution of aspartic acid with glutamic acid at position 67 of the BRCA1 RING domain might appear to be a neutral or mild cancer-risk modifier, potentially through the other defective mechanisms. Several investigations have gained much attention on taking advantage of the inherent weakness of the BRCA1 dysfunction in cancer therapy. Targeting the BRCA1 RING domain through the disruption of  $Zn^{2+}$  coordination sites by the platinum-based drugs might be effective for the eradication of cancers and recurrent

platinum-resistant cancers with lesser adverse effects than the empirical and conventional treatment. The cisplatin-modified BRCA1 RING domain was capable of forming the formations of the favourably intramolecular and intermolecular protein adducts by which cisplatin binding to the apo form of BRCA1 induced more folded structural rearrangement potentially at the vacant  $Zn^{2+}$ -binding sites. Moreover, cisplatin did not perturb the global conformation of the holo form of the BRCA1 RING protein, implying that cisplatin interacted with the other residues beyond the  $Zn^{2+}$ -binding sites. The preferential platinum-binding site for the formation of the monofunctional adduct between  $[Pt(NH_3)_2(OH)]^+$  and the BRCA1 RING domain was likely the His117. The inhibitory activity of the BRCA1-mediated E3 ubiquitin ligase was observed, and it was proportional to the concentration of the platinum complexes. The reactivity of the platinum complexes towards the BRCA1 RING domain was decreased in the following order: transplatin > cisplatin > oxaliplatin > carbaplatin. The resulting data demonstrated that the geometry and the properties of both the leaving and the non-leaving groups of the platinum complexes play a vital role in controlling the reactivity towards BRCA1. Taken together, the present data would provide a foundation for the utilization of the BRCA1 dysfunction, through the BRCA1 RING domain, as a potentially molecular target for platinum-based drugs for significantly improving the efficacy in cancer therapy.

## REFERENCES

- Ahmad S. Platinum-DNA interactions and subsequent cellular processes controlling sensitivity to anticancer platinum complexes. *Chem Biodivers.* 2010; 7(3):543-66.
- Albertella MR, Green CM, Lehmann AR, O'Connor MJ. A Role for polymerase  $\eta$  in the cellular tolerance to cisplatin-induced damage. *Cancer Res.* 2005; 65(21):9799-806.
- Amir E, Seruga B, Serrano R, Ocana A. Targeting DNA repair in breast cancer: A clinical and translational update. *Cancer Treat Rev.* 2010; 36(7):557-65.
- Ande SR, Chen J, Maddika S. The ubiquitin pathway: an emerging drug target in cancer therapy. *Eur J Pharmacol.* 2009; 625(1-3):199-205.
- Anderson E, Berg J, Black R, Bradshaw N, Campbell J, Cetnarskyj R, et al. Predicting breast cancer risk: implications of a "weak" family history. *Fam Cancer.* 2008; 7(4):361-6.
- Anderson PO, Knoben JE, Troutman WG. Handbook of clinical drug data. 10<sup>th</sup> ed. USA: McGraw-Hill companies; 2002. p.209-11.
- Ang WH, Myint M, Lippard SJ. Transcription inhibition by platinum-DNA cross-links in live mammalian cells. *J Am Chem Soc.* 2010; 132(21):7429-35.
- Areberg J, Björkman S, Einarsson L, Frankenberg B, Lundqvist H, Mattsson S, et al. Gamma camera imaging of platinum in tumours and tissues of patients after administration of <sup>191</sup>Pt-cisplatin. *Acta Oncol.* 1999; 38(2):221-8.
- Aris SM, Farrell NP. Towards antitumor active trans-platinum compounds. *Eur J Inorg Chem.* 2009; 2009(10):1293-302.
- Arnold FH, Zhang JH. Metal-mediated protein stabilization. *Trends Biotechnol.* 1994; 12(5):189-92.

- Arnold K, Bordoli L, Kopp J, Schwede T. The SWISS-MODEL Workspace: A web-based environment for protein structure homology modeling. *Bioinformatics* 2006; 22(2):195-201.
- Aryal S, Hu CM, Zhang L. Polymer-cisplatin conjugate nanoparticles for acid-responsive drug delivery. *ACS Nano*. 2010; 4(1):251-8.
- Ashworth A. A synthetic lethal therapeutic approach: poly(ADP) ribose polymerase inhibitors for the treatment of cancers deficient in DNA double-strand break repair. *J Clin Oncol*. 2008; 26(22):3785-90.
- Baldeyron C, Jacquemin E, Smith J, Jacquemont C, De Oliveira I, Gad S, et al. A single mutated BRCA1 allele leads to impaired fidelity of double strand break end-joining. *Oncogene*. 2002; 21(9):1401-10.
- Bassett E, King NM, Bryant MF, Hector S, Pendyala L, Chaney SG, et al. The role of DNA polymerase  $\eta$  in translesion synthesis past platinum-DNA adducts in human fibroblasts. *Cancer Res*. 2004; 64(18):6469-75.
- Bau DT, Fu YP, Chen ST, Cheng TC, Yu JC, Wu PE, et al. Breast cancer risk and the DNA double-strand break end-joining capacity of nonhomologous end-joining genes are affected by BRCA1. *Cancer Res*. 2004; 64(14):5013-19.
- Baumann P, Benson FE, West SC. Human Rad51 protein promotes ATP-dependent homologous pairing and strand transfer reactions *in vitro*. *Cell*. 1996; 87(4):757-66.
- Baumgartner KB, Schlierf TJ, Yang D, Doll MA, Hein DW. N-acetyltransferase 2 genotype modification of active cigarette smoking on breast cancer risk among hispanic and non-hispanic white women. *Toxicol Sci*. 2009; 112(1):211-20.
- Belguise-Valladier P, Maki H, Sekiguchi M, Fuchs RPP. Effect of single DNA lesions on *in vitro* replication with DNA polymerase III holoenzyme. *J Mol Biol*. 1994; 236(1):151-64.

- Berners-Price SJ, Frenkiel TA, Frey U, Ranford JD, Sadler PJ. Hydrolysis products of cisplatin: pKa determinations via [<sup>1</sup>H,<sup>15</sup>N] NMR spectroscopy. *J Chem Soc., Chem Commun.* 1992; 789-91.
- Bhattacharyya A, Ear US, Koller BH, Weichselbaum RR, Bishop DK. The breast cancer susceptibility gene *BRCA1* is required for subnuclear assembly of Rad51 and survival following treatment with the DNA cross-linking agent cisplatin. *J Biol Chem.* 2000; 275(31):23899-903.
- BIC Summary Sheet - The Breast Cancer Information Core Database [Internet]. Bethesda, USA: National Human Genome Research Institute, National Institutes of Health (NIH). [updated 2010 Sep 29; cited 2010 Nov 09]. Available from: <http://research.nhgri.nih.gov/bic/>
- Bose RN, Yang WW, Evanics F. Structural perturbation of a C4 zinc-finger module by *cis*-diamminedichloroplatinum(II): insights into the inhibition of transcription processes by the antitumor drug. *Inorg Chim Acta.* 2005; 358(10):2844-54.
- Boulikas T. Clinical overview on Lipoplatin: a successful liposomal formulation of cisplatin. *Expert Opin Invest Drugs.* 2009; 18(8):1197-218.
- Boyd NF, Stone J, Vogt KN, Connelly BS, Martin LJ, Minkin S. Dietary fat and breast cancer risk revisited: a meta-analysis of the published literature. *Br J Cancer.* 2003; 89(9):1672-85.
- Bradley LNJ, Yarema KJ, Lippard SJ, Essigmann JM. Mutagenicity and genotoxicity of the major DNA adduct of the antitumor drug *cis*-diamminedichloroplatinium(II). *Biochemistry.* 1993; 32(3):982-8.
- Brinton LA, Richesson D, Leitzmann MF, Gierach GL, Schatzkin A, Mouw T, et al. Menopausal hormone therapy and breast cancer risk in the NIH-AARP Diet and Health Study Cohort. *Cancer Epidemiol Biomarkers Prev.* 2008; 17(11):3150-60.

- Brunton LL, Editor. Goodman & Gilman's the pharmacological basis of therapeutics. 11<sup>th</sup> ed. USA: McGraw-Hill Companies; 2006. p.1332-5.
- Brzovic PS, Keffe JR, Nishikawa H, Miyamoto K, Fox III D, Fukuda M, et al. Binding and recognition in the assembly of an active BRCA1/BARD1 ubiquitin-ligase complex. *Proc Natl Acad Sci USA*. 2003; 100(10):5646-51.
- Brzovic PS, Lissounov A, Christensen DE, Hoyt DW, Klevit RE. A UbcH5/ubiquitin noncovalent complex is required for processive BRCA1-directed ubiquitination. *Mol Cell*. 2006; 21(6):873-80.
- Brzovic PS, Meza J, King MC, Klevit RE. The cancer-predisposing mutation C61G disrupts homodimer formation in the NH2-terminal BRCA1 RING finger domain. *J Biol Chem*. 1998; 273(14):7795-9.
- Brzovic PS, Rajagopal P, Hoyt DW, King MC, Klevit RE. Structure of a BRCA1-BARD1 heterodimeric RING-RING complex. *Nat Struct Biol*. 2001; 8(10):833-7.
- Buck M. A novel domain of BRCA1 interacts with p53 in breast cancer cells. *Cancer Lett*. 2008; 268(1):137-45.
- Bueso-Ramos CE, Manshouri T, Haidar MA, Yang Y, McCown P, Ordonez N, et al. Abnormal expression of MDM-2 in breast carcinomas. *Breast Cancer Res Treat*. 1996; 37(2):179-88.
- Burnouf D, Gauthier C, Chottard JC, Fuchs RPP. Single d(ApG)/cis-diamminedichloroplatinum(II) adduct-induced mutagenesis in *Escherichia coli*. *Proc Natl Acad Sci USA*. 1990; 87(16):6087-91.
- Byrne MP, Stites WE. Chemically crosslinked protein dimers: stability and denaturation effects. *Protein Sci*. 1995; 4(12):2545-58.
- Byrski T, Gronwald J, Huzarski T, Grzybowska E, Budryk M, Stawicka M, et al. Pathologic complete response rates in young women with BRCA1-positive breast cancers after neoadjuvant chemotherapy. *J Clin Oncol*. 2010; 28(3):375-9.

- Byrski T, Huzarski T, Dent R, Gronwald J, Zuziak D, Cybulski C, et al. Response to neoadjuvant therapy with cisplatin in BRCA1-positive breast cancer patients. *Breast Cancer Res Treat.* 2009; 115(2):359-63.
- Canitrot Y, Cazaux C, Fréchet M, Bouayadi K, Lesca C, Salles B, et al. Overexpression of DNA polymerase  $\beta$  in cell results in a mutator phenotype and a decreased sensitivity to anticancer drugs. *Proc Natl Acad Sci USA.* 1998; 95(21):12586-90.
- Casini A, Gabbiani C, Michelucci E, Pieraccini G, Moneti G, Dyson PJ, et al. Exploring metallodrug-protein interactions by mass spectrometry: comparisons between platinum coordination complexes and an organometallic ruthenium compound. *J Biol Inorg Chem.* 2009; 14(5):761-70.
- Casini A, Guerri A, Gabbiani C, Messori L. Biophysical characterisation of adducts formed between anticancer metallodrugs and selected proteins: New insights from X-ray diffraction and mass spectrometry studies. *J Inorg Biochem.* 2008; 102(5-6):995-1006.
- Casini A, Mastrobuoni G, Temperini C, Gabbiani C, Francese S, Moneti G, et al. ESI mass spectrometry and X-ray diffraction studies of adducts between anticancer platinum drugs and hen egg white lysozyme. *Chem Commun.* 2007; 14(2):156-8.
- Cepeda V, Fuertes MA, Castilla J, Alonso C, Quevedo C, Pérez JM. Biochemical mechanisms of cisplatin cytotoxicity. *Anticancer Agents Med Chem.* 2007; 7(1):3-18.
- Chang IY, Kim MH, Kim HB, Lee DY, Kim SH, Kim HY, et al., Small interfering RNA-induced suppression of ERCC1 enhances sensitivity of human cancer cells to cisplatin. *Biochem Biophys Res Commun.* 2005; 327(1):225-33.
- Chen A, Kleiman FE, Manley JL, Ouchi T, Pan ZQ. Autoubiquitination of the BRCA1-BARD1 RING ubiquitin ligase. *J Biol Chem.* 2002; 277(24):22085-92.

- Chen D, Ohta N, Ukai M, Masuda M, Yotsuyanagi T. Binding and aggregation of human  $\gamma$ -globulin by *cis*-diamminedichloroplatinum (II) through disulfide bond. *Biol Pharm Bull.* 1994; 17(12):1561-6.
- Chiba N, Parvin JD. Redistribution of BRCA1 among four different protein complexes following replication blockage. *J Biol Chem.* 2001; 276(42):38549-54.
- Choy H, Park C, Yao M. Current status and future prospects for satraplatin, an oral platinum analogue. *Clin Cancer Res.* 2008; 14(6):1633-8.
- Christensen DE, Klevit RE. Dynamic interactions of proteins in complex networks: identifying the complete set of interacting E2s for functional investigation of E3-dependent protein ubiquitination. *FEBS J.* 2009; 276(19):5381-9.
- Cibula D, Gompel A, Mueck AO, La Vecchia C, Hannaford PC, Skouby SO, et al. Hormonal contraception and risk of cancer. *Hum Reprod Update.* 2010; 16(6):631-50.
- Ciccarelli RB, Solomon MJ, Varshavsky A, Lippard SJ. In vivo effects of *cis*- and *trans*-diamminedichloroplatinum (II) on SV40 chromosomes: differential repair, DNA-protein crosslinking, and inhibition of replication. *Biochemistry.* 1985; 24(26):7533-40.
- Comess KM, Burstyn JN, Essigmann JM, Lippard SJ. Replication inhibition and translesion synthesis on templates containing site- specifically placed *cis*-diamminedichloroplatinum(II) DNA adducts. *Biochemistry.* 1992; 31(16):3975-90.
- Corda Y, Job C, Anin M-F, Leng M, Job D. Transcription by eukaryotic and prokaryotic RNA polymerases of DNA modified at a d(GG) or a d(AG) site by the antitumor drug *cis*-diamminedichloroplatinum(II). *Biochemistry.* 1991; 30(1):222-30.



- Cox MC, Barnham KJ, Frenkiel TA, Hoeschele JD, Mason AB, He Q-Y, et al. Identification of platination sites on human serum transferrin using  $^{13}\text{C}$  and  $^{15}\text{N}$  NMR spectroscopy. *J Biol Inorg Chem*. 1999; 4(5):621-31.
- Coyle YM. The effect of environment on breast cancer risk. *Breast Cancer Res Treat*. 2004; 84(3):273-88.
- Crider SE, Holbrook RJ, Franz KJ. Coordination of platinum therapeutic agents to met-rich motifs of human copper transport protein 1. *Metallomics*. 2010; 2(1):74-83.
- Cubo L, Thomas DS, Zhang J, Quiroga AG, Navarro-Ranninger C, Berners-Price SJ. [ $^1\text{H}$ ,  $^{15}\text{N}$ ] NMR studies of the aquation of *cis*-diamine platinum(II) complexes. *Inorg Chim Acta*. 2009; 362(3):1022-6.
- Custódio JBA, Cardoso CMP, Santos MS, Almeida LM, Vicente JAF, Fernandes MAF. Cisplatin impairs rat liver mitochondrial functions by inducing changes on membrane ion permeability: Prevention by thiol group protecting agents. *Toxicology*. 2009; 259(1-2):18-24.
- Dabholkar M, Vionnet J, Bostick-Bruton F, Yu JJ, Reed E. Messenger RNA levels of XPAC and ERCC1 in ovarian cancer tissue correlate with response to platinum-based chemotherapy. *J Clin Invest*. 1994; 94(2):703-8.
- Damia G, D'Incalci M. Targeting DNA repair as a promising approach in cancer therapy. *Eur J Cancer*. 2007; 43(12):1791-801.
- Damsma GE, Alt A, Brueckner F, Carell T, Cramer P. Mechanism of transcriptional stalling at cisplatin-damaged DNA. *Nat Struct Mol Biol*. 2007; 14(12):1127-33.
- Dantuma NP, Groothuis TA, Salomons FA, Neefjes J. A dynamic ubiquitin equilibrium couples proteasomal activity to chromatin remodeling. *J Cell Biol*. 2006; 173(1):19-26.

- Davies MS, Berners-Price SJ, Hambley TW. Slowing of cisplatin aquation in the presence of DNA but not in the presence of phosphate: improved understanding of sequence selectivity and the roles of monoaquated and diaquated species in the binding of cisplatin to DNA. *Inorg Chem.* 2000; 39(24):5603-13.
- de Paula QA, Mangrum JB, Farrell NP. Zinc finger proteins as templates for metal ion exchange: Substitution effects on the C-finger of HIV nucleocapsid NCp7 using M(chelate) species (M=Pt, Pd, Au). *J Inorg Biochem.* 2009; 103(10):1347-54.
- Dhar S, Lippard SJ. Mitaplatin, a potent fusion of cisplatin and the orphan drug dichloroacetate. *Proc Natl Acad Sci USA.* 2009; 106(52):22199-204.
- Dhar S, Liu Z, Thomale J, Dai H, Lippard SJ. Targeted single-wall carbon nanotube-mediated Pt(IV) prodrug delivery using folate as a homing device. *J Am Chem Soc.* 2008; 130(34):11467-76.
- Dizin E, Irminger-Finger I. Negative feedback loop of BRCA1-BARD1 ubiquitin ligase on estrogen receptor  $\alpha$  stability and activity antagonized by cancer-associated isoform of BARD1. *Int J Biochem Cell Biol.* 2010; 42(5):693-700.
- Du W, Li Z, Wang B, Zhang Y. A study on the interaction between cisplatin and urease. *Thermochimica Acta.* 1999; 333(2):109-14.
- Dumitrescu RG, Shields PG. The etiology of alcohol-induced breast cancer. *Alcohol.* 2005; 35(3):213-25.
- Eakin CM, Maccoss MJ, Finney GL, Klevit RE. Estrogen receptor  $\alpha$  is a putative substrate for the BRCA1 ubiquitin ligase. *Proc Natl Acad Sci USA.* 2007; 104(14):5794-9.
- Ebadi M, Iversen PL. Metallothionein in carcinogenesis and cancer chemotherapy. *Gen Pharmacol.* 1994; 25(7):1297-310.

- Eckardt JR, Bentsion DL, Lipatov ON, Polyakov IS, MacKintosh FR, Karlin DA, et al. Phase II Study of picoplatin as second-line therapy for patients with small-cell lung cancer. *J Clin Oncol*. 2009; 27(12):2046-51.
- Eguchi Y, Shimizu S, Tsujimoto Y. Intracellular ATP levels determine cell death fate by apoptosis or necrosis. *Cancer Res*. 1997; 57(10):1835-40.
- Eisen A, Lubinski J, Klijn J, Moller P, Lynch HT, Offit K, et al. Breast cancer risk following bilateral oophorectomy in BRCA1 and BRCA2 mutation carriers: an international case-control study. *J Clin Oncol*. 2005; 23(30):7491-6.
- El-Khateeb M, Appleton TG, Gahan LR, Charles BG, Berners-Price SJ, Bolton AM. Reactions of cisplatin hydrolytes with methionine, cysteine, and plasma ultrafiltrate studied by a combination of HPLC and NMR techniques. *J Inorg Biochem*. 1999; 77(1-2):13-21.
- Engel G. Estimation of binding parameters of enzyme-ligand complex from fluorometric data by a curve fitting procedure: Seryl-tRNA synthetase-tRNA<sup>Ser</sup> complex. *Anal Biochem*. 1974; 61(1):184-91.
- Esteban-Fernández D, Moreno-Gordaliza E, Cañas B, Palacios MA, Gómez-Gómez MM. Analytical methodologies for metallomics studies of antitumor Pt-containing drugs. *Metallomics*. 2010; 2(1):19-38.
- Evans DG, Shenton A, Woodward E, Lalloo F, Howell A, Maher ER. Penetrance estimates for *BRCA1* and *BRCA2* based on genetic testing in a Clinical Cancer Genetics service setting: risks of breast/ovarian cancer quoted should reflect the cancer burden in the family. *BMC Cancer*. 2008; 8:155.
- Fabbro M, Savage K, Hobson K, Deans AJ, Powell SN, McArthur GA, et al. BRCA1-BARD1 complexes are required for p53<sup>Ser-15</sup> phosphorylation and a G1/S arrest following ionizing radiation-induced DNA damage. *J Biol Chem*. 2004; 279(30):31251-8.

- Fan S, Ma YX, Wang C, Yuan RQ, Meng Q, Wang JA, et al. p300 Modulates the BRCA1 inhibition of estrogen receptor activity. *Cancer Res.* 2002; 62(1):141-51.
- Fan S, Ma YX, Wang C, Yuan RQ, Meng Q, Wang J-N, et al. Role of direct interaction in BRCA1 inhibition of estrogen receptor activity. *Oncogene.* 2001; 20(1):77-87.
- Fan S, Meng Q, Gao B, Grossman J, Yadegari M, Goldberg ID, et al. Alcohol stimulates estrogen receptor signaling in human breast cancer cell lines. *Cancer Res.* 2000; 60(20):5635-39.
- Fan S, Wang J, Yuan R, Ma Y, Meng Q, Erdos MR, et al. BRCA1 inhibition of estrogen receptor signaling in transfected cells. *Science.* 1999; 284(5418):1354-6.
- Farmer H, McCabe N, Lord CJ, Tutt AN, Johnson DA, Richardson TB, et al. Targeting the DNA repair defect in BRCA mutant cells as a therapeutic strategy. *Nature.* 2005, 434(7035):917-21.
- Fedier A, Steiner RA, Schwarz VA et al. The effect of loss of Brca1 on the sensitivity to anticancer agents in p53-deficient cells. *Int J Oncol.* 2003; 22(5):1169-73.
- Ferlay J, Shin HR, Bray F, Forman D, Mathers C, Parkin DM. GLOBOCAN 2008, Cancer Incidence and Mortality Worldwide: IARC CancerBase No. 10 [Internet]. Lyon, France: International Agency for Research on Cancer; 2010. [updated 2010 Aug; cited 2010 Nov 09]. Available from: <http://globocan.iarc.fr>
- Fong PC, Boss DS, Yap TA, Tutt A, Wu P, Mergui-Roelvink M, et al. Inhibition of poly(ADP-ribose) polymerase in tumors from BRCA mutation carriers. *N Engl J Med.* 2009; 361(2):123-34.
- Font A, Taron M, Gago JL, Costa C, Sánchez JJ, Carrato C, et al. BRCA1 mRNA expression and outcome to neoadjuvant cisplatin-based chemotherapy in bladder cancer. *Ann Oncol.* 2010. doi:10.1093/annonc/mdq333

- Ford D, Easton DF, Peto J. Estimates of the gene frequency of BRCA1 and its contribution to breast and ovarian cancer incidence. *Am J Hum Genet.* 1995; 57(6):1457-62.
- Foulkes WD. Traffic Control for BRCA1. *N Engl J Med.* 2010; 362(8):755-6.
- Frankel AD, Berg JM, Pabo CO. Metal-dependent folding of a single zinc finger from transcription factor IIIA. *Proc Natl Acad Sci USA.* 1987; 84(14):4841-5.
- Frey U, Ranford JD, Sadler PJ. Ring-opening reactions of the anticancer drug carboplatin: NMR characterization of cis-[Pt(NH<sub>3</sub>)<sub>2</sub>(CBDCA-O)(5'-GMP-N7)] in solution. *Inorg Chem.* 1993; 32(8):1333-40.
- Fuertes MA, Castilla J, Alonso C, Pérez JM. Cisplatin biochemical mechanism of action: from cytotoxicity to induction of cell death through interconnections between apoptotic and necrotic pathways. *Curr Med Chem.* 2003; 10(3):257-66.
- Furuta T, Ueda T, Aune G, Sarasin A, Kraemer KH, Pommier Y. Transcription-coupled nucleotide excision repair as a determinant of cisplatin sensitivity of human cells. *Cancer Res.* 2002; 62(17):4899-902.
- Ghezzi A, Aceto M, Cassino C, Gabano E, Osella D. Uptake of antitumor platinum(II)-complexes by cancer cells, assayed by inductively coupled plasma mass spectrometry (ICP-MS). *J Inorg Biochem.* 2004; 98(1):73-8.
- Gnerlich JL, Deshpande AD, Jeffe DB, Sweet A, White N, Margenthaler JA. Elevated breast cancer mortality in women younger than age 40 years compared with older women is attributed to poorer survival in early-stage disease. *J Am Coll Surg.* 2009; 208(3):341-7.
- Greenfield NJ. Using circular dichroism spectra to estimate protein secondary structure. *Nat Protoc.* 2006; 1(6):2876-90.

- Groessler M, Tsybin YO, Hartinger CG, Keppler BK, Dyson PJ. Ruthenium versus platinum: interactions of anticancer metallodrugs with duplex oligonucleotides characterized by electrospray ionisation mass spectrometry. *J Biol Inorg Chem* 2010; 15(5):677-88.
- Gudas JM, Nguyen H, Li T, Cowan KH. Hormone-dependent regulation of BRCA1 in human breast cancer cells. *Cancer Res.* 1995; 55(20):4561-5.
- Hall JM, Lee MK, Newman B, Morrow JE, Anderson LA, Huey B, et al. Linkage of early onset familial breast cancer to chromosome 17q21. *Science.* 1990; 250(4988):1684-9.
- Hansen TV, Ejlersen B, Albrechtsen A, Bergsten E, Bjerregaard P, Hansen T, et al. A common Greenlandic Inuit BRCA1 RING domain founder mutation. *Breast Cancer Res Treat.* 2009; 115(1):69-76.
- Harder HC, Rosenberg B. Inhibitory effects of anti-tumor platinum compounds on DNA, RNA and protein syntheses in mammalian cells in vitro. *Int J Cancer.* 1970; 6(2):207-16.
- Harper BW, Krause-Heuer AM, Grant MP, Manohar M, Garbutcheon-Singh KB, Aldrich-Wright JR. *Advances in Platinum Chemotherapeutics.* Chem Eur J. 2010; 16(24):7064-77.
- Hashizume R, Fukuda M, Maeda I, Nishikawa H, Oyake D, Yabuki Y, et al. The RING heterodimer BRCA1-BARD1 is a ubiquitin ligase inactivated by a breast cancer-derived mutation. *J Biol Chem.* 2001; 276(18):14537-40.
- Haupt Y, Maya R, Kazaz A, Oren M. Mdm2 promotes the rapid degradation of p53. *Nature.* 1997; 387(6630):296-9.
- Helleday T, Petermann E, Lundin C, Hodgson B, Sharma RA. DNA repair pathways as targets for cancer therapy. *Nat Rev Cancer.* 2008; 8(3):193-204.
- Heminger KA, Hartson SD, Rogers J, Matts RL. Cisplatin inhibits protein synthesis in rabbit reticulocyte lysate by causing an arrest in elongation. *Arch Biochem Biophys.* 1997; 344(1):200-7.

- Henderson BE, Paganini-Hill A, Ross RK. Decreased mortality in users of estrogen replacement therapy. *Arch Intern Med.* 1991; 151(1):75-8.
- Herceg Z, Wang ZQ. Functions of poly(ADP-ribose) polymerase (PARP) in DNA repair, genomic integrity and cell death. *Mutat Res.* 2001; 477(1-2):97-110.
- Hicks JK, Chute CL, Paulsen MT, Ragland RL, Howlett NG, Gueranger Q, et al. Differential roles for DNA polymerases eta, zeta, and REV1 in lesion bypass of intrastrand versus interstrand DNA cross-links. *Mol Cell Biol.* 2010; 30(5):1217-30.
- Hoeller D, Dikic I. Targeting the ubiquitin system in cancer therapy. *Nature.* 2009; 458(7237):438-44.
- Hoffmann J-S, Pillaire M-J, Garcia-Estefania D, Lapalu S, Villani G. In vitro bypass replication of the cisplatin-d(GpG) lesion by calf thymus DNA polymerase  $\beta$  and human immunodeficiency virus type I reverse transcriptase is highly mutagenic. *J Biol Chem.* 1996; 271(26):15386-92.
- Hoffmann JS, Pillaire MJ, Maga G, Fodust V, Htibseber U, Villani G. DNA polymerase  $\beta$  bypasses *in vitro* a single d(GpG)-cisplatin adduct placed on codon 13 of the *HRAS* gene. *Proc Natl Acad Sci USA.* 1995; 92(12):5356-60.
- Holford J, Raynaud F, Murrer BA, Grimaldi K, Hartley JA, Abrams M, et al. Chemical, biochemical and pharmacological activity of the novel sterically hindered platinum co-ordination complex, cis-[amminedichloro(2-methylpyridine)] platinum(II) (AMD473). *Anticancer Drug Des.* 1998; 13(1):1-18.
- Horwitz AA, Affar EB, Heine GF, Shi Y, Parvin JD. A mechanism for transcriptional repression dependent on the BRCA1 E3 ubiquitin ligase. *Proc Natl Acad Sci USA.* 2007; 104(16):6614-9.
- Hostetter AA, Chapman EG, DeRose VJ. Rapid cross-linking of an RNA internal loop by the anticancer drug cisplatin. *J Am Chem Soc.* 2009; 131(26):9250-7.

- Howard RA, Leitzmann MF, Linet MS, Freedman DM. Physical activity and breast cancer risk among pre- and postmenopausal women in the U.S. radiologic technologists cohort. *Cancer Causes Control*. 2009; 20(3):323-33.
- Huang JC, Zamble DB, Reardon JT, Lippard SJ, Sancar A. HMG-domain proteins specifically inhibit the repair of the major DNA adduct of the anticancer drug cisplatin by human excision nuclease. *Proc Natl Acad Sci USA*. 1994; 91(22):10394-8.
- Huen MSY, Sy SMH, Chen J. BRCA1 and its toolbox for the maintenance of genome integrity. *Nat Rev Mol Cell Biol*. 2010; 11(2):138-48.
- Hulka BS, Stark A. Breast cancer: cause and prevention. *Lancet* 1995; 346(8979):883-7.
- Husain A, He G, Venkatraman ES, Spriggs DR. BRCA1 up-regulation is associated with repair-mediated resistance to cis-diamminedichloroplatinum(II). *Cancer Res*. 1998; 58(6):1120-23.
- Ishidaa R, Takaokaa Y, Yamamotoa S, Miyazakia T, Otakab M, Watanabeb S, et al. Cisplatin differently affects amino terminal and carboxyl terminal domains of HSP90. *FEBS Lett*. 2008; 582(28):3879-83.
- Ivanov AI, Christodoulou J, Parkinson JA, Barnham KJ, Tucker A, Woodrow J, et al. Cisplatin binding sites on human albumin. *J Biol Chem*. 1998; 273(24):14721-30.
- James CR, Quinn JE, Mullan PB, Johnston PG, Harkin DP. BRCA1, a potential predictive biomarker in the treatment of breast cancer. *Oncologist*. 2007; 12(2):142-50.
- Jatoi I, Anderson WF, Rao SR, Devesa SS. Breast cancer trends among black and white women in the United States. *J Clin Oncol*. 2005; 23(31):7836-41.
- Jemal A, Siegel R, Xu J, Ward E. Cancer Statistics, 2010. *CA Cancer J Clin*. 2010; 60(5):277-300.



- Jensen DE, Proctor M, Marquis ST, Gardner HP, Ha SI, Chodosh LA, et al. BAP1: a novel ubiquitin hydrolase which binds to the BRCA1 RING finger and enhances BRCA1-mediated cell growth suppression. *Oncogene*. 1998; 16(9):1097-112.
- Jerremalm E, Videhult P, Alvelius G, Griffiths WJ, Bergman T, Eksborg S, et al. Alkaline hydrolysis of oxaliplatin-isolation and identification of the oxalato monodentate intermediate. *J Pharm Sci*. 2002; 91(10):2116-21.
- Jordan P, Carmo-Fonseca M. Cisplatin inhibits synthesis of ribosomal RNA *in vivo*. *Nucleic Acids Res*. 1998; 26(12):2831-6.
- Jung Y, Mikata Y, Lippard SJ. Kinetic studies of the TATA-binding protein interaction with cisplatin-modified DNA. *J Biol Chem*. 2001; 276(47):43589-96.
- Kahlenborn C, Modugno F, Potter DM, Severs WB. Oral contraceptive use as a risk factor for premenopausal breast cancer: a meta-analysis. *Mayo Clin Proc*. 2006; 81(10):1290-302.
- Kartalou M, Essigmann JM. Recognition of cisplatin adducts by cellular proteins. *Mutat Res*. 2001; 478(1-2):1-21.
- Katiyar P, Ma Y, Riegel A, Fan S, Rosen EM. Mechanism of BRCA1-mediated inhibition of progesterone receptor transcriptional activity. *Mol Endocrinol*. 2009; 23(8):1135-46.
- Kehn K, Berro R, Alhaj A, Bottazzi ME, Yeh WI, Klase Z, et al. Functional consequences of cyclin D1/BRCA1 interaction in breast cancer cells. *Oncogene*. 2007; 26(35):5060-9.
- Kelland L. The resurgence of platinum-based cancer chemotherapy. *Nat Rev Cancer*. 2007; 7(8):573-84.
- Kelley MR, Fishel ML. DNA repair proteins as molecular targets for cancer therapeutics. *Anticancer Agents Med Chem*. 2008; 8(4):417-25.

- Kennedy RD, Quinn JE, Mullan PB, Johnston PG, Harkin DP. The role of BRCA1 in the cellular response to chemotherapy. *J Natl Cancer Inst.* 2004; 96(22):1659-68.
- Kenny FS, Hui R, Musgrove EA, Gee JM, Blamey RW, Nicholson RI, et al. Overexpression of cyclin D1 messenger RNA predicts for poor prognosis in estrogen receptor-positive breast cancer. *Clin Cancer Res.* 1999; 5(8):2069-76.
- Knudson Jr AG. Mutation and cancer: statistical study of retinoblastoma. *Proc Natl Acad Sci USA.* 1971; 68(4):820-3.
- Konstantakou EG, Voutsinas GE, Karkoulis PK, Aravantinos G, Margaritis LH, Stravopodis DJ. Human bladder cancer cells undergo cisplatin-induced apoptosis that is associated with p53-dependent and p53-independent responses. *Int J Oncol.* 2009; 35(2):401-16.
- Krizek BA, Merkle DL, Berg JM. Ligand variation and metal ion binding specificity in zinc finger peptides. *Inorg Chem.* 1993; 32(6):937-40.
- Kroemer G, Zamzami N, Susin SA. Mitochondrial control of apoptosis. *Immunol Today.* 1997; 18(1):44-51.
- Krum SA, Miranda GA, Lin C, Lane TF. BRCA1 associates with processive RNA polymerase II. *J Biol Chem.* 2003; 278(52):52012-20.
- Kuroki R, Inaka K, Taniyama Y, Kidokoro S, Matsushima M, Kikuchi M, et al. Enthalpic destabilization of a mutant human lysozyme lacking a disulfide bridge between cysteine-77 and cysteine-95. *Biochemistry.* 1992; 31(35):8323-8.
- Lafarge S, Sylvain V, Ferrara M, Bignon YJ. Inhibition of BRCA1 leads to increased chemoresistance to microtubule-interfering agents, an effect that involves the JNK pathway. *Oncogene.* 2001; 20(45):6597-606.
- Lee CC, Mackay JA, Frechet JMJ, Szoka FC. Designing dendrimers for biological applications. *Nat Biotechnol.* 2005; 23(12):1517-26.

- Lehmann AR. Replication of damaged DNA by translesion synthesis in human cells. *FEBS Lett.* 2005; 579(4):873-6.
- Leist M, Single B, Castoldi AF, Kühnle S, Nicotera PJ. Intracellular adenosine triphosphate (ATP) concentration: a switch in the decision between apoptosis and necrosis. *Exp Med.* 1997; 185(8):1481-86.
- Lew JQ, Freedman ND, Leitzmann MF, Brinton LA, Hoover RN, Hollenbeck AR, et al. Alcohol and risk of breast cancer by histologic type and hormone receptor status in postmenopausal women: the NIH-AARP Diet and Health Study. *Am J Epidemiol.* 2009; 170(3):308-17.
- Li L, Ryser S, Dizin E, Pils D, Krainer M, Jefford CE, et al. Oncogenic BARD1 isoforms expressed in gynecological cancers. *Cancer Res.* 2007; 67(24):11876-85.
- Li S, Chen PL, Subramanian T, Chinnadurai G, Tomlinson G, Osborne CK, et al. Binding of CtIP to the BRCT repeats of BRCA1 involved in the transcription regulation of p21 is disrupted upon DNA damage. *J Biol Chem.* 1999; 274(16):11334-8.
- Lieberman HB. DNA damage repair and response proteins as targets for cancer therapy. *Curr Med Chem.* 2008; 15(4):360-7.
- Lieberthal W, Triaca V, Levine J. Mechanisms of death induced by cisplatin in proximal tubular epithelial cells: apoptosis vs. necrosis. *Am J Physiol.* 1996; 270(4):700-8.
- Litman R, Gupta R, Brosh Jr RM, Cantor SB. BRCA-FA pathway as a target for anti-tumor drugs *Anticancer Agents Med Chem.* 2008; 8(4):426-30.
- Liu Y, Lashuel HA, Choi S, Xing X, Case A, Ni J, et al. Discovery of inhibitors that elucidate the role of UCH-L1 activity in the H1299 lung cancer cell line. *Chem Biol.* 2003; 10(9):837-46.

- Liu Y, Xing H, Han X, Shi X, Liang F, Cheng G, et al. Apoptosis of HeLa cells induced by cisplatin and its mechanism. *J Huazhong Univ Sci Technol Med Sci.* 2008; 28(2):197-9.
- Ljungman M, Zhang F, Chen F, Rainbow AJ, McKay BC. Inhibition of RNA polymerase II as a trigger for the p53 response. *Oncogene.* 1999; 18(3):583-92.
- Loh SN. The missing Zinc: p53 misfolding and cancer. *Metallomics.* 2010; 2(7):442-9.
- Lucas MF, Pavelka M, Alberto ME, Russo N. Neutral and acidic hydrolysis reactions of the third generation anticancer drug oxaliplatin. *J Phys Chem B.* 2009; 113(3):831-8.
- MacLachlan TK, Somasundaram K, Sgagias M, Shifman Y, Muschel RJ, Cowan KH, et al. BRCA1 effects on the cell cycle and the DNA damage response are linked to altered gene expression. *J Biol Chem.* 2000; 275(4):2777-85.
- MacLachlan TK, Takimoto R, El-Deiry WS. BRCA1 directs a selective p53-dependent transcriptional response towards growth arrest and DNA repair targets. *Mol Cell Biol.* 2002; 22(12):4280-92.
- Magyar JS, Godwin HA. Spectropotentiometric analysis of metal binding to structural zinc-binding sites: accounting quantitatively for pH and metal ion buffering effects. *Anal Biochem.* 2003; 320(1):39-54.
- Mahoney MC, Bevers T, Linos E, Willett WC. Opportunities and strategies for breast cancer prevention through risk reduction. *CA Cancer J Clin.* 2008; 58(6):347-71.
- Mailand N, Bekker-Jensen S, Fastrup H, Melander F, Bartek J, Lukas C, et al. RNF8 ubiquitylates histones at DNA double-strand breaks and promotes assembly of repair proteins. *Cell.* 2007; 131(5):887-900.
- Mallery DL, Vandenberg CJ, Hiom K. Activation of the E3 ligase function of the BRCA1/BARD1 complex by polyubiquitin chains. *EMBO J.* 2002; 21(24):6755-62.

- Mamanta EL, Poma EE, Kaufmann WK, Delmastro DA, Grady HL, Chaney SG. Enhanced replicative bypass of platinum-DNA adducts in cisplatin-resistant human ovarian carcinoma cell lines. *Cancer Res.* 1994; 54(13):3500-5.
- Mansouri A, Ridgway LD, Korapati AL, Zhang Q, Tian L, Wang Y, et al. Sustained activation of JNK/p38 MAPK pathways in response to cisplatin leads to Fas ligand induction and cell death in ovarian carcinoma cells. *J Biol Chem.* 2003; 278(21):19245-56.
- Mark WY, Liao JC, Lu Y, Ayed A, Laister R, Szymczyna B, et al. Characterization of segments from the central region of BRCA1: an intrinsically disordered scaffold for multiple protein-protein and protein-DNA interactions?. *J Mol Biol.* 2005; 345(2):275-87.
- Martin RM, Middleton N, Gunnell D, Owen CG, Smith GD. Breast-feeding and cancer: the Boyd Orr cohort and a systematic review with meta-analysis. *J Natl Cancer Inst.* 2005; 97(19):1446-57.
- Matthews JM, Kowalski K, Liew CK, Sharpe BK, Fox AH, Crossley M, et al. A class of zinc fingers involved in protein-protein interactions biophysical characterization of CCHC fingers from fog and U-shaped. *Eur J Biochem.* 2000; 267(4):1030-8
- Mavaddat N, Antoniou AC, Easton DF, Garcia-Closas M. Genetic susceptibility to breast cancer. *Mol Oncol.* 2010; 4(3):174-91.
- McEvoy GK, Snow EK, Miller J, Kester L, Welsh Jr OH, Heydorn JD, et al. editors. American hospital formulary service (AHFS) – Drug information. Bethesda: American Society of Health-System Pharmacists; 2009. p.990-1005.
- Mettin C. Global breast cancer mortality statistics. *CA Cancer J Clin.* 1999; 49(3):138-44.
- Miki Y, Swensen J, Shattuck-Eidens D, Futreal PA, Harshman K, Tavtigian S, et al. A strong candidate for the breast and ovarian cancer susceptibility gene BRCA1. *Science.* 1994; 266(5182):66-71.

- Miao R, Yang G, Miao Y, Mei Y, Hong J, Zhao C, et al. Interactions of platinum(II) complexes with sulfur-containing peptides studied by electrospray ionization mass spectrometry and tandem mass spectrometry. *Rapid Commun Mass Spectrom.* 2005; 19(8):1031-40.
- Morris JR, Boutell C, Keppler M, Densham R, Weekes D, Alamshah A, et al. The SUMO modification pathway is involved in the BRCA1 response to genotoxic stress. *Nature.* 2009; 462(7275):886-90.
- Morris JR, Pangon L, Boutell C, Katagiri T, Keep NH, Solomon E. Genetic analysis of BRCA1 ubiquitin ligase activity and its relationship to breast cancer susceptibility. *Hum Mol Genet.* 2006; 15(4):599-606.
- Moynahan ME, Cui TY, Jasin M. Homology-directed dna repair, mitomycin c resistance, and chromosome stability is restored with correction of a Brcal mutation. *Cancer Res.* 2001; 61(12):4842-50.
- Muheim A, Todd RJ, Casimiro DR, Gray HB, Arnold FH. Ruthenium-mediated protein cross-linking and stabilization. *J Am Chem Soc.* 1993; 115(12):5312-3.
- Muggia F. Platinum compounds 30 years after the introduction of cisplatin:Implications for the treatment of ovarian cancer. *Gynecol Oncol.* 2009; 112(1):275-81.
- Mullan PB, Quinn JE, Harkin DP. The role of BRCA1 in transcriptional regulation and cell cycle control. *Oncogene.* 2006; 25(43):5854-63.
- Murakawa Y, Sonoda E, Barber LJ, Zeng W, Yokomori K, Kimura H, et al. Inhibitors of the proteasome suppress homologous DNA recombination in mammalian cells. *Cancer Res.* 2007; 67(18):8536-43.
- Murray MM, Mullan PB, Harkin DP. Role played by BRCA1 in transcriptional regulation in response to therapy. *Biochem Soc Trans.* 2007; 35(5):1342-6.
- Musah RA. The HIV-1 nucleocapsid zinc finger protein as a target of antiretroviral therapy. *Curr Top Med Chem.* 2004; 4(15):1605-22.

- Nadeau G, Boufaied N, Moisan A, Lemieux KM, Cayanan C, Monteiro ANA, et al. BRCA1 can stimulate gene transcription by a unique mechanism. *EMBO Rep.* 2000; 1(3): 260-265.
- Nagata C, Mizoue T, Tanaka K, Tsuji I, Wakai K, Inoue M, et al. Tobacco smoking and breast cancer risk: an evaluation based on a systematic review of epidemiological evidence among the Japanese population. *Jpn J Clin Oncol.* 2006; 36(6):387-94.
- Neault JF, Benkirane A, Malonga H, Tajmir-Riahi HA. Interaction of cisplatin drug with Na,K-ATPase: drug binding mode and protein secondary structure. *J Inorg Biochem.* 2001; 86(2-3):603-9.
- Neault JF, Tajmir-Riahi HA. Interaction of cisplatin with human serum albumin. Drug binding mode and protein secondary structure. *Biochim Biophys Acta.* 1998; 1384(1):153-9.
- Newcomb PA, Egan KM, Trentham-Dietz A, Titus-Ernstoff L, Baron JA, Hampton JM, et al. Prediagnostic use of hormone therapy and mortality after breast cancer. *Cancer Epidemiol Biomarkers Prev.* 2008; 17(4):864-71.
- Nijman SM, Luna-Vargas MP, Velds A, Brummelkamp TR, Dirac AM, Sixma TK, et al. A genomic and functional inventory of deubiquitinating enzymes. *Cell.* 2005; 123(5):773-86.
- Nishikawa H, Ooka S, Sato K, Arima K, Okamoto J, Klevit RE, et al. Mass spectrometric and mutational analyses reveal Lys-6-linked polyubiquitin chains catalyzed by BRCA1-BARD1 ubiquitin ligase. *J Biol Chem.* 2004; 279(6):3916-24.
- Nishikawa H, Wu W, Koike A, Kojima R, Gomi H, Fukuda M, et al. BRCA1-associated protein 1 interferes with BRCA1/BARD1 RING heterodimer activity. *Cancer Res.* 2009; 69(1):111-9.

- Noda S, Yoshimura S, Sawada M, Naganawa T, Iwama T, Nakashima S, et al. Role of ceramide during cisplatin-induced apoptosis in C6 glioma cells. *J Neurooncol.* 2001; 52(1):11-21.
- Ober M, Lippard SJ. A 1,2-d(GpG) cisplatin intrastrand cross-link influences the rotational and translational setting of DNA in nucleosomes. *J Am Chem Soc.* 2008; 130(9):2851-61.
- Ohta T, Fukuda M. Ubiquitin and breast cancer. *Oncogene.* 2004; 23(11):2079-88.
- O'Donovan PJ, Livingston DM. BRCA1 and BRCA2: breast/ovarian cancer susceptibility gene products and participants in DNA double-strand break repair. *Carcinogenesis.* 2010; 31(6):961-7.
- Ohndorf UM, Rould MA, He Q, Pabo CO, Lippard SJ. Basis for recognition of cisplatin-modified DNA by high-mobility-group proteins. *Nature.* 1999; 399(6737):708-12.
- Oost TK, Sun C, Armstrong RC, Al-Assaad AS, Betz SF, Deckwerth TL, et al. Discovery of potent antagonists of the antiapoptotic protein XIAP for the treatment of cancer. *J Med Chem.* 2004; 47(18):4417-26.
- Orlowski RZ, Dees EC. The role of the ubiquitination-proteasome pathway in breast cancer: Applying drugs that affect the ubiquitin-proteasome pathway to the therapy of breast cancer. *Breast Cancer Res.* 2003; 5(1):1-7.
- Parvin JD. The BRCA1-dependent ubiquitin ligase, gamma-tubulin, and centrosomes. *Environ Mol Mutagen.* 2009; 50(8):649-53.
- Pavelka M, Lucas MF, Russo N. On the hydrolysis mechanism of the second-generation anticancer drug carboplatin. *Chemistry.* 2007; 13(36):10108-16.
- Patmasiriwat P, Bhothisuwan K, Sinilnikova OM, Chopin S, Methakijvaroon S, Badzioch M, et al. Analysis of breast cancer susceptibility genes BRCA1 and BRCA2 in Thai familial and isolated early-onset breast and ovarian cancer. *Hum Mutat.* 2002; 20(3):230.



- Peleg-Shulman T, Najajreh Y, Gibson D. Interactions of cisplatin and transplatin with proteins: Comparison of binding kinetics, binding sites and reactivity of the Pt-protein adducts of cisplatin and transplatin towards biological nucleophiles. *J Inorg Biochem.* 2002; 91(1):306-11.
- Pestell RG, Albanese C, Reutens AT, Segall JE, Lee RJ, Arnold A. The cyclins and cyclin-dependent kinase inhibitors in hormonal regulation of proliferation and differentiation. *Endocr Rev.* 1999; 20(4):501-34.
- Petrović D, Stojimirović B, Petrović B, Bugarcic ZM, Bugarcic ZD. Studies of interactions between platinum(II) complexes and some biologically relevant molecules. *Bioorg Med Chem.* 2007; 15(12):4203-11.
- Pillaire MJ, Margot A, Villani G, Sarasin A, Defais M, Gentil A. Mutagenesis in monkey cells of a vector containing a single d(GpG *cis*-diamminedichloroplatinum(II) adduct placed on codon 13 of the human *H-ras* protooncogene. *Nucleic Acids Res.* 1994; 22(13):2519-24.
- Pizarro AM, Sadler PJ. Unusual DNA binding modes for metal anticancer complexes. *Biochimie.* 2009; 91(10):1198-211.
- Pjura P, Matthews BW. Structures of randomly generated mutants of T4 lysozyme show that protein stability can be enhanced by relaxation of strain and by improved hydrogen bonding via bound solvent. *Protein Sci.* 1993; 2(12):2226-32.
- Pongsavee M, Patmasiriwat P, Saunders GF. Functional analysis of familial Asp67Glu and Thr1051Ser BRCA1 mutations in breast/ovarian carcinogenesis. *Int J Mol Sci.* 2009; 10(9):4187-97.
- Powell SN, Bindra RS. Targeting the DNA damage response for cancer therapy. *DNA Repair.* 2009; 8(9):1153-65.
- Price M, Monteiro ANA. Fine tuning chemotherapy to match BRCA1 status. *Biochem Pharmacol.* 2010; 80(5):647-53.

- Provencher SW, Glöckner J. Estimation of globular protein secondary structure from circular dichroism. *Biochemistry*. 1981; 20(1):33-7.
- Quinn JE, Carser JE, James CR, Kennedy RD, Harkin DP. BRCA1 and implications for response to chemotherapy in ovarian cancer. *Gynecol Oncol*. 2009; 113(1):134-42.
- Quinn JE, James CR, Stewart GE, Mulligan JM, White P, Chang GK, et al. BRCA1 mRNA expression levels predict for overall survival in ovarian cancer after chemotherapy. *Clin Cancer Res*. 2007; 13(24):7413-20.
- Quinn JE, Kennedy RE, Mullan PB, Gilmore PM, Carty M, Johnston PG, et al. BRCA1 functions as a differential modulator of chemotherapy-induced apoptosis. *Cancer Res*. 2003; 63(19):6221-8.
- Raaphorst GP, Leblanc M, Li LF. A Comparison of response to cisplatin, radiation and combined treatment for cells deficient in recombination repair pathways. *Anticancer Res*. 2005; 25(1A):53-58.
- Rahman N, Seal S, Thompson D, Kelly P, Renwick A, Elliott A, et al. PALB2, which encodes a BRCA2-interacting protein, is a breast cancer susceptibility gene. *Nature Genet*. 2007; 39(2):165-7.
- Ramsay DT, Kent JC, Hartmann RA, Hartmann PE. Anatomy of the lactating human breast redefined with ultrasound imaging. *J Anat*. 2005; 206(6):525-34.
- Ransburgh DJ, Chiba N, Ishioka C, Toland AE, Parvin JD. Identification of breast tumor mutations in BRCA1 that abolish its function in homologous DNA recombination. *Cancer Res*. 2010; 70(3):988-95.
- Ratanaphan A, Canyuk B, Wasiksiri S, Mahasawat P. In vitro platination of human breast cancer suppressor gene 1 (BRCA1) by the anticancer drug carboplatin. *Biochim Biophys Acta*. 2005; 1725(2):145-51.
- Ratanaphan A, Wasiksiri S, Canyuk B, Prasertsan P. Cisplatin-damaged BRCA1 exhibits altered thermostability and transcriptional transactivation. *Cancer Biol Ther*. 2009; 8(10):890-8.

- Reed JC. Apoptosis-based therapies. *Nat Rev - Drug Discov.* 2002; 1(2):111-21.
- Reedijk J. Why does cisplatin reach guanine-N7 with competing S-donor ligands available in the cell?. *Chem Rev.* 1999; 99(9):2499-510.
- Rocca A, Viale G, Gelber RD, Bottiglieri L, Gelber S, Pruneri G, et al. Pathologic complete remission rate after cisplatin-based primary chemotherapy in breast cancer: correlation with p63 expression. *Cancer Chemother Pharmacol.* 2008; 61(6):965-71.
- Roddam AW, Pirie K, Pike MC, Chilvers C, Crossley B, Hermon C, et al. Active and passive smoking and the risk of breast cancer in women aged 36-45 years: a population based case-control study in the UK. *Br J Cancer.* 2007; 97(3):434-9.
- Roehm PC, Berg JM. Sequential metal binding by the RING finger domain of BRCA1. *Biochemistry.* 1997; 36(33):10240-5.
- Rogakou EP, Pilch DR, Orr AH, Ivanova VS, Bonner WM. DNA double-stranded breaks induce histone H2AX phosphorylation on serine 139. *J Biol Chem.* 1998; 273(10):5858-68.
- Rosen EM, Fan S, Pestell RG, Goldberg ID. BRCA1 gene in breast cancer. *J Cell Physiol.* 2003; 196(1):19-41.
- Rosenberg B, VanCamp L, Krigas T. Inhibition of cell division in *Escherichia coli* by electrolysis products from a platinum electrode. *Nature.* 1965; 205(4972):698-9.
- Rosenberg B, VanCamp L, Trosko JE, Mansour VH. Platinum compounds: a new class of potent antitumour agents. *Nature.* 1969; 222(5191):385-6.
- Rosenberg JM, Sato PH. Cisplatin inhibits *in vitro* translation by preventing the formation of complete initiation complex. *Mol. Pharmacol.* 1993; 43(3):491-7.
- Rowling PJE, Cook R, Itzhaki LS. Toward classification of BRCA1 missense variants using a biophysical approach. *J Biol Chem.* 2010; 285(26):20080-7.

- Ruffner H, Joazeiro CA, Hemmati D, Hunter T, Verma IM. Cancer-predisposing mutations within the RING domain of BRCA1: loss of ubiquitin protein ligase activity and protection from radiation hypersensitivity. *Proc Natl Acad Sci USA*. 2001; 98(9):5134-9.
- Saga Y, Hashimoto H, Yachiku S, Iwata T, Tokumitsu M. Reversal of acquired cisplatin resistance by modulation of metallothionein in transplanted murine tumors. *Int J Urol*. 2004; 11(6):407-15.
- Sato K, Hayami R, Wu W, Nishikawa T, Nishikawa H, Okuda Y, et al. Nucleophosmin/B23 is a candidate substrate for the BRCA1-BARD1 ubiquitin ligase. *J Biol Chem*. 2004; 279(30):30919-22.
- Sato PH, Rosenberg JM, Sato RI. Differences in the inhibition of translation by cisplatin, transplatin, and certain related compounds. *Biochem Pharmacol*. 1996; 52(12):1895-902.
- Schimmer AD, Dalili S, Batey RA, Riedl SJ. Targeting XIAP for the treatment of malignancy. *Cell Death Differ*. 2006; 13(2):179-88.
- Scully R, Chen J, Plug A, Xiao Y, Weaver D, Feunteun J, et al. Association of BRCA1 with Rad51 in mitotic and meiotic cells. *Cell*. 1997; 88(2):265-75.
- Shimizu M, Rosenberg B. A similar action to UV-irradiation and a preferential inhibition of DNA synthesis in *E. coli* by antitumor platinum compounds. *J Antibiot (Tokyo)*. 1973; 26(4):243-5.
- Shuck SC, Short EA, Turchi JJ, Eukaryotic nucleotide excision repair: from understanding mechanisms to influencing biology. *Cell Res*. 2008; 18(1):64-72.
- Silver DP, Richardson AL, Eklund AC, Wang ZC, Szallasi Z, Li O, et al. Efficacy of neoadjuvant cisplatin in triple-negative breast cancer. *J Clin Oncol*. 2010. 28(7):1145-53.

- Sirohi B, Arnedos M, Popat S, Ashley S, Nerurkar A, Walsh G, et al. Platinum-based chemotherapy in triple-negative breast cancer. *Annals of Oncology*. 2008; 19(11):1847-52.
- Smith DB, Newlands ES, Rustin GJS, Begent RHJ, Howells N, McQuade B, et al. Comparison of ondansetron and ondansetron plus dexamethasone as antiemetic prophylaxis during cisplatin-containing chemotherapy. *Lancet*. 1991; 338(8765):487-90.
- Snouwaert JN, Gowen LC, Latour AM, Mohn AR, Xiao A, DiBiase L, et al. BRCA1 deficient embryonic stem cells display a decreased homologous recombination frequency and an increased frequency of non-homologous recombination that is corrected by expression of a brca1 transgene. *Oncogene*. 1999; 18(55):7900-7.
- Sobhian B, Shao G, Lilli DR, Culhane AC, Moreau LA, Xia B, et al. RAP80 targets BRCA1 to specific ubiquitin structures at DNA damage sites. *Science*. 2007; 316(5828):1198-202.
- Starita LM, Horwitz AA, Keogh MC, Ishioka C, Parvin JD, Chiba N. BRCA1/BARD1 ubiquitinate phosphorylated RNA polymerase II. *J Biol Chem*. 2005; 280(26):24498-505.
- Starita LM, Parvin JD. The multiple nuclear functions of BRCA1: transcription, ubiquitination and DNA repair. *Curr Opin Cell Biol*. 2003; 15(3):345-50.
- Stathopoulos GP, Antoniou D, Dimitroulis J, Michalopoulou P, Bastas A, Marosis K, et al. Liposomal cisplatin combined with paclitaxel versus cisplatin and paclitaxel in non-small-cell lung cancer: a randomized phase III multicenter trial. *Ann Oncol*. 2010; 21(11):2227-32.
- Stewart DJ, Benjamin RS, Luna M, Feun L, Caprioli R, Seifert W, et al. Human tissue distribution of platinum after cis-diamminedichloroplatinum. *Cancer Chemother Pharmacol*. 1982; 10(1):51-4.

- Strauss BS. The 'A rule' of mutagen specificity: a consequence of DNA polymerase bypass of non-instructional lesions? *Bioessays*. 1991; 13(2):79-84.
- Stucki M, Clapperton JA, Mohammad D, Yaffe MB, Smerdon SJ, Jackson SP. MDC1 directly binds phosphorylated histone H2AX to regulate cellular responses to DNA double-strand breaks. *Cell*. 2005; 123(7): 1213-26.
- Sun X, Tsang C-N, Sun H. Identification and characterization of metaldrug binding proteins by (metallo)proteomics. *Metallomics*. 2009; 1(1):25-31.
- Sun Y. E3 ubiquitin ligases as cancer targets and biomarkers. *Neoplasia*. 2006; 8(8):645-54.
- Suo Z, Lippard SJ, Johnson KA. Single d(GpG)/cis-diammineplatinum(II) adduct-induced inhibition of DNA polymerization. *Biochemistry*. 1999; 38(2):715-26.
- Suzuki Y, Nakabayashi Y, Takahashi R. Ubiquitin-protein ligase activity of X-linked inhibitor of apoptosis protein promotes proteasomal degradation of caspase-3 and enhances its anti-apoptotic effect in Fas-induced cell death. *Proc Natl Acad Sci USA*. 2001; 98(15):8662-7.
- Swisher EM, Sakai W, Karlan BY, Wurz K, Urban N, Taniguchi T. Secondary BRCA1 mutations in BRCA1-mutated ovarian carcinomas with platinum resistance. *Cancer Res*. 2008; 68(8):2581-6.
- Sy SMH, Huen MSY, Chen J. PALB2 is an integral component of the BRCA complex required for homologous recombination repair. *Proc Natl Acad Sci USA*. 2009; 106(17):7155-60.
- Szabo CI, Worley T, Monteiro AN. Understanding germ-line mutations in BRCA1. *Cancer Biol Ther*. 2004; 3(6):515-20.
- Takeshita T, Wu W, Koike A, Fukuda M, Ohta T. Perturbation of DNA repair pathways by proteasome inhibitors corresponds to enhanced chemosensitivity of cells to DNA damage-inducing agents. *Cancer Chemother Pharmacol*. 2009; 64(5):1039-46.

- Taron M, Rosell R, Felip E, Mendez P, Souglakos J, Ronco MS, et al. BRCA1 mRNA expression as an indicator of chemoresistance in lung cancer. *Hum Mol Genet.* 2004; 13(20):2443-9.
- Tassone P, Martino MTD, Ventura M, Pietragalla A, Cucinotto I, Calimeri T, et al. Loss of BRCA1 function increases the antitumor activity of cisplatin against human breast cancer xenografts in vivo. *Cancer Biol Ther.* 2009; 8(7):648-53.
- Tassone P, Tagliaferri P, Perricelli A, Blotta S, Quaresima B, Martelli ML, et al. BRCA1 expression modulates chemosensitivity of BRCA1-defective HCC1937 human breast cancer cells. *Br J Cancer.* 2003; 88(8):1285-91.
- Thakar A, Parvin JD, Zlatanova J. BRCA1/BARD1 E3 ubiquitin ligase can modify histones H2A and H2B in the nucleosome particle. *J Biomol Struct Dyn.* 2010; 27(4):399-406.
- Thompson D, Easton DF, the Breast Cancer Linkage Consortium. Cancer incidence in BRCA1 mutation carriers. *J Natl Cancer Inst.* 2002; 94(18):1358-65.
- Timerbaev AR, Hartinger CG, Aleksenko SS, Keppler BK. Interactions of antitumor metallodrugs with serum proteins: advances in characterization using modern analytical methodology. *Chem Rev.* 2006; 106(6):2224-48.
- Todd RC, Lippard SJ. Inhibition of transcription by platinum antitumor compounds. *Metallomics.* 2009; 1(4):280-91.
- Toh S, Hernández-Díaz S, Logan R, Rossouw JE, Hernán MA. Coronary heart disease in postmenopausal recipients of estrogen plus progestin therapy: does the increased risk ever disappear? A randomized trial. *Ann Intern Med.* 2010; 152(4):211-7.
- Topping RP, Wilkinson JC, Scarpinato KD. Mismatch repair protein deficiency compromises cisplatin-induced apoptotic signaling. *J Biol Chem.* 2009; 284(21):14029-39.
- Tornaletti S. Transcription arrest at DNA damage sites. *Mutat Res.* 2005; 577(1-2):131-45.

- Trynda-Lemiesz L, Kozłowski H, Keppler BK. Effect of *cis*-, *trans* diamminedichloroplatinum(II) and DBP on human serum albumin. *J Inorg Biochem.* 1999; 77(3-4):141-6.
- Tsuzuki M, Wu W, Nishikawa H, Hayami R, Oyake D, Yabuki Y, et al. A truncated splice variant of human BARD1 that lacks the RING finger and ankyrin repeats. *Cancer Lett.* 2006 Feb 20;233(1):108-16.
- Turnbull C, Rahman N. Genetic predisposition to breast cancer: past, present, and future. *Annu Rev Genomics Hum Genet.* 2008; 9(1):321-45.
- Tutt A, Robson M, Garber JE, Domchek SM, Audeh MW, Weitzel JN, et al. Oral poly(ADP-ribose) polymerase inhibitor olaparib in patients with BRCA1 or BRCA2 mutations and advanced breast cancer: a proof-of-concept trial. *Lancet.* 2010; 376(9737):235-44.
- Vaisman A, Varchenko M, Umar A, Kunkel TA, Risinger, JI, Barrett JC, et al. The role of hMLH1, hMSH3, and hMSH6 defects in cisplatin and oxaliplatin resistance: correlation with replicative bypass of platinum-DNA adducts. *Cancer Res.* 1998; 58(16):3579-85.
- van Rijt SH, Sadler PJ. Current applications and future potential for bioinorganic chemistry in the development of anticancer drugs. *Drug Discov Today.* 2009; 14(23-24):1089-97.
- Varma AK, Brown RS, Birrane G, Ladias JA. Structural basis for cell cycle checkpoint control by the BRCA1-CtIP complex. *Biochemistry.* 2005; 44(33):10941-6.
- Varshavsky A. Discovery of cellular regulation by protein degradation. *J Biol Chem.* 2008; 283(50):34469-89.
- Vassilev LT, Vu BT, Graves B, Carvajal D, Podlaski F, Filipovic Z, et al. In vivo activation of the p53 pathway by small-molecule antagonists of MDM2. *Science.* 2004; 303(5659):844-8.



- Vaux DL, Silke J. IAPs, RINGs and ubiquitylation. *Nat Rev Mol Cell Biol.* 2005; 6(4):287-97.
- Vaz DC, Rodrigues JR, Sebald W, Dobson CM, Brito RM. Enthalpic and entropic contributions mediate the role of disulfide bonds on the conformational stability of interleukin-4. *Protein Sci.* 2006; 15(1):33-44.
- Vichi P, Coin F, Renaud J-P, Vermeulen W, Hoeijmakers JHJ, Moras D, et al. Cisplatin- and UV-damaged DNA lure the basal transcription factor TFIID/TBP. *EMBO J.* 1997; 16(24):7444-56.
- Wang B, Elledge SJ. Ubc13/Rnf8 ubiquitin ligases control foci formation of the Rap80/Abraxas/Brcal/Brc36 complex in response to DNA damage. *Proc Natl Acad Sci USA.* 2007; 104(52):20759-63.
- Wang C, Fan S, Li Z, Fu M, Rao M, Ma Y, et al. Cyclin D1 antagonizes BRCA1 repression of estrogen receptor alpha activity. *Cancer Res.* 2005; 65(15):6557-67.
- Wang D, Lippard S. Cellular processing of platinum anticancer drugs. *Nat Rev Drug Discov.* 2005; 4(4):307-20.
- Wang JY, Ho T, Trojanek J, Chintapalli J, Grabacka M, Stoklosa T, et al. Impaired homologous recombination DNA repair and enhanced sensitivity to DNA damage in prostate cancer cells exposed to anchorage-independence. *Oncogene.* 2005; 24(23):3748-58.
- Wang RH, Yu H, Deng CX. A requirement for breast cancer associated gene 1 (BRCA1) in the spindle checkpoint. *Proc Natl Acad Sci USA.* 2004; 101(49):17108-13.
- Wang W, Figg WD. Secondary BRCA1 and BRCA2 alterations and acquired chemoresistance. *Cancer Biol Ther.* 2008; 7(7):1004-5.
- Wang XW, Zhan Q, Coursen JD, Khan MA, Kontny HU, Yu L, et al. GADD45 induction of a G2/M cell cycle checkpoint. *Proc Natl Acad Sci USA.* 1999; 96(7):3706-11.

- Watts FZ, Brissett NC. Linking up and interacting with BRCT domains. *DNA Repair*. 2010; 9(2):103-8.
- Wei L, Lan L, Hong Z, Yasui A, Ishioka C, Chiba N. Rapid recruitment of BRCA1 to DNA double-strand breaks is dependent on its association with Ku80. *Mol Cell Biol*. 2008; 28(24):7380-93.
- Welsh C, Day R, McGurk C, Masters JRW, Wood RD, Koberle B. Reduced levels of XPA, ERCC1 and XPF DNA repair proteins in testis tumor cell lines. *Int J Cancer*. 2004; 110(3):352-61.
- Williams RS, Green R, Glover JNM. Crystal structure of the BRCT repeat region from the breast cancer-associated protein BRCA1. *Nat Struct Biol*. 2001; 8(10):838-42.
- Williams RS, Lee MS, Hau DD, Glover JN. Structural basis of phosphopeptide recognition by the BRCT domain of BRCA1. *Nat Struct Mol Biol*. 2004; 11(6):519-25.
- Williamson EA, Dadmanesh F, Koeffler HP. BRCA1 transactivates the cyclin-dependent kinase inhibitor p27<sup>Kip1</sup>. *Oncogene*. 2002; 21(20): 3199-206.
- Wu B, Dröge P, Davey CA. Site selectivity of platinum anticancer therapeutics. *Nat Chem Biol*. 2008; 4(2):110-2.
- Wu LC, Wang ZW, Tsan JT, Spillman MA, Phung A, Xu XL, et al. Identification of a RING protein that can interact in vivo with the *BRCA1* gene product. *Nat Genet*. 1996; 14(4):430-40.
- Wu W, Sato K, Koike A, Nishikawa H, Koizumi H, Venkitaraman AR, et al. HERC2 is an E3 ligase that targets BRCA1 for degradation. *Cancer Res*. 2010; 70(15):6384-92.
- Wu Z, Liu Q, Liang X, Yang X, Wang N, Wang X, et al. Reactivity of platinum-based antitumor drugs towards a Met- and His-rich 20 mer peptide corresponding to the N-terminal domain of human copper transporter 1. *J Biol Inorg Chem*. 2009; 14(8):1313-23.

- Wu-Baer F, Ludwig T, Baer R. The UBXN1 protein associates with autoubiquitinated forms of the BRCA1 tumor suppressor and inhibits its enzymatic function. *Mol Cell Biol.* 2010; 30(11):2787-98.
- Xia Y, Pao GM, Chen H-W, Verma IM, Hunter T. Enhancement of BRCA1 E3 ubiquitin ligase activity through direct interaction with the BARD1 protein. *J Biol Chem.* 2003; 278(7):5255-63.
- Xu J, Baase WA, Quillin ML, Baldwin EP, Matthews BW. Structural and thermodynamic analysis of the binding of solvent at internal sites in T4 lysozyme. *Protein Sci.* 2001; 10(5):1067-78.
- Xu J, Fan S, Rosen EM. Regulation of the estrogen-inducible gene expression profile by the breast cancer susceptibility gene BRCA1. *Endocrinology.* 2005; 146(4):2031-47.
- Xue Y, Wang S, Feng X. Effect of metal ion on the structural stability of tumour suppressor protein p53 DNA-binding domain. *J Biochem.* 2009; 146(2):193-200.
- Yang ES, Xia F. BRCA1 16 years later: DNA damage-induced BRCA1 shuttling. *FEBS J.* 2010; 277(15):3079-85.
- Yang Y, Kitagaki J, Dai RM, Tsai YC, Lorick KL, Ludwig RL, et al. Inhibitors of ubiquitin-activating enzyme (E1), a new class of potential cancer therapeutics. *Cancer Res.* 2007; 67(19):9472-81.
- Yang Y, Ludwig RL, Jensen JP, Pierre SA, Medaglia MV, Davydov IV, et al. Small molecule inhibitors of HDM2 ubiquitin ligase activity stabilize and activate p53 in cells. *Cancer Cell.* 2005; 7(6):547-59.
- Yarden RI, Pardo-Reoyo S, Sgagias M, Cowan KH, Brody LC. BRCA1 regulates the G2/M checkpoint by activating Chk1 kinase upon DNA damage. *Nat Genet.* 2002; 30(3):285-9.

- Yerushalmi R, Hayes MM, Gelmon KA, Chia S, Bajdik C, Norris B, et al. A phase II trial of a neoadjuvant platinum regimen for locally advanced breast cancer: pathologic response, long term follow-up, and correlation with biomarkers. *Clin Breast Cancer*. 2009; 9(3):166-72.
- Zhang BL, Sun WY, Tang WX. Determination of the association constant of platinum(II) to metallothionein. *J Inorg Biochem*. 1997; 65(4):295-8.
- Zdraveski ZZ, Mello JA, Marinus MG, Essigmann JM. Multiple pathways of recombination define cellular responses to cisplatin. *Chem Biol*. 2000; 7(1):39-50.
- Zhai X, Beckmann H, Jantzen H-M, Essigmann JM. Cisplatin-DNA adducts inhibit ribosomal RNA synthesis by hijacking the transcription factor human upstream binding factor. *Biochemistry*. 1998; 37(46):16307-15.
- Zhang H, Somasundaram K, Peng Y, Tian H, Bi D, Weber BL, et al. BRCA1 physically associates with p53 and stimulates its transcriptional activity. *Oncogene*. 1998; 16(13):1713-21.
- Zhang J, Powell SN. The role of the BRCA1 tumor suppressor in DNA double-strand break repair. *Mol Cancer Res*. 2005; 3(10):531-9.
- Zhao T, King FL. A mass spectrometric comparison of the interactions of cisplatin and transplatin with myoglobin. *J Inorg Biochem*. 2010; 104(2):186-92.
- Zhao T, King FL. Direct determination of the primary binding site of cisplatin on cytochrome c by mass spectrometry. *J Am Soc Mass Spectrom*. 2009; 20(6):1141-7.
- Zhong Q, Boyer TG, Chen PL, Lee WH. Deficient nonhomologous end-joining activity in cell-free extracts from Brcal-null fibroblasts. *Cancer Res*. 2002; 62(14):3966-70.
- Zhu Y, Hub J, Hu Y, Liu W. Targeting DNA repair pathways: a novel approach to reduce cancer therapeutic resistance. *Cancer Treat Rev*. 2009; 35(7):590-6.

## **APPENDIX**

**Figure 52.** Information of pET28a(+)\_BARD1 (Addgene plasmid 12646).

Gene/insert name:	BRCA1-associated RING domain 1 (BARD1)
Nucleotide:	76-981
Insert size (bp):	906
Species of gene(s):	<i>H. sapiens</i> (human)
Vector backbone:	pET28a(+)
Type of vector:	Bacterial expression
Cloning site 5':	<i>Nco</i> I
Cloning site 3':	<i>Xho</i> I
Bacteria resistance:	Kanamycin
Plasmid provided in:	<i>E. coli</i> DH5 $\alpha$
Principal investigator:	Rachel Klevit

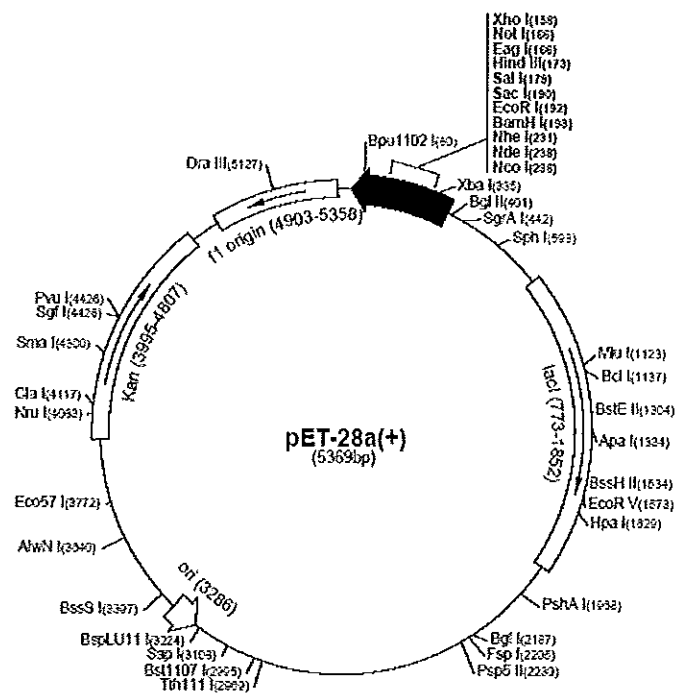
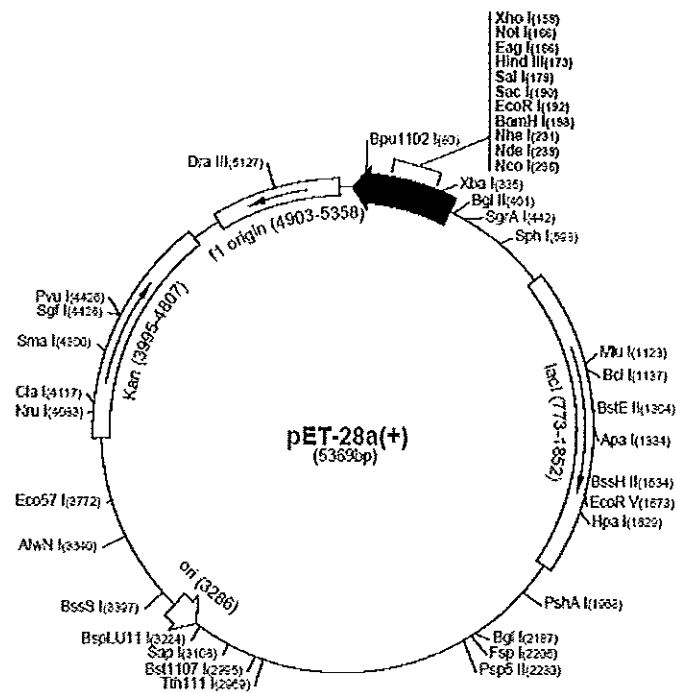


Figure 53. Information of pET28a(+)\_UbchH5c (Addgene plasmid 12643).

Gene/insert name:	Ubiquitin conjugating enzyme (UbchH5c)
Nucleotide:	1-444
Insert size (bp):	444
Species of gene(s):	<i>H. sapiens</i> (human)
Vector backbone:	pET28a(+)
Type of vector:	Bacterial expression
Cloning site 5':	<i>NcoI</i>
Cloning site 3':	<i>XhoI</i>
Bacteria resistance:	Kanamycin
Plasmid provided in:	<i>E. coli</i> DH5 $\alpha$
Principal investigator:	Rachel Klevit



**Figure 54.** Information of pET15\_ubiquitin (Addgene plasmid 12647).

Gene/insert name:	Ubiquitin
Nucleotide:	1-231
Insert size (bp):	231
Species of gene(s):	<i>H. sapiens</i> (human)
Vector backbone:	pET15
Type of vector:	Bacterial expression
Cloning site 5':	<i>Bam</i> HI
Cloning site 3':	<i>Kpn</i> I
Bacteria resistance:	Ampicillin
Plasmid provided in:	<i>E. coli</i> DH5 $\alpha$
Principal investigator:	Rachel Klevit

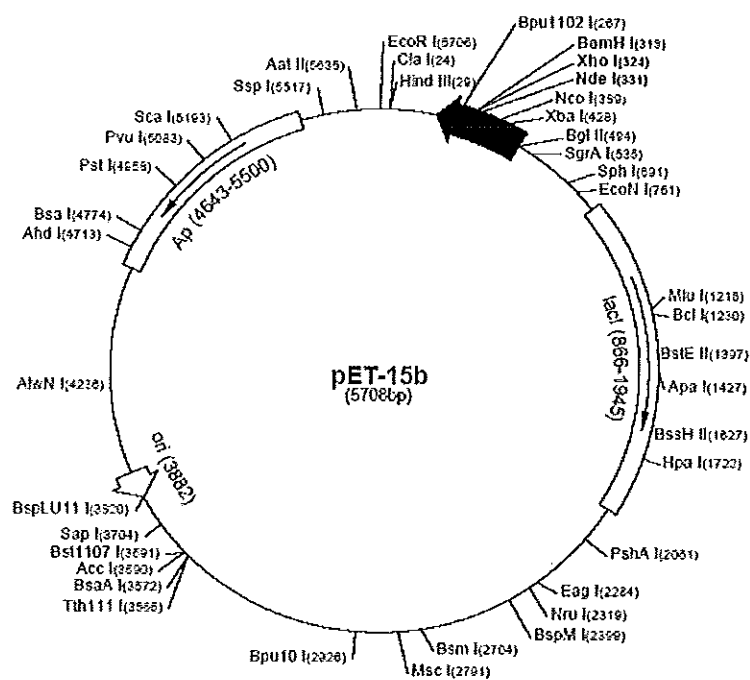




**Figure 55.** Nucleotide sequence of the *BARD1* gene fragment (nucleotide 76-981)  
(GenBank no. NM\_000465).

```
1 CCTCTGGCGG CCCGCCGTCC CAGACGCGGG AAGAGCTTGG CCGGTTTCGA GTCGCTGGCC
61 TGCAGCTTCC CTGTGGTTTC CCGAGGCTTC CTTGCTTCCC GCTCTGCGAG GAGCCTTTCA
121 TCCGAAGGCG GGACGATGCC GGATAATFCG CAGCCGAGGA ACCGGCAGCC GAGGATCCGC
181 TCCGGGAACG AGCCTCGTTC CGCGCCCGCC ATGGAACCGG ATGGTFCGCGG TGCCTGGGCC
241 CACAGTCGCG CCGCGCTCGA CCGCCTGGAG AAGCTGCTGC GCTGCTCGCG TTGTACTAAC
301 ATTCTGAGAG AGCCTGTGTG TTTAGGAGGA TGTGAGCACA TCTTCTGTAG TAATTGTGTA
361 AGTGACTGCA TTGGAAGTGG ATGTCCAGTG TGTTACACCC CGGCCTGGAT ACAAGACTTG
421 AAGATAAATA GACAACTGGA CAGCATGATT CAACTTTGTA GTAAGCTTCG AAATTTGCTA
481 CATGACAATG AGCTGTCAGA TTTGAAAGAA GATAAACCTA GGAAAAGTTT GTTTAATGAT
541 GCAGGAAACA AGAAGAATTC AATTAAAATG TGGTTTAGCC CTCGAAGTAA GAAAGTCAGA
601 TATGTTGTGA GTAAAGCTTC AGTGCAAACC CAGCCTGCAA TAAAAAAGA TGCAAGTGCT
661 CAGCAAGACT CATATGAATT TGTTTCCCA AGTCCTCCTG CAGATGTTTC TGAGAGGGCT
721 AAAAAGGCTT CTGCAAGATC TGGAAAAAAG CAAAAAAGA AAACTTTAGC TGAAATCAAC
781 CAAAAATGGA ATTTAGAGGC AGAAAAAGAA GATGGTGAAT TTGACTCCAA AGAGGAATCT
841 AAGCAAAAGC TGGTATCCTT CTGTAGCCAA CCATCTGTTA TCTCCAGTCC TCAGATAAAT
901 GGTGAAATAG ACTTACTAGC AAGTGGCTCC TTGACAGAAT CTGAATGTTT TGGAAGTTTA
961 ACTGAAGTCT CTTTACCATT GGCTGAGCAA ATAGAGTCTC CAGACACTAA GAGCAGGAAT
```

**Figure 56.** Nucleotide sequence of the full-length *UbcH5c* gene (GenBank no. HSU39318).

```
1 ATGGCGCTGA AACGGATTAA TAAGGAACTT AGTGATTTGG CCCGTGACCC TCCAGCACAA
61 TGTTCCTGCAG GTCCAGTTGG GGATGATATG TTTCATTGGC AAGCCACAAT TATGGGACCT
121 AATGACAGCC CATATCAAGG CGGTGTATTC TTTTGTGACAA TTCATTTTCC TACAGACTAC
181 CCCTTCAAAC CACCTAAGGT TGCATTTACA ACAAGAATTT ATCATCCAAA TATTAACAGT
241 AATGGCAGCA TTTGTCTCGA TATTCTAAGA TCACAGTGGT CGCCTGCTTT AACAAATTTCT
301 AAAGTTCTTT TATCCATTTG TTCACTGCTA TGTGATCCAA ACCCAGATGA CCCCCTAGTG
361 CCAGAGATTG CACGGATCTA TAAAACAGAC AGAGATAAGT ACAACAGAAT ATCTCGGGAA
421 TGGACTCAGA AGTATGCCAT GTGA
```

**Figure 57.** Nucleotide sequence of the full-length ubiquitin gene (GenBank no. NM\_021009).

```
1 ATGCAGATCT TCGTGAAGAC TCTGACTGGT AAGACCATCA CCCTCGAGGT TGAGCCCAGT
61 GACACCATCG AGAATGTCAA GGCAAAGATC CAAGATAAGG AAGGCATCCC TCCTGACCAG
121 CAGAGGCTGA TCTTTGCTGG AAAACAGCTG GAAGATGGGC GCACCCGTGC TGA CTACAAC
181 ATCCAGAAAG AGTCCACCC T GCACCTGGTG CTCCGTCTCA GAGGTGGGTG A
```

## VITAE

**Name** Mr. Apichart Atipairin

**Student ID** 4653006

### **Educational Attainment**

Degree	Name of Institution	Year of Graduation
Bachelor of Pharmacy (B.Pharm.) (First-Class Honours)	Faculty of Pharmaceutical Sciences, Prince of Songkla University	2002

### **Scholarship Awards during Enrolment**

Graduate Study Scholarship for Ph.D. 2003-2005, Prince of Songkla University

### **Work position and Address**

Lecturer, School of Pharmacy, Walailak University, 222 Thaiburi, Thasala District, Nakhonsithammarat 80160, Thailand

### **List of Publication and Proceedings**

**Atipairin A, Canyuk B, Ratanaphan A.** Substitution of aspartic acid with glutamic acid at position 67 of the BRCA1 RING domain retains ubiquitin ligase activity and zinc(II) binding with a reduced transition temperature. *J Biol Inorg Chem.* 2010. DOI:10.1007/s00775-010-0718-y. Impact factor (2009): 3.415

**Atipairin, A, Canyuk B, Ratanaphan A.** The RING heterodimer BRCA1-BARD1 is a ubiquitin ligase inactivated by the platinum-based anticancer drugs. *Breast Cancer Res Treat.* 2010. DOI:10.1007/s10549-010-1182-7. Impact factor (2009): 4.696

**Atipairin A**, Canyuk B, Ratanaphan A. Cisplatin affects the conformation of apo-form, not holo-form, of BRCA1 RING finger domain and confers thermal stability. *Chem. Biodivers.* 2010; 7(8):1949-67. Impact factor (2009): 1.926

**Atipairin A**, Canyuk B, Ratanaphan A. Substitution of aspartic acid with glutamic acid at position 67 of BRCA1 RING domain exhibits thermal instability. The 2<sup>nd</sup> Biochemistry and molecular biology for regional sustainable development. May 6-7 2009, Khon Kaen, Thailand.

**Atipairin A**, Canyuk B, Ratanaphan A. Molecular cloning and expression of the D67E mutant breast cancer susceptibility gene 1 (BRCA1) protein. The 5<sup>th</sup> Princess Chulabhorn international science congress: Evolving genetics and its global impact. August 16-20 2004, Bangkok, Thailand.

Ratanaphan A, Canyuk B, **Atipairin, A**, Wasiksiri S. Molecular cloning and expression of the C-terminal region of human BRCA1 (BRCT) protein induced by the bacterial *pho A* promoter. XIX International congress of genetics, genomes - the linkage to life. July 6-12 2003, Melbourne, Australia.

Ratanaphan A, Canyuk B, Wasiksiri S, **Atipairin A**, Mahasawat P. Human breast cancer suppressor gene 1 (BRCA1): Analysis of DNA damage and gene expression. The 3<sup>rd</sup> Indochina conference on pharmaceutical sciences (Pharma Indochina III), Pharmacy for better quality of life. May 21-23 2003, Bangkok, Thailand.